MODELING REEF-CORAL RESPONSE TO CLIMATE CHANGE

by

CHRISTOPHER WILLIAM CACCIAPAGLIA

B.S., Florida Institute of Technology

A dissertation submitted to the Department of Biological Sciences
of the Florida Institute of Technology in partial fulfillment
of the requirements for the degree of

DOCTOR OF PHILOSOPHY
in
BIOLOGICAL SCIENCES

Melbourne, Florida
December 2016

MODELING REEF-CORAL RESPONSE TO CLIMATE CHANGE

A DISSERTATION

By

CHRISTOPHER WILLIAM CACCIAPAGLIA

Approved as to style and content by:

Robert van Woesik, Ph.D., Chairperson Professor Department of Biological Sciences	Ralph G. Turingan, Ph.D., Professor Department of Biological Sciences
Mark Bush, Ph.D., Professor Department of Biological Sciences	Nezamoddin Nezamoddini-Kachouie, Ph.D., Assistant Professor, Department of Mathematical Sciences
	Richard B. Aronson, Ph.D., Professor and Head Department of Biological Sciences

December 2016

ABSTRACT

MODELING REEF-CORAL RESPONSE TO CLIMATE CHANGE

by Christopher William Cacciapaglia,
B.S. Florida Institute of Technology

Chairperson of Advisory Committee: Robert van Woesik, Ph.D.

Coral reefs are one of the most diverse ecosystems on the planet. They provide goods and services to millions of people living in the coastal tropics. Recently, however, rising sea-surface temperatures have been threatening reef corals, causing episodes of thermal stress that lead to coral bleaching, mortality, and changes in reef composition. This increase in ocean temperature, along with the melting of glaciers and polar ice caps, is also causing an increase in sea level, which is threatening to 'drown' reefs that cannot keep up with sea-level rise. Some early models predicted that nearly all coral species would be unable to survive the +2–3^{o}C increase in sea-surface temperature predicted by the year 2100. However, ocean warming was most often modeled without considering geographical variation. Indeed, within that spatial variation are locations that may act as climate-change refugia, where temperatures are not rapidly increasing, and in which corals can persist into the future. This study aims to identify potential climate-change refuges for coral reefs in the Indian and Pacific Oceans.

Species-distribution models are increasingly being used as a tool to identify suitable habitats for terrestrial and marine species under future climate change. These models consider: (i) the contemporary distribution of species, (ii) the environmental conditions in which the species is found, and (iii) the forecasted environmental conditions from climate models. These models fit the distribution of a species to its current habitat and use projected climate to predict where the species will most likely persist into the future.

The first model in this study identified twelve potential climate refuges in the Indo-Pacific. In the Indian Ocean, climate-change refugia were identified in south western Madagascar, the Maldives, the Chagos Archipelago, Western Australia, and the Seychelles. In the Pacific Ocean, climate-change refugia were identified in northern Indonesia, Micronesia, the northern Marshall Islands, the southern Great Barrier Reef, the Solomon Islands, Vanuatu, and French Polynesia. All twelve of these reef-coral refugia deserve high-conservation status. Nine of the twelve species examined were predicted to lose 24–50% of their current habitat, with most reduction predicted to occur between the latitudes 5º–15º, in both hemispheres. Yet when these species were modeled with a 1ºC capacity to adapt, they were predicted to retain much of their current distribution. By contrast, the thermally tolerant *Porites lobata* is expected to expand its current distribution by 8%, particularly southward along Australia's western and eastern coasts.

In the second model, light-blocking turbidity reduced the harmful effect of increased sea-surface temperature in 9% of the Indo-Pacific's shallow water reefs. Turbidity-driven mitigation was identified in the northwestern Hawaiian Islands, northern Philippines, the Ryukyu Islands (Japan), eastern Vietnam, western and eastern Australia, New Caledonia, the northern Red Sea, and the Arabian Gulf. Turbidity also prevented coral growth by reducing light for photosynthesis in 16% of shallow-water reefs in the Indo-Pacific.

In the third model, genetic isolation reduced *Porites lobata*'s predicted suitable habitat by over 60%, irrespective of climate-change scenario. These results indicate that genetic isolation will likely play a major role in the persistence of coral species under climate change. Most loss in suitable habitat occurred in the Pacific Ocean and small, isolated populations were most vulnerable to climate change.

In the fourth model, sea-level rise threatens to outpace vertical accretion in habitats that are unable to support reef-building corals in a warming ocean. In locations where primary reef-accreting species were able to withstand the regional increase in thermal stress, reefs were predicted to be able to vertically accrete and keep pace with sea-level rise. These locations were aligned with previously identified climate and turbidity-driven refugia. The largest effect of erosion was biological erosion, considered as function of human-population density. Reefs were predicted to drown primarily at the distributional edge of the representative reef-accreting species.

Although the models in this study show significant habitat loss as the oceans are predicted to warm, the work also highlights regions where corals might survive over the next century. This study provides critical information on where we should invest conservation effort, and identifies refugia that deserve protection and consideration as global sanctuaries.

TABLE OF CONTENTS

LIST OF TABLES

LIST OF FIGURES

LIST OF SUPPLEMENTARY FIGURES

ACKNOWLEDGEMENTS

Dr. Robert van Woesik, thank you for being the best adviser possible in every aspect of my research experience. Every step of the way you have offered me the freedom, support, encouragement, and enthusiasm necessary to push me towards my talents – and helped me learn the things I couldn't work out on my own. Thank you for every opportunity; from volunteering in the lab as an undergraduate, to finalizing this dissertation as a graduate student. So much has happened during this time, and I couldn't have done it without your guidance.

I am grateful for the support offered by the members of my committee, Dr. Rich Aronson, Dr. Mark Bush, Dr. Ralph Turingan, Dr. Nezamoddin Nezamoddini-Kachouie, and previous committee member, Dr. Christin Pruett. Your advice and direction in both methodology and application of my research have been extremely valuable. I would like to thank Dr. Bush and Dr. Aronson in particular for the opportunity to work outside of my lab doing research. It was a very valuable experience to learn about different ecosystems and collaborate.

I would like to thank Sandy van Woesik and my lab mates: Dr. Carly Randall, Dr. Adán Guillermo Jordán-Garza, and Kelly McCaffrey as well as the many other graduate students who have helped me with everything from editing to colors to offering advice from an engineering point of view.

I would like to thank the administrative members of the biology department. Thank you for your outstanding patience as I aimlessly fumbled through the paperwork required to get through the steps of this program.

I am thankful for my friends at the university outside of academia, particularly the members of the cross country program. Pete Mazzone, you have always been there for me throughout my undergraduate and graduate degrees, and I would not be who I am today without your guidance and friendship. I also would like to thank my teammates, who have not only kept me sane throughout the years, but are responsible for some of my fondest memories.

Lastly, I would like to thank my family and friends. I love you all.

CHAPTER 1. INTRODUCTION AND RESEARCH QUESTIONS

Coral reefs are one of the world's most diverse ecosystems. Coral reefs provide resources and ecosystem services that benefit both the nearby human populations and the associated coral-reef organisms (Costanza et al. 1998). In the last three decades, however, reef corals in some tropical regions have experienced unprecedented thermal stress events (Glynn 1993; Hoegh-Guldberg 1999; Aronson et al. 2000). Such thermal stress has led to extensive coral bleaching, coral mortality, and dramatic shifts in coral-community composition (Loya et al. 2001; van Woesik et al. 2011; Burman et al. 2012). These recent, unprecedented thermal-stress events have led to compositional shifts toward more thermally tolerant corals (Glynn 1984; Glynn 1988; Glynn 1991; Loya et al. 2001).

The International Panel on Climate Change (IPCC 2013) has shown that the average ocean temperature of the upper 75 m of the oceans has increased by 0.11°C (±0.09 to 0.13°C) per decade, over the last sixty years. This rate of change is likely to increase in a 'business as usual', Representative Concentration Pathway (RCP) 8.5 scenario (IPCC 2013) (Figure 1.1). Such rapid rates of climate change are faster than corals have experienced in the past several hundred millennia (Hoegh-Guldberg et al. 2007). Several authors suggest that corals on modern reef corals are at the highest risk of extinction since the Cretaceous-Tertiary mass extinction event, approximately 65 million years ago (Veron 1995; Wood 1999; Veron 2008). Hoegh-Guldberg et al.

(2007) even suggested that because corals are already living near their thermal maximum, further increases in temperatures will most likely lead to local, regional, and global extinction of many coral species.

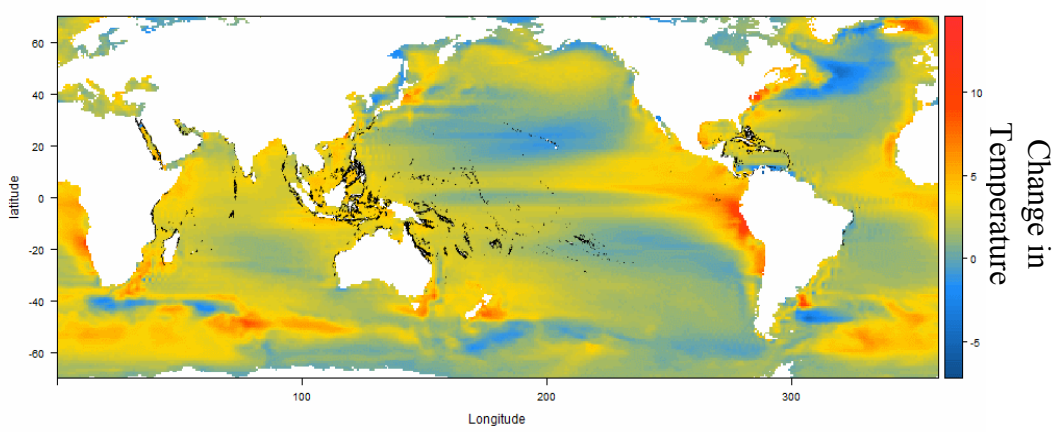

Figure 1.1 Predicted change in mean sea-surface temperature (˚C) between 2012 and 2100 under a Representative Concentration Pathways 8.5 (business as usual) scenario. The black dots are where modern coral reefs are located. Sea-surface temperature data were gathered from Bio-ORACLE (Ocean Rasters for Analysis of Climate and Environment) (http://www.oracle.ugent.be/). Current raster data from Bio-ORACLE was derived from Aqua-MODIS (Moderate Resolution Imaging Spectroradiometer) satellite for the years 2002-2009 (Tyberghein et al. 2012), which are in grids of 5 arc minutes (c. 9.2 km).

In support of such dire climate scenarios, most global models predict that few reef corals will survive beyond the 2°C temperature rise predicted for the tropical oceans within the next hundred years (Frieler et al., 2013). Yet, such predictions disagree with field studies of climate-change impacts on coral reefs, which show persistence of corals in some oceanic regions (Thompson & van Woesik, 2009; McClanahan et al., 2011; Pandolfi et al., 2011), and persistence of corals in specific nearshore and

turbid habitats (van Woesik et al., 2012a). The disagreement between the global models and field studies stems from treating ocean warming in the models as spatially homogenous. By contrast, there are some regions that are warming more slowly than other regions (Thompson and van Woesik 2009; Burrows et al 2011). Regions that are warming the slowest may act as climate-change refuges, defined here as areas greater than 100 km^2, to which corals can migrate to and persist in, without having to rapidly adapt until the year 2100 (Ashcroft 2010). This study aims at identifying potential climate-change refuges for coral reefs in the Indian and Pacific Oceans. The primary research questions of this study are:

(1) Where are the climate-change refugia in the Indo-Pacific?

(2) Where does turbidity mitigate thermal stress in the Indo-Pacific?

(3) How does genetic isolation and local adaptation affect species persistence under climate change?

(4) Where will coral reefs in the Indo-Pacific be able to accumulate carbonate vertically, and keep up with the rate of modern sea-level rise?

SPECIES-DISTRIBUTION MODELS

Determining the response of organisms to climate change is most frequently assessed using species-distribution models (Elith and Leathwick 2009). Species-distribution models gather data on existing species distributions and on the environmental

conditions within those distributions. In combination with climate models, the species-distribution models are capable of predicting future distributions (Cacciapaglia and van Woesik 2015). Species-distribution models assume (i) that each individual of the population is able to tolerate all the environmental conditions across the broad geographic range of the population, and (ii) that there are no genotypes within the geographical range of a given species that can tolerate environmental conditions outside the native geographic range. The present study tests these assumptions, and questions their validity, by determining whether the isolation of subpopulations have detrimental consequences in predicting suitable habitats across the Indo-Pacific under different climate-change scenarios by the year 2100.

Generalist coral species, such as *Porites lobata* and *Acropora hyacinthus*, clearly have inherent traits that allow for range expansion (Figure 1.2). Rare species, by definition, have restricted geographic ranges and are generally considered vulnerable because of their small population size. Although it is well known that populations with low genetic diversity have low adaptive potential, it is unclear how rare, endemic species can survive at all (Birkeland et al., 2013). Yet they do survive! Some rare species are even able to survive through climatic extremes, often in microrefugia (10–100 km^2), while some widespread species perish (Mosblech et al., 2011; van Woesik et al., 2012b). However, classifying species as either generalists or specialists does not capture the spectrum of life-history strategies that exists in

nature. Instead, the extent of the distribution of each species may tell us more about how each species will fare under climate change.

The modeling approach in the present study uses contemporary environmental conditions in which the species are found and the forecasted environmental conditions from Global Climate Models (GCMs). The range in sea-surface temperature (SST) and the range of photosynthetically active radiation (PAR)

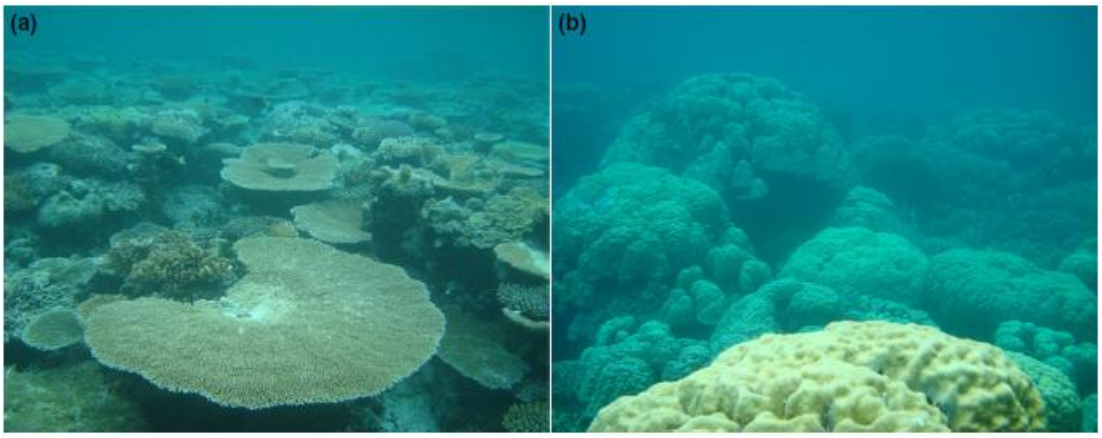

Figure 1.2 **(a)** Tabulate *Acropora hyacinthus* and **(b)** massive *Porites lobata* colonies (Palau). Photos by Rob van Woesik.

were preferred environmental variables because the *range* of both variables influences the scope of aerobic performance, or physiological response (Portner and Farrell, 2008). In addition, "range limits are commonly niche limits", as suggested by Lee-Yaw et al. (2016). Temperature and PAR are used in the present study because thermal stress occurs only when water temperature is outside of the normal

range for an extended period, but only when solar irradiance (or PAR) is high. Thermal stress and coral bleaching is based on the response of coral to both irradiance and temperature; reduce irradiance under high temperature, and the likelihood of coral bleaching is substantially reduced (Takahashi et al., 2004). Therefore, both temperature and irradiance influence photosynthesizing organisms such as corals. Other temperature indices were excluded from this study to (i) avoid collinearity between variables, (ii) because averages do not capture the niche space, and (iii) because the range of SST includes both the minimum and maximum temperatures, thereby increasing model parsimony.

Data from GCMs are generally used for the forecasted environmental conditions. These models are presently coarse grained (1^{o}), and considerable research is aiming toward downscaling the GCMs to align with contemporary environmental variables. The downscaling technique uses in-situ data to refine GCMs, and assumes that the future data will respond similarly. This approach accounts for bias between the in-situ data and the modeled data. Any bias between models and in-situ data is usually overshadowed by intentional deviations of the modeled data from the downscaling operation.

A variety of species distribution models were tested in the present study, including ensemble modeling. We chose not to use the black-box methodology of neural networks, Maxent had pseudo-absence problems, and the area under receiver operating characteristic curve (AUC) scores of Generalized Additive Models were

consistently lower than the Generalized Linear Model. The random forest models yielded higher AUC scores, but the model output showed very pixelated results, increasing the AUC in a hit-miss pixel fashion, and the results looked very unlike what would be expected from a biological system with interconnected habitats. Therefore, this study primarily focused on Generalized Linear Models, using the binomial family of distributions and the logit link function, which was considered the best model for the system of interest. This model was later extended to incorporate a random effect by using a Generalized Linear Mixed Effects Model.

Species-distribution models also assume that the environment constantly selects against unsuitable genotypes. The models however treat each species as a single, homogenous population. The inherent response of phenotypic plasticity is not considered in such models. Moreover, some tropical populations may have an inherent capacity to survive outside of contemporary habitats. Populations with such capacities would have latent genotypes that arm some individuals with an inherent capacity to tolerate non-analogue future environments with ocean warming. Most species-distribution models do not account for adaptive processes of a population to a changing environment (but see Chevin et al. 2010, and Cacciapaglia and van Woesik 2015). Although modeling adaptation is relatively straightforward, empirically determining whether sufficient adaptation will occur by the year 2100 is difficult, especially when it involves disentangling the effects of acclimation, or plasticity, from adaptation.

TURBID REFUGIA

Turbidity can reduce irradiance during temperature-stress events and buffer corals from mortality (van Woesik et al 2012b). Although highly turbid environments often exclude corals completely (Yentsch et al. 2002), and turbidity can reduce irradiance, which reduces reef-accretion rates (Anthony and Fabricius 2000; Edinger et al. 2000; Fabricius and De'ath 2004), turbid environments can also prevent bleaching (Wagner et al 2010). Because coral bleaching is caused by excess irradiance and is exacerbated by high temperature (Brown 1997; Hoegh-Guldberg 1999), turbidity can potentially buffer corals from the combination of high temperature and irradiance, and act as climate refuges. Reducing irradiance during temperature-stress events relieves the symbiont's photosystem, and can prevent corals from bleaching (Warner et al. 1999; Iglesias-Prieto and Trench 1994). Such reductions in irradiance are most common nearshore, where turbidity is elevated (van Woesik et al. 2012a) (Figure 1.3).

Figure 1.3 *Cyphastrea chalcidicum* in turbid nearshore conditions near the entrance to a rivermouth on Palau's western coast. Photo by Rob van Woesik

Turbidity depends on the rate of water movement and on the size of the sediments in the water column. Turbidity is best conceptualized through Stokes's Law (Larcombe and Wolfe 1999). Small particles will stay suspended in moving fluids for longer periods than large particles, and high-velocity fluids can retain more sediments than low-velocity fluids. High-velocity currents are associated with adverse weather conditions but are also a function of tidal amplitude. For example, Maxwell and Henderson (1968) showed that fine sediments were rare on the ocean floor along the inner Great Barrier Reef, where diurnal tidal fluctuations were > 3 m. Consistent water flow perpetually kept fine sediments in suspension. Fine sediments were only apparent on the ocean floor in the leeward of islands, where reefs still were able to accrete (Kleypas 1996; van Woesik and Done 1997). Yet, extremely high and

consistent turbidity, apparent at localities where the diurnal tides were > 6 m along the Great Barrier Reef, caused narrow photic zones and provided limited opportunities for coral growth and reef development (Kleypas 1996; van Woesik and Done 1997). Turbidity was examined in this study to determine if, and where, a reduction in irradiance (high turbidity) would mitigate an increase in sea-surface temperature in the Indian and Pacific Oceans.

REEF CONNECTIVITY

A widely distributed species may appear to be tolerant to a wide-range of environmental conditions, based on its current distribution and the range of environmental conditions across that distribution. Local adaptation, however, will distort the overall tolerance of the population. Local adaptation is not captured by species-distribution models, because the models assume that a widely distributed species can tolerate the *entire* range of the environmental conditions in which it is found. Neglecting local adaptation in species-distribution models unrealistically predicts that the future range of the species is larger than can be realistically expected. For example, species-distribution models predict that some ubiquitous species, such as *Porites lobata,* will increase their distribution under projected climate change scenarios (Cacciapaglia and van Woesik, 2015).

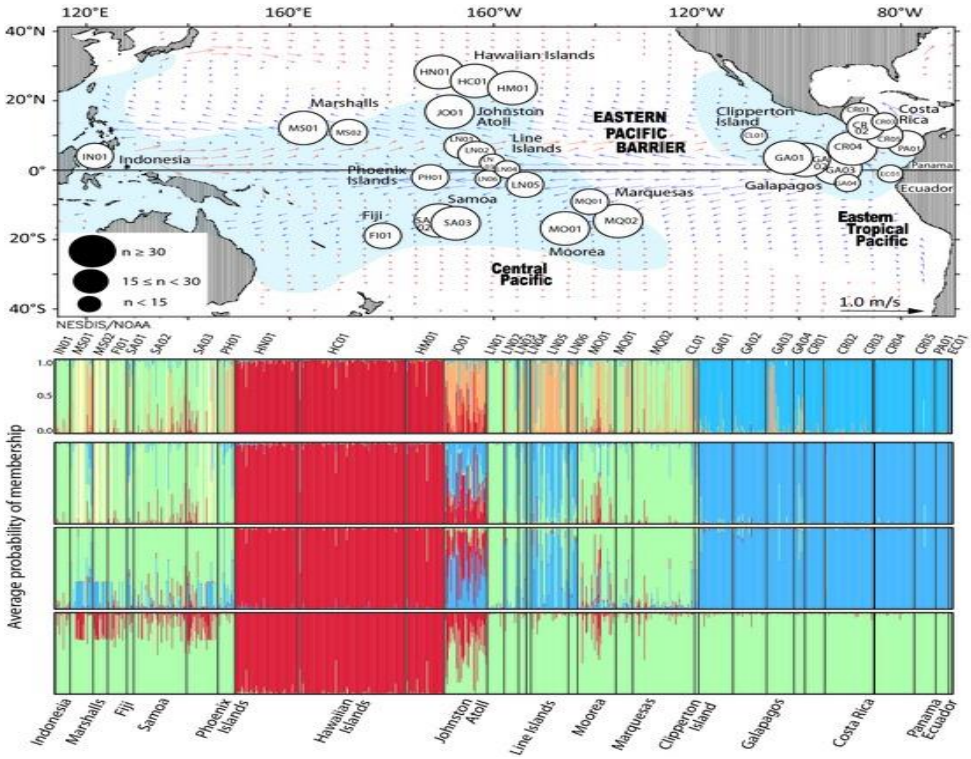

Figure 1.4 Extent of genetic isolation of *Porites lobata* individuals through the Pacific Ocean and Indonesia. Figure from Baums et al. 2012.

Not only is local adaptation not addressed in many species-distribution models, but genetic isolation among widely distributed species is not captured by these models either, although the two are strongly linked. Many species inhabit a wide geographic extent, with some species distributed over millions of km^2. This extent can be so large that in some cases gene flow between some individuals is non-existent. For example, recent genetic studies of *Porites lobata,* a dominant reef-building coral in the Pacific and Indian Oceans, shows four relatively isolated

megaregions (Baums et al. 2012) (Figure 1.4). This lack of long-term genetic connectivity can have major implications when modeling these populations. The present study will examine the assumption of treating populations as genetically isolated regions, and examine the response of the species to climate change under a more realistic model that incorporates genetic isolation of the subpopulations.

REEF-ACCRETION RATES

For a reef to grow, rates of reef accretion must exceed rates of erosion. As the climate warms and land ice begins to melt, sea-level rise will accelerate. The average global rate of sea-level rise has been 1.7 mm yr^{-1} during the 19^{th} century, but since 1993 sea-level rise has been about 2.8 mm yr^{-1} (IPCC 2013). This increase in sea-level rise is not homogenous across the oceans (Figure 1.5), and in some places sea-level rise is increasing faster than in other places, because of differential increases in temperatures, differences in ocean salinities, and differential effects of tectonics and glacial isostatic adjustment.

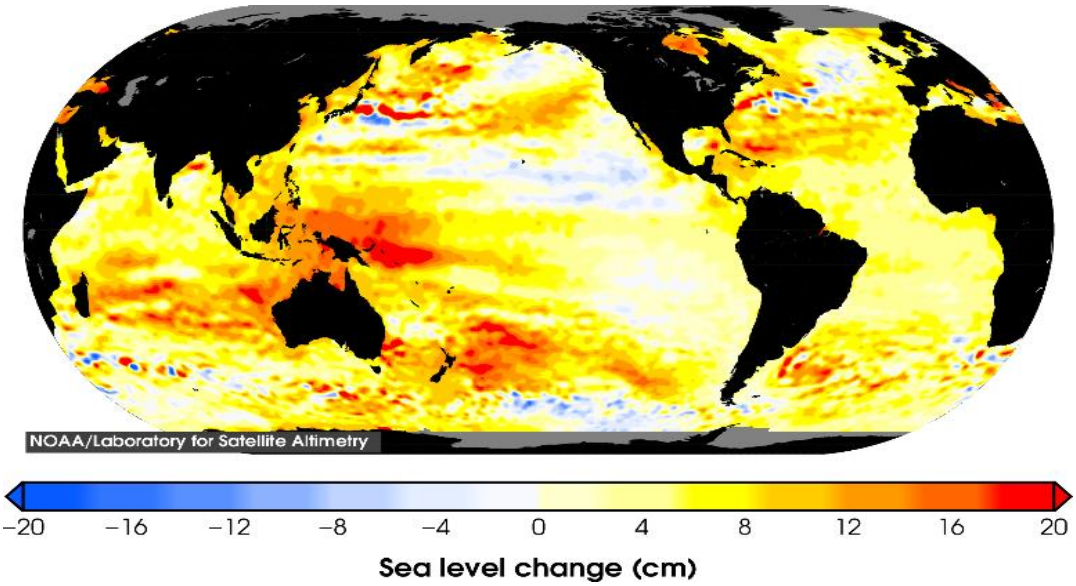

Figure 1.5 Total sea level change since 1993. Map of total sea level change from TOPEX/Poseidon, Jason-1, and Jason-2 between 1993 and 2015. Figure from NOAA Laboratory for Satellite Altimetry.

To maintain access to irradiance, reefs must accrete vertically at a pace fast enough to keep up with sea-level rise. Keeping up with sea-level rise requires reefs to maintain reef-building coral species. Climate change is influencing coral-community composition (Loya et al. 2001), and some localities are losing more species than other localities (Cacciapaglia and van Woesik 2015). This change in composition will likely influence the capacity of reefs to accrete, and therefore to keep up with sea-level rise.

The rates of reef accretion depend on the composition and densities of organisms that are able to accrete calcium carbonate, and on the rates of carbonate erosion (Adey 1978; Davies 1983; Perry et al. 2008; van Woesik 2013). Carbonate

accumulates through the accretion of corals and coralline algae, and erodes by physical (e.g., cyclones), chemical (e.g., ocean acidification), and biological (e.g., fishes, echinoids, and boring infauna) processes (Davies 1983; Edinger et al. 2000; Perry et al. 2008; Perry et al. 2012; van Woesik 2013). Examining the fate of the composition of coral communities, and particularly the fate of reef-building corals, in a spatio-temporal framework, alongside rates of sea-level rise, may provide a first-order approximation of regions where reefs are likely and unlikely to keep up with sea-level rise.

RESEARCH OBJECTIVES

Objective 1: Model the response to ocean warming of a suite of coral species within the Indian and Pacific Oceans to identify the location of potential reef-coral climate refugia. Determine whether widely distributed coral species, are less likely to suffer from ocean warming than narrowly distributed species, and determine how much coral habitat, lost under projected climate change, can be prevented by a 1^{o}C capacity for adaptation by 2100?

Objective 2: Locate turbid areas in the Indo-Pacific region that may mitigate the loss of corals predicted from an increase in sea surface temperature under climate change.

Objective 3: Examine the effect of genetic connectivity on the response of *Porites lobata* to ocean warming.

Objective 4: Identify areas within the Indo-Pacific region that are vulnerable to sea level rise, and areas where reef accretion will likely be able to keep up with sea level rise.

DISSERTATION STRUCTURE

Chapter 1 is an introductory chapter that defines the rationale for the the research questions, and the study objectives, and provides a short review of the literature. This rest of the dissertation includes four main data chapters presented as manuscripts that highlight answers to the above research objectives. Chapter 2 is a species distribution model that identifies climate-change refugia in the Indian and Pacific Oceans, and identifies the response of species to climate change when adaptation is considered. Chapter 3 is a model that highlights where turbidity may mitigate the harmful interaction between light and temperature under future climate scenarios. Chapter 4 incorporates genetic connectivity into a species-distribution model of corals to identify how genetic isolation may influence reef persistence into the future under climate change scenarios. Chapter 5 includes a combined species-distribution model with a reef accretion model identifying where reefs will likely be able to accrete at a

rate fast enough to keep up with predicted sea level rise. The final chapter, Chapter 6, provides a synthesis of the abovementioned chapters.

The manuscripts associated with this study are:

Cacciapaglia, Chris, and Robert van Woesik (2015) Reef-coral refugia in a rapidly changing ocean. *Global Change Biology* 21: 2272-2282

Cacciapaglia, Chris, and Robert van Woesik (2016) Climate-change refugia: shading reef corals by turbidity. *Global Change Biology* 22: 1145-1154

Cacciapaglia, Chris, and Robert van Woesik. (In review) Marine species distribution modeling and the effects of genetic isolation under climate change. *Journal of Biogeography*

Cacciapaglia, Chris, and Robert van Woesik (In prep.) Locating where coral reefs will keep up with sea-level rise in the Indo-Pacific. *Nature Climate Change*

CHAPTER 2. CLIMATE REFUGIA

ABSTRACT

This study sought to identify climate-change thermal-stress refugia for reef corals in the Indian and Pacific Oceans. A species distribution modeling approach was used to identify refugia for twelve coral species that differed considerably in their local response to thermal stress. We hypothesized that the local response of coral species to thermal stress might be similarly reflected as a regional response to climate change. We assessed the contemporary geographic range of each species, and determined their temperature and irradiance preferences using a k-fold algorithm to randomly select training and evaluation sites. That information was applied to downscaled outputs of global-climate models to predict where each species is likely to exist by the year 2100. Our model was run with and without a 1°C capacity to adapt to the rising ocean temperature. The results show a positive exponential relationship between the current area of habitat that coral species occupy and the predicted area of habitat that they will occupy by 2100. There was considerable decoupling between scales of response, however, and with further ocean warming some 'winners' at local scales will likely become 'losers' at regional scales. We predicted that nine of the twelve species examined will lose 24–50% of their current habitat. Most reductions are predicted to occur between the latitudes 5°–15°, in both hemispheres. Yet when we modeled a 1°C capacity to adapt, two ubiquitous species, *A. hyacinthus* and *A. digitifera*, were predicted to retain much of their current habitat.

By contrast, the thermally tolerant *Porites lobata* is expected to increase its current distribution by 14%, particularly southward along the east and west coasts of Australia. Five areas were identified as Indian-Ocean refugia, and seven areas were identified as Pacific-Ocean refugia for reef corals under climate change. All twelve of these reef-coral refugia deserve high-conservation status.

INTRODUCTION

Coral reefs support the world's most diverse marine assemblages, and they provide goods and services for adjacent human populations (Costanza et al. 1997; Costanza et al. 2014). However, rapid climate change is increasing the frequency and intensity of temperature anomalies, and is consequently causing coral mortality and changes to the species composition of many coral reefs worldwide (Loya et al. 2001; Hughes et al. 2003; Hoegh-Guldberg et al. 2007). Indeed, the International Panel on Climate Change (IPCC 2013) has shown that the average ocean surface temperature has increased by 0.11°C (±0.09 to 0.13°C) per decade over the last sixty years. This rate of change is highly likely to increase under a 'business as usual' climate-change scenario, identified as Representative Concentration Pathway (RCP) 8.5 (Figure 1.1, pg2).

The average sea surface temperature is predicted to increase 3.1^{o}C by 2100, under a RCP 8.5 climate-change scenario, if radiative forcing continues to rise, without stabilization and mitigation. Such a rapid rate of ocean warming has been unprecedented in the past several hundred millennia (Hoegh-Guldberg et al. 2007), and some authors suggest that corals on modern coral reefs are at the highest risk of extinction since the Cretaceous-Tertiary mass extinction event, approximately 65 million years ago (Veron 1995; Wood 1999; Veron 2008). Hoegh-Guldberg et al. (2007) even suggested that because corals are already living near their thermal

maximum, further increases in temperatures will most likely lead to local, regional, and even global extinction of many coral species.

THERMAL STRESS

The global models that examine climate-change effects on reef corals rightly express concern that ocean warming will have serious consequences. Yet most global models suggest that few reef corals will survive beyond the 2^{o}C temperature rise predicted for the tropical oceans within the next hundred years (Frieler et al. 2012). Such predictions, however, disagree with field studies of climate-change impacts on coral reefs that show persistence in some regions (Thompson and van Woesik 2009; McClanahan et al. 2011), and persistence in some habitats (van Woesik et al. 2012a). The disagreement between the global models and contemporary field studies is likely a consequence of the global models treating the tropical oceans as homogenous, and the large 'pixel' size of the global models (ranging from ~ 2,500 km^2 to 49,000 km^2), which therefore ignore refugia on coral reefs that are generally found at a local scale of 10-100 km² (van Woesik et al. 2012a).

Thermal stresses have been spatially variable in the oceans in the past, and are likely to be spatially variable in the future (Thompson and van Woesik, 2009). For example, reef corals in Kenya have been subjected to frequent and extreme thermal-stress events, particularly in 1998, which caused extensive coral bleaching and mortality (McClanahan 2004). By contrast, corals on reefs south of Kenya, in

Mozambique and Madagascar, have been subjected to fewer and less extreme thermal anomalies than Kenya (Maina et al. 2008), and have consequently shown less extensive coral bleaching and mortality (McClanahan et al. 2011). Similarly the eastern and central tropical Pacific Ocean, including the Marshall Islands, have experienced frequent (3-5 years) anomalously high temperatures over the last few decades, whereas in Micronesia (Pohnpei, Kosrae, Chuuk, and Yap), west of the Marshall Islands, the anomalously high temperatures have been less frequent (~ 50 years) (Thompson & van Woesik 2009). Still, the western Pacific Ocean has been warming faster than elsewhere (England et al. 2014), and extensive bleaching has been recorded in the coral triangle (Guest et al. 2012), which includes the Philippines and Indonesia, supporting the world's most diverse reefs. Such spatial and temporal variability prompts the critical question: Where are the climate-change refugia? Indeed, one of the most immediate challenges we face with a rapidly changing climate is to predict where coral species are most likely to survive, and then protect those refugia from regional and local impacts.

REFUGIA

Refugia have been defined as areas that will support reef-coral populations, and to which reef corals can retreat to, persist in, and subsequently expand from, under changing environmental conditions (Ashcroft 2010; Keppel et al. 2012). Refugia can be identified by either: 1) examining biogeographic patterns using paleo-proxies

(Mosblech et al. 2011) or genetic markers (Avise 2000), or 2) investigating the processes that are likely to create refugia. The first approach has been useful to examine refugia through glacial and interglacial events (Colinvaux et al. 2002), whereas the latter approach is potentially more useful for identifying contemporary and future refugia, which are a consequence of unprecedented rates of environmental change that are caused by the emissions of greenhouse gases (Keppel et al. 2012).

Refugia can be defined as either macrorefugia or microrefugia (Mosblech et al. 2011). Macrorefugia are commensurate with the regional scales of global climate models, whereas microrefugia usually exist at local scales (van Woesik et al. 2012a). Macrorefugia are viewed as large areas where the current climatic conditions are maintained by the year 2100, and hence will allow organisms to persist without the necessity to rapidly adapt. Microrefugia are similar to macrorefugia, in that they allow organisms to persist under climate change, although they are small pockets, with benign environmental conditions, located in regions that are not necessarily environmentally conducive to species persistence. Although macrorefugia are easier to detect than microrefugia, because microrefugia are limited by the grain size of the environmental and species-presence data, both are of conservation interest (Ashcroft 2010).

We used a species distribution modeling approach to identify macrorefugia in the Pacific and Indian Oceans. First we assessed the contemporary geographic range of a given species, and the climatic envelope within that range. That

information was then combined with downscaled information from global climate models to predict where each species is likely to exist in the future. This study had two main objectives: 1) construct a framework to quantify the range shifts of corals species by the year 2100, using downscaled global-climate models under the 'business as usual scenario', and 2) quantify regions where coral species are most likely to be retained, lost, and gained by the year 2100. Within our model predictions we also included a capacity for species to adapt to thermal stress, which we set at 1ºC change by the year 2100, or a rate of 0.05ºC increase in thermal tolerance per generation for *Acropora* species (van Woesik and Jordan Garza 2011). We hypothesized that the response of the coral species to thermal stress at local scales, of 10–100 km², would be similar to the response of coral species to climate-change related thermal stress at regional scales, of 1000–10,000 km².

MATERIALS AND METHODS

ENVIRONMENTAL PARAMETERS

Sea-surface temperature (SST) data were gathered from Bio-ORACLE (Ocean Rasters for Analysis of Climate and Environment) (http://www.oracle.ugent.be/). Current raster data from Bio-ORACLE was derived from Aqua-MODIS (Moderate Resolution Imaging Spectroradiometer) satellite for the years 2002—2009 (Tyberghein et al. 2012), which were adjusted spatially using bi-linear interpolation to grids of 5 arc minutes (c. 9.2 km). The range of Sea Surface Temperature (SST) values (°C), between the latitudes 37˚N–37˚S, were calculated as the maximum minus the minimum temperature for the 8-year time span at each grid cell. The short, eight-year time frame was used to match the time frame of the Photosynthetically Available Radiation (PAR). PAR (E m^{-2} d^{-1}) data that were derived from Sea-Viewing Wide Field-of-View Sensor (SeaWiFS) (http://gdata1.sci.gsfc.nasa.gov/daac-bin/G3/gui.cgi?instance_id=ocean_month) from 1998—2007. Individual monthly raster files were stacked in a geographic information system QGIS (www.qgis.org), and then imported into R (R Core Team, 2014), where all values greater than zero were used to determine the range for the 10 years. The grid size of PAR was in 5 arcmin (c. 9.2 km). A shapefile of depth was made using NOAAs bathymetric database in R with the getNOAA.bathy function in the 'marmap' package. This shapefile was used to mask out all depths greater than 20 m, at least for the present analysis to get a sense of shallow-reef response.

CORAL DISTRIBUTIONS

We examined the global distribution of reefs using ReefBase (www.reefbase.org). Shapefiles of reefs were downloaded to QGIS and used as the base layer. We examined the distribution of twelve coral species that were found in the Indian and Pacific Oceans using Veron (2000), IUCN's Red List http://www.iucnredlist.org/technical-documents/spatial-data, and Wallace (1999). The twelve species were selected based on their long-term response to a major thermal stress in Okinawa, Japan (Loya et al. 2001; van Woesik et al. 2011). Long-term 'winners' (van Woesik et al. 2011) on the reefs of Okinawa were: 1) *Acropora digitifera,* 2) *Acropora hyacinthus,* 3) *Goniastrea aspera,* and 4) *Porites lobata* (Figure 2.2). Coral species that did not appear to change in abundance were: 5) *Cyphastrea chalcidicum*, 6) *Dipsastraea speciosa*, 7) *Favites halicora*, and 8) *Leptastrea pruinosa.* Long-term 'losers' on the reefs of Okinawa were: 9) *Porites horizontalata,* 10) *Montipora aequituberculata,* 11) *Seriatopora hystrix,* and 12) *Stylophora pistillata* (Table 2.1). We hypothesized that the response of the coral species to thermal stress on the local reefs of Okinawa might be similarly reflected as a regional response to climate change.

The distributions of all twelve coral species were recorded as either present or absent within the ecoregions defined by Veron et al. (2009). Presence points were randomly selected from the reefs within 'ecoregions' (*sensu* Veron et al. 2009) that allegedly supported each coral species. Absence points were selected from

ecoregions from which we were 95% certain the coral species of interest was absent. These certainties were determined using a probability-of-detection algorithm at depths less than 20 m. Constraining the depth of the species absence points allowed specific determination of the environmental parameters that were most likely affecting each particular species. We extracted both the range of sea surface temperature and the range of photosynthetically available radiation from the raster files to characterize the environmental 'climate' where the species were present, and where the species were absent (N = 3000 points, at grid cells of 9.2 km). The environmental data points were weighted by the number of 'ecoregions' in which each species was either present or absent.

SPECIES DETECTABILITY

To estimate the probability that a species was truly absent from a particular ecoregion (Veron et al. 2009) in which it was not detected, we used all available coral-related published studies as a proxy for sampling effort. The likelihood of finding a species in an ecoregion was assumed to be greatest on the first survey, with an increased likelihood of a species being truly absent from a particular ecoregion on subsequent surveys. These likelihoods were expressed as a geometric distribution, as follows:

$$P_i = 1 - (1 - p_i)^{n_i+1} \qquad (1),$$

where P is the probability that a species was absent from ecoregion i, p is the probability of detection within the ecoregion, and n is the sampling effort in

ecoregion *i*. In this context, sampling effort relates to the number of failures in detecting a species and the probability of detection (*p*), which is dependent on the size of the ecoregion, and the number of adjacent ecoregions supporting the species. We also assumed that as the size of an ecoregion increases, the probability of detection decreases, as follows:

$$S_i = \left(\frac{minsize}{size_i}\right)^4 \quad (2),$$

where for ecoregion *i,* S_i an ecoregion-size ratio, *minsize* is the size of the smallest ecoregion, and $size_i$ is the size of the ecoregion of interest, and 4 is a scaling constant. The probability of a false negative should also theoretically increase as the number of adjacent regions supporting a species increases. The adjacency relationship was considered as follows:

$$Adj_i = 0.6^{a_i} \quad (3),$$

where *Adj* is the adjacency relationship for ecoregion *i*, and *a* is the number of adjacent ecoregions. This relationship decreases the detection probability by 40% for each adjacent ecoregion containing the species. Incorporating size (S_i) and Adjacency (Adj_i) into our probability of detection (p_i) allowed us to determine the probability that a particular species of interest was found, given our estimated detection probability, and the sampling effort. Credible intervals were estimated to determine the likelihood that a species was truly absent in a given ecoregion by rearranging the geometric cumulative distribution function as follows:

$$n_i = \left(\frac{\log(1-.95)}{\log(1-p_i))} - 1\right) \quad (4)$$

where n_i is the sampling effort in ecoregion i required to achieve a 95% probability of observing a success, with the given detection probability p for ecoregion i. A confidence ceiling was calculated because the probability of finding a new species tapers off and reaches an asymptote within increased sampling. The ceiling was accomplished by using the maximum sampling effort of all ecoregions (n_i), in the cumulative distribution function (P_i), from equation 1, to limit P_i. The relationship between observed failures and the ceiling was expressed as:

$$Pf_i = \frac{P_i}{maxP \cdot P_i} \quad (5),$$

where Pf_i is the probability that the species is truly absent from an ecoregion (i), in which it was not detected (including a ceiling), P is the probability that the species was absent from an ecoregion in which it was not detected (not including a ceiling), and $maxP$ is the ceiling.

RIVER BUFFERING

The 12 largest tropical river outflow areas were masked out in accordance with the size of the drainage basins, following the function Distance from river mouth= 3992.7268*dbasin$^{.2735}$)/1000 where dbasin is the size of the drainage basin in km^2 .

SPECIES-DISTRIBUTION MODEL

We used a logistic regression model to predict the coral species using the logit-link function and a binomial error distribution, as follows:

$$y_i = log(p_i/1\text{-}p_i) = b_o + b_1x_i + b_2z_i + b_3x_i.z_i + e_i \qquad (6),$$

where y_i was the observed binary response (presence or absence) at site i, p was the probability of presence, and $(1-p)$ was the probability of absence, x_i and z_i were the explanatory environmental variables at site i, and e was the binomial error term. We used a k-fold algorithm (in the R package 'dismo', Hijmans et al 2013) to randomly select training and evaluation sites, which created a vector that assigned each row in the data matrix to a group between 1 to k. Both presence and absence data were partitioned and used for training (80%) and testing (20%). The k-fold algorithm was repeated 100 times, and the model run that recorded the highest Area under the Receiver Operating Characteristic Curve (AUC) was subsequently used for further analyses. To increase sensitivity (i.e., the true positive fraction) and specificity (i.e., the true negative fraction), we used a threshold where the sum of the sensitivity and specificity was highest. Values above the threshold were transformed to presence values (1), and values below the threshold were transformed to absence values (0). We then used the AUC to describe the relationship between the correctly predicted presences (sensitivity), and the incorrectly predicted absences (1-specificity). AUC values close to 1 suggested that the sites that were predicted to have high suitability were also sites where the species of interest was present.

Similarly, sites that were predicted to have low suitability were also sites where the species of interest was absent. An AUC of 0.5 suggested that the predictions were no better than random.

CONSTRAINTS AND MASKS

Geographical masks were designed to eliminate false negatives, without lowering the credibility of the model. Four masks were applied to the model outputs. First, a mask was applied to constrain dispersal, limiting the potential range of dispersion to no more than a conservative 10 km per year beyond the contemporary range of each coral species (Miller and Munday 2003; Shanks et al. 2003). The dispersal mask coupled the logistic model with contemporary spawning (van Woesik 2010) and genetic studies (Ayre and Hughes 2000), which show evidence of high local retention of larvae. The dispersal mask also realistically restricted potential dispersal capacity under ocean warming (O'Connor et al. 2007; Figueireo et al. 2014). To implement the dispersal mask, all longitudes outside of 5°N or 5°S (*c.* 550 km) of the sampled presence points were masked from the model. Second, to focus on shallow-reef systems, all coral reefs greater than 20 m were masked out. Third, because freshwater causes coral mortality, the 12 largest subtropical and tropical river outflow areas were masked out depending on the size of their drainage basins (see supplementary document for details). Fourth, localities that experienced temperatures < 18ºC, for any time of the year, were masked out of all model runs because reef corals are

unlikely to survive temperatures below 18ºC for more than three months (Veron 1995), and reef accretion is unlikely below these temperatures (Kleypas 1999).

PREDICTIONS

After training the model and verifying the outputs with AUC scores, the models were run using future sea-surface temperatures, while keeping photosynthetically available radiation constant. The mask constraining the corals to a minimum temperature of 18°C was modified in accordance with the 'business as usual' RCP 8.5 climate-change scenario. The SST data that is predicted to occur by 2100 data was downloaded from http://www.oracle.ugent.be/download.html; this data stemmed from the World Climate Research Programme Coupled Model Intercomparison Project (WCRP CMIP3) multi-model database (http://esg.llnl.gov:8080/index.jsp) for A2 (>800 ppm until 2100), and was calculated using predicted values from 2087-2096. The data were adjusted spatially using bi-linear interpolation to grids of 5 arc minutes (c. 9.2 km), which was the same grid size as the present SST data.

We were particularly interested in comparing the contemporary estimates of habitat occupancy of each species with the predicted estimates of habitat occupancy by the year 2100. The coarse-grained (9.2 km) grid tended to over-estimate occupied reef area, and therefore the estimates of habitat occupancy are merely relative estimates that are most useful for comparative purposes between current and future

occupancy, and should not be used as estimates of absolute reef area. The highest AUC value from each of the 100 *k*-fold outputs was chosen to run each model. This procedure was repeated 25 times for each species to quantify the uncertainties as confidence intervals for each distribution, and for predicted changes in distributions through time. An adaptation scenario was also incorporated into the future model by reducing the predicted 2100 thermal range by 1ºC, which was an approximately 0.012ºC range increase per year, or, for an *Acropora*, amounted to approximately 0.05 ºC range increase per generation (van Woesik and Jordan Garza 2011).

Table 2.1 Contemporary estimates of relative-habitat occupancy of twelve coral species in the Pacific and Indian Oceans, and changes in relative-habitat occupancy by 2100. The coarse-grained (9.2 km) grid tended to over-estimate occupied reef area, and therefore the estimates of habitat occupancy are merely relative estimates that are useful for comparative purposes, and should not be used as estimates of absolute changes in coral-reef area. This table depicts: (1) Area under the Receiver Operating Characteristic Curve (AUC) scores, (2) change in relative-habitat occupancy between current and future models, and (3) significance of environmental conditions for the model runs. The 'Current habitat' indicates the relative area of habitat (using the 9.2 km coarse grid) in which the coral species will be found in 2014. 'Future habitat' is the predicted habitat occupancy in the year 2100. 'Lost habitat' is the relative area of habitat that is predicted to be lost by 2100. 'New habitat' is where the species currently does not occur, but will likely occur and occupy habitat in the year 2100. SST and PAR range (Pr(>|z|)) indicates significance (*) of the environmental parameters in the model. Percentage habitat change is either positive (+) or negative (-), which is the difference between the present species habitat occupancy, and the habitat occupancy predicted by the model by 2100. All ± signs are 95% confidence intervals.

Species	**Coral Morphology**	**AUC**	**Current Habitat km²**	**Lost Habitat km²**	**New Habitat km²**	**SST range (*Pr(>|z|)*)**	**PAR range (*Pr(>|z|)*)**	**SST:PAR interaction (*Pr(>|z|)*)**	**Percentage Habitat Change**
Porites lobata	Massive	0.98	5,148,364 ±76,503	29,135 ±5,194	747,486 ±30,178	0.157	0.888	0.072	+14% ±0.7%
Stylophora pistillata	Branching	0.80	4,754,730 ±159,862	392,493 ±55,460	331,273 ±33,537	<.001*	0.004*	<.001*	+0.6% ±0.8%
Montipora aequituberculata	Foliose	0.81	4,831,538 ±64,630	372,734 ±21,363	316,671 ±24,267	0.016*	0.015*	0.001*	+0.2% ±0.6%
Goniastrea aspera	Massive	0.93	4,536,698 ±107,342	1,506,761 ±109,669	383,517 ±14,288	0.190	<.001*	0.014*	-24% ±3.1%
Favia speciosa	Massive	0.77	3,794,371 ±281,193	1,429,924 ±170,181	416,221 ±56,388	0.644	0.020*	0.285	-25.9% ±6%
Favites halicora	Massive	0.92	4,367,782 ±105,582	1,607,213 ±89,007	360,343 ±14,175	0.004*	0.029*	0.853	-27.6% ±2.8%
Acropora hyacinthus	Tabulate	0.98	4,418,005 ±83,431	1,633,415 ±76,707	342,701 ±12,198	0.672	<.001*	0.003*	-28.1% ±2.3%
Cyphastrea chalcidicum	Encrusting	0.95	4,366,384 ±106,755	1,639,216 ±104,426	365,462 ±16,010	0.001*	0.030*	0.852	-28.3% ±3%
Acropora digitifera	Branching	0.96	4,295,530 ±110,146	1,709,384 ±84,191	343,369 ±13,594	0.576	<.001*	0.007*	-30.6% ±2.8%
Seriatopora hystrix	Branching	0.97	4,190,195 ±118,109	1,704,489 ±72,177	306,614 ±12,810	0.095	<.001*	0.045*	-31.7% ±2.4%
Leptastrea pruinosa	Encrusting	0.93	4,090,089 ±123,979	1,743,593 ±79,780	323,801 ±12,357	0.039*	0.038*	0.173	-33.1% ±2.6%
Porites horizontalata	Branching	0.96	2,805,764 ±27,586	1,794,596 ±14,343	295,357 ±4,871	<.001*	0.484	<.001*	-50% ±0.8%

RESULTS

CHANGES IN SPECIES DISTRIBUTIONS

The logistic regression model showed that the range of photosynthetically available radiation (PAR) was a significant predictor of the distribution ($p<0.05$) of ~80% of the selected twelve coral species, whereas sea surface temperature (SST) was a significant predictor of only ~50% of the twelve coral species in this study (Table 2.1). The interaction between SST and PAR was a significant predictor of 60% of the corals (Table 2.1). The model showed that the ubiquitous, reef-crest dwelling tabulate coral *Acropora hyacinthus* is predicted to lose 28 % (±2.3%) of its current habitat by 2100 (Figure 2.1a, Table 2.1). Most of the loss is predicted to occur in the Philippines, Indonesia, Papua New Guinea, the northern Great Barrier Reef, and along the southern Japanese archipelago (Figure 2.1a). Yet with a 1^{o}C potential to adapt, which is approximately 0.05°C per generation, *A. hyacinthus* is expected to only lose 5.6% (±1.8%) of its current reef habitat (Figure 2.1b). Similarly for the dominant Indo-Pacific coral *Acropora digitifera*, the model predicted that the species will lose 31% (±2.8%) of its reef habitat by 2100 (Figure 2.1), but with a 1^{o}C potential to adapt, *A. digitifera* will only lose 5.9% (±1.6%) of its current habitat.

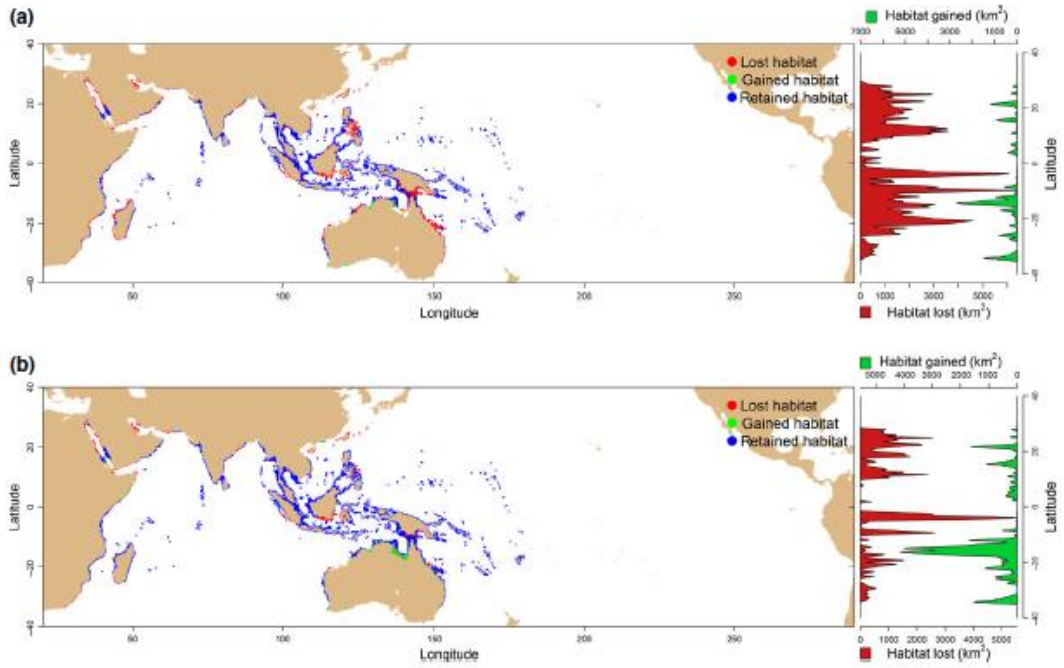

Figure 2.1 *Acropora hyacinthus*. (a) Predicted lost (red), gained (green), and retained (blue) habitat under a 'business as usual' RCP 8.5 climate-change scenario in 2100; (b) Predictions for the habitat changes by 2100 with a 1ºC adaptation under a 'business as usual' RCP 8.5 climate-change scenario.

Our results also suggest that *Porites lobata* will gain approximately 14% (±0.7%) new habitat (Table 2.1), and is expected to extend its global distribution by 2100 (Figure 2.2), particularly into southeastern and southwestern Australia, and southern Japan. *Stylophora pistillata* and *Montipora aequituberculata* are predicted to maintain their occupied habitat by 2100 (Table 2.1*)*. *Goniastrea aspera* is predicted to lose about 24% (± 3%) of its current habitat. *Dipsastraea speciosa and Favites halicora* are predicted to lose around one fourth of their current habitat, whereas *Cyphastrea chalcidicum, Seriatopora hystrix,* and *Leptastrea pruinosa* are

all predicted to lose between to 28% and 33% of their current habitats (Table 2.1). The most extreme loss is predicted for the branching *Porites horizontalata* with 50% loss of habitat (Table 2.1). There was a significant ($p < 0.001$) positive exponential relationship between the current area of habitat that coral species occupy and the predicted area of habitat that will be occupied by 2100 (Figure 2.3).

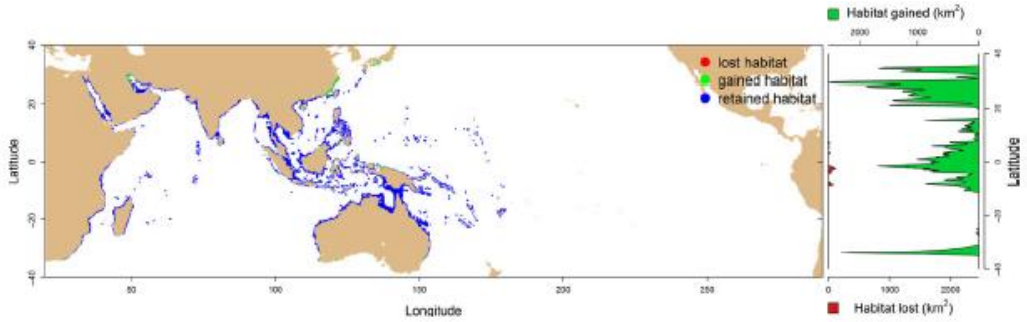

Figure 2.2 *Porites lobata.* Predicted lost (red), gained (green), and retained (blue) habitat under a 'business as usual' RCP 8.5 climate-change scenario in 2100.

REFUGIA

The present study identified areas where current climatic conditions are likely to be maintained by the year 2100. Five areas were identified as climate-change refugia for reef corals in the Indian Ocean: (i) south western Madagascar, (ii) the Maldives, (iii) the Chagos Archipelago, (iv) Western Australia, and (v) the Seychelles. Seven areas were identified as climate-change refugia for reef corals in the Pacific Ocean:

(vi) northern Indonesia, (vii) Micronesia, (viii) the northern Marshall Islands, (ix) the southern Great Barrier Reef, (x) the Solomon Islands, (xi) Vanuatu, and (xii) French Polynesia (Figure 2.3). Taken together, the predicted change in the spatial distribution of the twelve coral species, showed considerable fragmentation, and a particularly high loss of coral species richness between the latitudes 5–15^{o} in both hemispheres (Figure 2.3; for a detailed, global perspective, of the predicted changes by 2100 see the Google Earth Refugia.kmz file in the online supplementary files).

DISCUSSION

LATITUDINAL SHIFTS

Over the next 85 years, thermally sensitive coral species, such as *Acropora hyacinthus,* will most likely lose up to 26–30% of their current habitat because of higher sea surface temperatures. Most reductions in habitat are predicted to occur between the latitudes 5°–15°, in both hemispheres, particularly in the Philippines, southern Indonesia, and Papua New Guinea. Other habitat reductions will likely occur along the northern Great Barrier Reef, the Red Sea, and along the reefs of eastern Africa. By contrast, the global increases in minimum temperature at high latitudes are predicted to expand the latitudinal extent of several species to places that were previously considered too cold for coral growth.

The results in the present study largely agree with other studies on range expansion 'out-of-the-tropics', including the study by Baird et al. (2012) that showed the southern expansion of four *Acropora* species along the east coast of Australia. This southern expansion will likely continue until corals become light limited at high latitudes. The most unexpected result of the present study was the lack of northward expansion of several species along the western Pacific Ocean, particularly along the Japanese islands by 2100. The results of our model contrast with the recent study by Yamano et al. (2011) that showed northern range expansion of *Acropora hyacinthus* over the last two decades along the main islands of Japan. The differences in the modeled results and the results by Yamano et al. (2011) maybe a consequence of the

difference in the time frames of the studies. While Yamano showed range expansion from 1988 to 2010, the global climate models show extreme temperature ranges around the Japanese islands by 2100 (Figure 2.1), which may preclude temperature sensitive *Acropora hyacinthus* and *A. digitifera* from the northern Japanese islands (Figure 2.3a). The modeled results suggest that the recent northern expansion of reef corals along the Japanese islands may be, therefore, short-lived. Indeed, Veron (1992) showed considerable turnover in species composition on the northernmost reefs of Japan over the last 6000 years. Alternatively, the modeled results in the present study may miss the fine-grained microrefugia where *Acropora* species might persist in the northern Japanese islands in 2100.

More disturbing, perhaps, is the prediction that some Indo-Pacific *Acropora* species, at least the *Acropora* species that were analyzed in the present study, will not be able to live in parts of the tropics. Particularly striking is the predicted change in the spatial distribution of coral species richness, and the projected heterogeneous nature of that richness between the latitudes 5^{o}–15^{o}, in both hemispheres (Figure 2.3). If, however, thermally sensitive corals, such as *A. hyacinthus,* are able to adapt to a 1^{o}C increase in temperature, over the next 85 years, the predictive model shows limited habitat loss. Yet, whether these species can adapt to rapid climate change is still an open question.

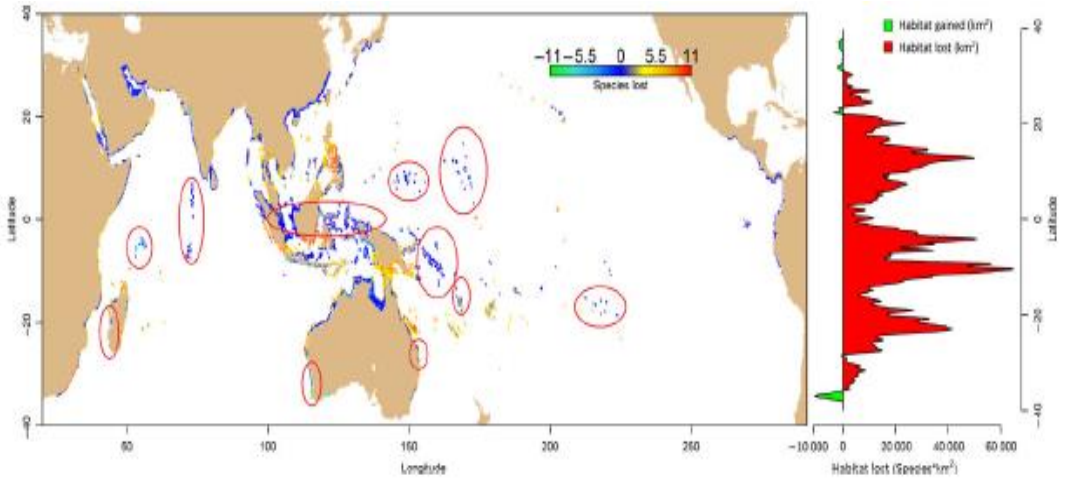

Figure 2.3 Spatial distribution of the 12 coral species examined in the present study in the coral triangle in 2014 compared with the predicted spatial diversity of the 12 coral species examined in 2100 under a 'business as usual' RCP 8.5 climate-change scenario. The red circles highlight the predicted macrorefugia.

SPECIES TRAITS

The vulnerability of a coral species to increasing thermal stress is a combination of the duration and intensity of thermal exposure, and the inherent sensitivity of the species (Moritz and Agudo 2013). Some coral species are invariably resistant to thermal stress, whereas other coral species are sensitive to thermal stress, and are being lost from regional-reef systems (Loya et al. 2001). Still other coral species are physiologically sensitive to thermal stress in the short term, yet their ubiquitous distribution and high fecundity allows rapid recovery, and hence persistence over the long term. We hypothesized that the response of coral species to thermal stress at local scales, using isolated field studies, might be similarly reflected as a response to

climate change at regional scales. We showed, instead, considerable decoupling between scales of response, and that some 'winners' at local scales are likely to be 'losers' at regional scales. For example, ten years after a thermal stress event on Okinawa the long-term 'winners' were *Acropora digitifera, Acropora hyacinthus, Goniastrea aspera,* and *Porites lobata* (van Woesik et al. 2011). The present study showed that *Porites lobata* is likely to be one of the few long-term 'winners' under further ocean warming.

At a time of much warmer oceans than today (~ 10ºC warmer on average), during the Eocene (56 – 34 million years before present), (Zachos et al. 2001), coral reefs supported mainly encrusting and massive coral colonies, and supported few multiple-branched coral colonies (Coates and Jackson 1985; Budd et al. 1992). Recent studies have also shown that branching coral morphologies are more susceptible to thermal stresses than massive and encrusting colonies (Loya et al. 2011; McClanahan 2004). The results in Table 2.1, however, do not conform to the conventional paradigm that all encrusting and massive colonies should survive in preference to branching corals, at least by 2100. For example, the present study predicted that the branching coral *Stylophora pistillata* will maintain its distribution, whereas some massive faviids are predicted to lose up to 28% of their current habitat (Table 2.1). The shift away from the conventional coral-morphology paradigm in the present study may be a consequence of numerous factors, including inherent

differences in life-history traits other than morphology, and potentially a latent effect of analyzing widely distributed species.

ADAPTATION AND PERSISTENCE

Recent genetic studies have shown that the widely distributed corals *Pocillopora, Stylophora,* and *Seriatopora* in the Indian and Pacific Oceans have geographically restricted haplotypes, which suggests local adaptation, and minimal gene flow between some clades across oceanic regions (Foresman, 2013). In the present study, we characterized the environmental conditions in which the present-day species were located, which we assumed reflected their environmental tolerance (i.e., their fundamental niche). These environmental conditions were then used to estimate the potential distribution of the coral species under climate change. The most obvious, overarching trend in our study was the significant ($p < 0.001$) positive exponential relationship between the current area of habitat occupancy and the predicted area of habitat occupancy by 2100 (Figure 2.3). The results suggest that widely distributed species will lose relatively less area than geographically restricted species. Yet, local adaptation is not captured by species distribution models, because the models assume that a widely distributed species can also tolerate the entire range of the environmental conditions in which it is found. Although a broad geographic distribution does not necessarily render the entire population tolerant to a wide array of global temperature changes, and does not guarantee immunity to regional

extinction (van Woesik et al. 2012b), geographic ubiquity does suggest that portions of a widely distributed species might have an inherent capacity to adapt to climate change. Recent studies have shown that the most vulnerable species to climate-change forcing are environmentally sensitive, stenotopic coral species (cf. Vaughan 1919, Burman et al 2012). For example, the loss of stenotopic corals from many reefs has left the eurytopic, generalist species as the dominant corals on most contemporary Floridian reefs. The transition in dominance from stenotopic to eurytopic coral species, mirrors similar transitions elsewhere in the Caribbean, both in recent decades and in the geologic past (Edinger and Risk 1994). However, in a recent study, van Woesik et al. (2012b) showed that vulnerability to changing climates in the past was largely attributed to species traits, and was not simply a function of geographic distribution in the Caribbean.

Generalist coral species clearly have inherent traits that allow for range expansion. Is the issue then simply that only generalists will tract with climate-change temperatures? Rare species, by definition have restricted geographic ranges, and are generally considered 'vulnerable' because of their small population size. Some rare species are even able to survive through climate extremes, often in microrefugia (10–100 km^2), whereas some widespread species perish (Mosblech et al. 2011; van Woesik et al. 2012b). For example, in a recent study in Palau, corals on nearshore reefs bleached less and suffered lower mortality than corals on patch reefs and outer reefs, even though the temperatures nearshore were higher than elsewhere.

A higher than average vertical attenuation of light, caused by naturally high suspended particulate matter, appeared to buffer the local nearshore corals from thermal stress. Such microrefugia are often lost using the predictions from coarse-grain global climate models (Donner et al 2009; van Hooidonk et al. 2013), and such microrefugia were not 'captured' in the present study.

DEEP-REEF REFUGIA

Mesophotic reefs, between 30 and 150 m, are also considered to be important refugia for shallow reefs (Riegl and Pillar 22003). Although we did not consider deep, mesophotic reefs as refugia in the present study, there are several caveats when assuming that mesophotic reefs will act as shallow-reef refugia. For example, there was a recent discovery of large stands of *Seriatopora hystrix* at 35-45 m (Sinniger et al. 2013) near the Okinawan study site (Loya et al. 2011), mentioned above. Although these corals are extensive on the mesophotic reefs, *Seriatopora hystrix* was not recorded on the shallow reefs for over 10 years (van Woesik et al. 2011). Similarly, van Oppen et al. (2011) showed clear genetic differences between shallow and deep *Seriatopora hystrix* populations on the Great Barrier Reef, but showed homogenous, genetic populations across the shallow and mesophotic reefs in Western Australia. Therefore, the existence of adjacent mesophotic reefs does not directly infer larval connectivity with shallow reefs (see also Serrano et al. 2014). Considerable work needs to be done to firstly map mesophotic reefs adjacent to

shallow coral reefs, secondly to determine the extent of genetic connectivity between the mesophotic reefs and the adjacent shallow reef-coral populations, and thirdly to identify microrefugia.

In conclusion, the present study identified twelve climate-change macrorefugia, which we define as areas that will support reef-coral populations, and to which reef corals can retreat to, persist in, and subsequently expand from, under a 'business as usual' climate-change scenario, identified as Representative Concentration Pathway (RCP) 8.5, that is expected by 2100. In the Indian Ocean, reef-coral climate-change refugia were identified in south western Madagascar, the Maldives, the Chagos Archipelago, Western Australia, and the Seychelles. In the Pacific Ocean, climate-change refugia were identified in northern Indonesia, Micronesia, the northern Marshall Islands, the southern Great Barrier Reef, the Solomon Islands, Vanuatu, and French Polynesia. All twelve reef-coral refugia need protection from local and regional disturbances and land-use change, and they clearly deserve the highest conservation status because they may be the only locations where modern coral reefs can survive climate change.

CHAPTER 3. TURBID REFUGIA

ABSTRACT

Coral reefs have recently experienced an unprecedented decline as the world's oceans continue to warm. Yet global climate models reveal a heterogeneously warming ocean, which has initiated a search for refuges, where corals may survive in the near future. We hypothesized that some turbid-nearshore environments may act as climate-change refuges, shading corals from the harmful interaction between high sea-surface temperatures and high irradiance. We took a hierarchical Bayesian approach to determine the expected distribution of 12 coral species in the Indian and Pacific Oceans, between the latitudes 37°N and 37°S, under Representative Concentration Pathway 8.5 (W m^{-2}) by 2100. The turbid-nearshore refuges identified in this study were located between latitudes 20–30°N, and 15–25°S, where there was a strong coupling between turbidity and tidal fluctuations. Our model predicts that turbidity will mitigate high temperature bleaching for 9% of shallow reef habitat (to 30 m depth) — habitat that was previously considered inhospitable under ocean warming. Our model also predicted that turbidity will protect some coral species more than others from climate-change associated thermal stress. We also identified locations where consistently high turbidity will likely reduce irradiance to < 250 μmol m^{-2} s^{-1}, and predict that 16% of reef-coral habitat $\leq$ 30 m will preclude coral growth and reef development. Thus, protecting the turbid-nearshore refuges identified in this study, particularly in the northwestern Hawaiian Islands, the

northern Philippines, the Ryukyu Islands (Japan), eastern Vietnam, western and eastern Australia, New Caledonia, the northern Red Sea, and the Arabian Gulf, should become part of a judicious global strategy for reef-coral persistence under climate-change.

INTRODUCTION

Coral reefs are one of the world's most diverse and valuable marine ecosystems (Moberg and Folke 1999; Cesar 2003). A rapidly changing climate, however, has increased the frequency and intensity of thermal anomalies in the subtropical and tropical oceans (IPCC 2013). These events have led to widespread coral mortality, and to changes in coral-community composition (Loya *et al.,* 2001; Hoegh-Guldberg *et al.,* 2007; Pandolfi *et al.,* 2011). The Intergovernmental Panel on Climate Change (IPCC) reported in 2013 that the average global ocean temperature will likely increase 3 degrees by 2100, and some studies suggest that this increase in temperature will be outside the physiological range of most coral species (Hoegh-Guldberg *et al.,* 2007, Frieler *et al.,* 2013). Yet the heterogeneously warming ocean has instigated a search for refuges, where corals may survive in the near future.

Sea-surface temperatures (SSTs) and irradiance are the two most important factors determining where scleractinian corals grow (Darwin 1842). The physiological susceptibility of corals to climate-change-related stress is also dependent on the tolerance of both the corals (Baird *et al.,* 2009) and their symbionts to the combination of high SSTs and high irradiance (Warner *et al.,* 1999; Takahashi *et al.,* 2004). High-seasonal SSTs and high-irradiance intensity can lead to the over reduction of the photosynthetic reaction centers in coral symbionts, producing harmful photosynthetic byproducts, including oxygen radicals, which damage both the symbionts and the coral host (Iglesias-Prieto and Trench 1992; Iglesias-Prieto

and Trench 1994). Prolonged, elevated SSTs, during periods of high-seasonal irradiance, can lead to chronic photoinhibition and to the loss of symbiotic dinoflagellates, which leads to coral bleaching (Brown 1997; Hoegh-Guldberg 1999). Coral bleaching can be temporary, from which some species recover (Warner *et al.,* 1999), or can be fatal, especially for coral species that depend heavily on their symbionts.

Reducing irradiance during temperature-stress events relieves the symbiont's photosystem, and can prevent corals from bleaching (Warner *et al.,* 1999; Iglesias-Prieto and Trench 1994). Such reductions in irradiance are most common nearshore, where turbidity is elevated (Anthony *et al*. 2004; Anthony and Connolly 2004; van Woesik *et al.,* 2012). In a recent study of a thermal-stress event in Palau, coral bleaching was lowest on turbid nearshore reefs, although the SSTs were higher nearshore than on neighboring reefs where coral bleaching and mortality was extensive (van Woesik *et al.,* 2012). Similarly, corals on the warm, turbid nearshore reefs of Florida did not bleach as extensively in 2005 as corals on the warm, yet clear-water outer reefs of Florida (Wagner *et al.,* 2010). In both localities, turbidity appeared to relieve the corals from high irradiance stress, through shading, during periods of anomalously high SSTs.

The main objective of this study was to identify turbid nearshore environments in the Pacific and Indian Oceans that may act as climate-change

refuges, shading corals from the harmful interaction between high sea-surface temperatures and high irradiance. Secondary objectives were to (i) predict species-specific differences in coral responses to climate-change, (ii) to identify locations where consistently high turbidity will likely reduce irradiance to < 250 μmol m^{-2} s^{-1}, thus precluding reef-coral habitat, and (iii) determine whether the purported turbid refuges were a consequence of ephemeral pulses in ocean productivity, or stable refuges that were tidally driven.

METHODS

REEFS AND CORALS

The global distribution of coral reefs was used as a base layer for all analyses using the shapefiles from ReefBase (www.reefbase.org). Reef shapefiles were imported into R (R Core Team, 2014) using the package 'rgdal' (Bivand *et al.,* 2014). Coral reefs in the Indian and Pacific Oceans of depths < 30 m were extracted from the NOAAs bathymetric database in R, with the getNOAA.bathy function in the 'marmap' package (Pante and Simon-Bouhet 2013), and stored as a raster file with a 1-minute resolution. The data were buffered and resampled to 9.2 km resolution, which was commensurate with the environmental variables used in this study (see below).

Twelve Indo-Pacific coral species were examined for responses to ocean warming, irradiance, and different turbidity regimes. The 12 coral species were selected based on their short-term response to thermal stress (Loya *et al.,* 2001), which included six thermally tolerant species: 1) *Coelastrea aspera,* 2) *Porites lobata,* 3) *Cyphastrea chalcidicum*, 4) *Dipsastraea speciosa*, 5) *Favites halicora*, and 6) *Leptastrea pruinosa;* and six thermally intolerant species: 7) *Porites horizontalata,* 8) *Montipora aequituberculata,* 9) *Acropora hyacinthus,* 10) *Acropora digitifera,* 11) *Seriatopora hystrix,* and 12) *Stylophora pistillata* (*Coelastrea aspera* and *Dipsastraea speciosa* were previously referred to as *Goniastrea aspera* and *Favia speciosa* in Cacciapaglia and van Woesik 2015; Figure

3.1). Distribution maps were generated using Veron (2000) and the International Union for the Conservation of Nature (IUCN) Red List (http://www.iucnredlist.org/technical-documents/spatial-data). The species distributions were recorded as either present or absent within 141 ecoregions that were defined by Veron *et al.,* (2009). Three thousand presence sites were randomly selected from reefs within ecoregions that supported each coral species. The number of absence sites were selected from ecoregions in accordance with the area of reef habitat in which we were 95% certain that the coral species were absent (Cacciapaglia and van Woesik, 2015).

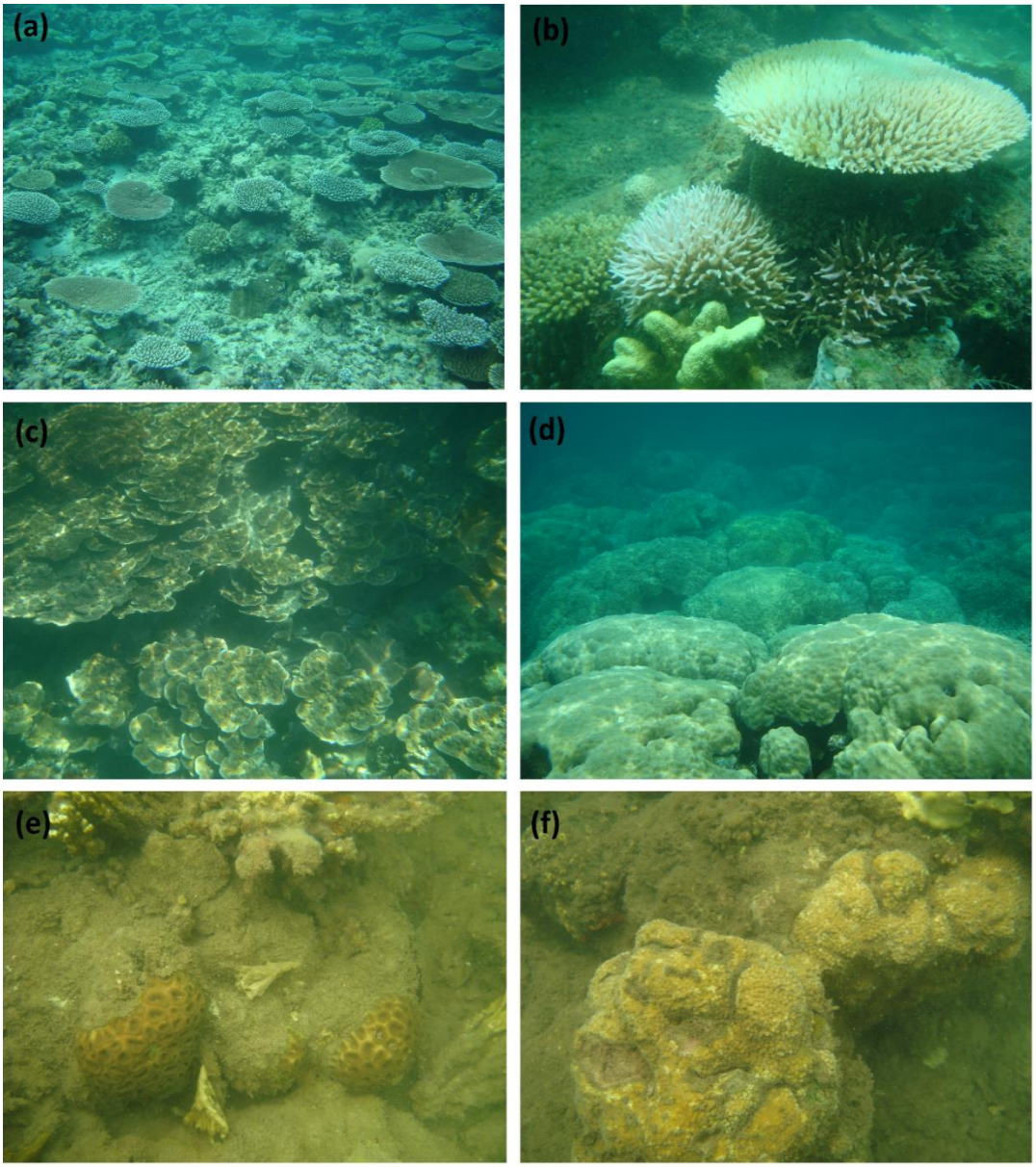

Figure 3.1 (**a**) Tabulate *Acropora hyacinthus* and corymbose *Acropora digitifera* in nearshore clear-water in Palau, Micronesia; (**b**) needle-shaped *Seriatopora hystrix*, showing a bleached colony in full sunlight (left), and an unbleached *S. hystrix* colony shaded by a corymbose *Acropora* colony (top right), during a summer thermal stress anomaly event in Bolinao, nearshore in the Philippines; (**c**) foliose, *Montipora aequituberculata* (left) and (**d**) massive *Porites lobata* (right) in turbid nearshore habitats in Palau; (**e**) *Dipsastraea speciosa* (left) and (**f**) *Cyphastrea chalcidicum* in turbid nearshore conditions near the entrance to a rivermouth on Palau's western coast.

ENVIRONMENTAL VARIABLES

Environmental variables were derived at each site where the coral species of interest was present, and for each site where the coral species of interest was absent. Irradiance was assessed as Photosynthetically Available Radiation (PAR, µmol m^{-2} s^{-1}), between the wavelengths 400 and 700 nm, using the satellite Sea-Viewing Wide Field-of-View Sensor (SeaWiFS) (http://gdata1.sci.gsfc.nasa.gov/daac-bin/G3/gui.cgi?instance_id=ocean_month) at a resolution of 9 x 9 km^2. Turbidity was assessed as the diffuse attenuation coefficient of the downwelling spectral irradiance wavelength 490 nm (K_{d490}), also using SeaWiFS (Pierson *et al.,* 2008). To transform K_{d490} to the diffuse extinction coefficient of PAR (K_{dPAR}), we used the following relationship (following Pierson *et al.,* (2008)):

$$K_{dPAR} = 0.6677.\ K_{d490}^{0.6763} \quad (7),$$

To determine irradiance at different depths we used the following relationship:

$$Irrad_{zm} = exp^{-K_{dPAR}.Z_{max}} \quad (8),$$

where $Irrad_{zm}$ is the proportion of irradiance reaching depth Z_{max} (Gallegos and Moore, 2000). After a sensitivity analysis (see supplementary document), we were interested in quantifying irradiance (µmol $m^{-2}s^{-1}$) reaching 3 m ($Irrad_{3m}$), to include the narrow photic zones on nearshore reefs (Adey 1976; Kleypas *et al.,* 1999). In accordance with previous studies, we also assumed that reef-building corals

were unable to grow and accrete carbonate structures in habitats at or below 3 m with average irradiance of < 250 µmol m^{-2} s^{-1} (Kleypas *et al.,* 1999). Tidal data were acquired from the integrated climate data center (http://icdc.zmaw.de/las/getUI.do), and chlorophyll *a* data were acquired from Giovanni Ocean Color (http://gdata1.sci.gsfc.nasa.gov/daac-bin/G3/gui.cgi?instance_id=ocean_month).

Sea-surface temperature (SST) data were derived from Aqua-MODIS (Moderate Resolution Imaging Spectroradiometer) satellite, collected at 5 arcmin (*c.* 9.2 km^2) grid-size pixels, for the years 2002—2009. The SST data were downloaded from Bio-ORACLE (Ocean Rasters for Analysis of Climate and Environment) (http://www.oracle.ugent.be/) (Tyberghein *et al.,* 2012). The range in SST for each grid point, *i*, between the latitudes 37˚N – 37˚S was calculated as the maximum minus the minimum temperature, for the 8-year period. Monthly data files were imported into R as raster files (using 'raster' (Hijmans *et al.,* 2014), and all values greater than zero were used to determine the range and mean temperature for the 8-year period. Future temperature predictions, for the year 2100, were also downloaded from Bio-ORACLE. The predicted data stemmed from the World Climate Research Programme Coupled Model Inter-comparison Project (WCRP CMIP3) for A2 (>800 ppm until 2100), which was equivalent to a 'business as usual' Representative Concentration Pathway (RCP) 8.5 (W m^{-2}). The predicted climate data were adjusted to the same grid size (*c.* 9.2 km^2) as the present SST data.

DATA ANALYSIS

The relationships between the presence of a particular coral species and the environmental variables of interest were examined using a logistic regression, and a logit-link function. To differentiate the effects of turbidity from PAR and temperature we used a Bayesian generalized linear mixed model from the R package 'blme' (Dorie 2014), using the following hierarchical system:

$$Y_i \sim \text{binomial}(p_i, n) \quad (9a),$$

$$y_i = log(p_i/1\text{-}p_i) = \beta_o + \beta_1 * x_i + \beta_2 * z_i + \beta_3 * x_i * z_i + a_i \quad (9b),$$

$$a_i \sim gamma(0, \sigma_a^2) \quad (9c),$$

where y_i is the observed binary response of a species (presence or absence) at site i, p_i is the probability of a species being present at site i, and $(1 - p_i)$ is the probability of species being absent at site i. The binomial distribution is the sum of the Bernoulli distributed cases of presence or absence of species considered for all sites n. The coefficient β_o is the intercept of the model, β_1, β_2, and β_3 are slopes that define the extent of the relationship between the response variable and the environmental covariates, x_i (range of SST) and z_i (range of PAR) at site i, and here turbidity was expressed as a random effect, a_i, which followed a gamma distribution. This random effect estimated an intercept at each turbidity value for the fixed effects of SST range and PAR range. We rounded the effect of turbidity into bins to reduce the likelihood of encountering no-analog conditions, which effectively reduced the uncertainty of the future predictions. The bin size for the effect of turbidity was determined using

Akaike's Information Criterion (AIC) to achieve the most parsimonious model. To determine the role that turbidity played in predicting future species distributions, this model was run twice, once with and once without the random effect of turbidity.

Using a mixed effects model with a random intercept, as in equation 3, we also assessed the contribution of the range in tidal amplitude and chlorophyll *a* concentrations on turbidity effects. These analyses were undertaken to examine whether the purported turbid refuges were merely a consequence of ephemeral pulses in ocean productivity, or whether they were consistent refuges that were tidally driven. If the tidal signatures were tightly coupled with chlorophyll *a* signatures, then the turbid refuges were deemed stable. If the tidal signatures were decoupled from the chlorophyll *a* signatures, then the turbid refuges were deemed ephemeral and unstable. To test whether turbid refuges were stable or not, we compared the chlorophyll *a* signatures with the tidal amplitude in an area known for regional upwelling, off the western coast of the Americas, and compared those signatures with an area where regional upwelling is less common. Fifteen thousand data sites were selected from the tidal and chlorophyll *a* data in a known upwelling area off the western coast of the Americas (between latitudes 37 North and South, from the 180th meridian to the Pacific coast of the Americas), and fifteen thousand data sites were selected in a non-upwelling area (between 37 North and South, and longitudes 50 East to the 180th meridian). A Bayesian generalized linear mixed model was then fitted using the sampled chlorophyll *a* and tidal data using latitude as a random effect.

The error terms of the random effects were then plotted across latitudes to examine the geographical coupling between tidal amplitude and chlorophyll *a* concentration. If the tidal signatures were tightly coupled with chlorophyll *a* signatures, then the turbid refuges were deemed stable. If the tidal signatures were decoupled from the chlorophyll *a* signatures, then the turbid refuges were deemed ephemeral and unstable.

MODEL EVALUATIONS AND CONSTRAINTS

Training (80%) and evaluation (20%) sites were randomly selected from all the presence and absence data combined, using a *k*-fold algorithm using the package 'dismo' in R, Hijmans *et al.,* (2014). This algorithm was repeated 100 times, and the model with the highest area under the receiver operating characteristic curve (AUC) was used in further analyses. A threshold, calculated as the greatest sum of sensitivity (i.e., the true positive fraction) and specificity (i.e., the true negative fraction), was used to transform the probability of a species being present into a Bernoulli presence-absence distribution. Values above this threshold were transformed to presence values (1), and values below the threshold were transformed to absence values (0). AUC values close to 1 indicated that the evaluation sites accurately predicted the (20% of k-folded) data that were not used in training the model. To gain some degree of confidence in the comparisons, coral habitat that was mitigated by turbidity was

evaluated by randomly comparing the non-turbid model runs with the turbid model runs, one-hundred times.

The model outputs were masked using five conservative constraints to eliminate false negatives, without lowering the credibility of the model (Dorie 2014). The masks followed Cacciapaglia and van Woesik (2015), and included: (i) limited geographical range extension, via larval dispersal, to no more than 10 km per year; (ii) the exclusion of the area surrounding the 12 largest subtropical and tropical river outflow areas, masked out in accordance with their drainage size (Cacciapaglia and van Woesik, 2015); (iii) reef localities that experienced temperatures < 18ºC, for any time of the year, (Kleypas 1997; Kleypas *et al.,* 1999); (iv) sites outside the contiguous tropical-ocean region in which the coral species was found; (v) any sites that experienced < 250 μmol m^{-2} s^{-1} (i.e., 21.6 E m^{-2} d^{-1}) $Irrad_{3m}$ (Kleypas *et al.,* 1999) were masked out of all models (all R code to run the models are provided in an online supplementary document).

RESULTS

Turbidity was predicted to mitigate the harsh interaction between high sea-surface temperatures and high irradiance by shading 9% of coral habitat previously considered inhospitable under ocean warming (Figure 3.2; Table 3.1). Turbidity was predicted to facilitate, in particular, the survival of corals in the northwestern Hawaiian Islands, the northern Philippines, the Ryukyu Islands (Japan), eastern Vietnam, northern, western, and eastern Australia, New Caledonia, the northern Red Sea, and the Arabian Gulf Figure 3.2). The predictive models also showed that extremely high turbidity will likely preclude 16% of the reef-coral habitat, mainly between eastern Sumatra (Indonesia) and southern Malaysia, the southwestern coast of Kalimantan (Indonesia), the Gulf of Martaban (Myanmar), the southern coast of China, western India, and southern Papua New Guinea (Figure 3.2; Table 3.2).

Table 3.1. Nearshore-coral habitat (≤ 30 m) that is predicted to be facilitated by turbidity in the Pacific and Indian Oceans by 2100 under Representative Concentration Pathway 8.5 (W m^{-2}); note that *Coelastrea aspera* and *Dipsastraea speciosa* were previously known as *Goniastrea aspera* and *Favia speciosa*, respectively. Note also that the estimates of habitat occupancy are relative estimates, because of the coarse-grained (9.2 km) nature of the grid, which tended to over-estimate occupied reef area. Therefore, these estimates are useful for comparative purposes only, and should not be used as estimates of absolute changes in coral-reef area.

Coral species	**Contemporary habitat (km^2)**	**Facilitated by turbidity (km^2)**	**95% confidence**	**Percentage facilitated**
Dipsastraea speciosa	3 126 586	980 740	1 470 985	31.4%
Acropora hyacinthus	3495198	405621	942 103	11.6%
Montipora aequituberculata	3 944 055	403 278	682 997	10.2%
Stylophora pistillata	3 848 554	334 382	755 679	8.7%
Cyphastrea chalcidicum	3 564 230	306 431	730 174	8.6%
Coelastrea aspera	3 630 042	313419	647383	8.6%
Seriatopora hystrix	3 384 351	249 712	568 435	7.4%
Favites halicora	3 521 092	233 007	603 490	6.6%
Acropora digitifera	3 546 122	190 728	40 4951	5.4%
Leptastrea pruinosa	3 384 330	171 993	423 246	5.1%
Porites lobata	4 465 534	134 273	140 109	3.0%
Porites horizontalata	2 170 448	46 051	113 385	2.1%

SPECIES-SPECIFIC DIFFERENCES

Porites lobata, the most widely distributed coral species in the Pacific and Indian Oceans, is predicted to only benefit slightly from positive turbidity effects, potentially increasing reef habitat by 3%, with an increase in water temperature under Representative Concentration Pathway 8.5 (W m^{-2}) by 2100. Similarly, *Porites horizontalata*, the most narrowly distributed coral species, is predicted to only benefit slightly from turbidity effects (2%; Table 3.1). The massive coral species *Dipsastraea speciosa* and the foliose species *Montipora aequituberculata* are predicted to benefit most from the shading effects of moderate turbidity (Table 3.1). In the Pacific Ocean, some turbid locations along the eastern coast of Australia and New Caledonia were predicted to shade corals from future thermal stress, particularly the species *Acropora digitifera, A. hyacinthus, Cyphastrea chalcidicum, Dipsastraea speciosa, Coelastrea aspera, Montipora aequituberculata,* and *Stylophora pistillata* (Table 3.2). In eastern Sumatra (Indonesia) turbid locations were predicted to shade *Porites lobata,* and in eastern Vietnam turbid locations were predicted to shade *Acropora digitifera, A. hyacinthus, Cyphastrea chalcidicum, Dipsastraea speciosa, Coelastrea aspera, Montipora aequituberculata,* and *Stylophora pistillata* (Table 3.2). In the Philippines, turbid locations were predicted to shade several coral species from climate-change temperatures, including *Acropora digitifera, A. hyacinthus, Cyphastrea chalcidicum, Dipsastraea speciosa, Coelastrea aspera, Leptastrea pruinosa, Montipora aequituberculata,* and *Stylophora pistillata.* The Ryukyu

Islands, in southern Japan, are predicted to be an important locations in the Pacific Ocean for shading *Dipsastraea speciosa* from ocean warming (Table 3.3).

Table 3.2. Nearshore-coral habitat (≤ 30 m) that is predicted to be suppressed by turbidity in the Pacific and Indian Oceans by 2100 under Representative Concentration Pathway 8.5 (W m^{-2}).

Coral species	**Contemporary habitat (km^2)**	**mean**	**95% confidence**	**Percentage suppressed**
Dipsastraea speciosa	3 126 586	1 091 771	1 328 524	34.9%
Stylophora pistillata	3 848 554	1 016 088	2 062 453	26.4%
Montipora aequituberculata	3 944 055	855 062	1 442 528	21.7%
Seriatopora hystrix	3 384 351	561 007	799 483	16.6%
Favites halicora	3 521 092	516 405	800 260	14.7%
Porites lobata	4 465 534	615 326	36 235	13.8%
Acropora digitifera	3 546 122	469 572	613 302	13.2%
Leptastrea pruinosa	3 384 330	444 314	467 320	13.1%
Coelastrea aspera	3 630 042	467 323	543 983	12.9%
Cyphastrea chalcidicum	3 564 230	411 167	418 336	11.5%
Acropora hyacinthus	3 495 198	375 453	565 577	10.7%
Porites horizontalata	2 170 448	147 593	94 150	6.8%

In the Indian Ocean, along the western coast of Australia, turbid locations were predicted to shade *Dipsastraea speciosa, Montipora aequituberculata,* and *Stylophora pistillata,* and, to a less of an extent, shade *Acropora hyacinthus, A. digitifera, Cyphastrea chalcidicum, Favites halicora,* and *Coelastrea aspera* (online supplementary document) (Table 3.3). Southern and eastern Madagascar were predicted to shade most coral species. Turbidity was also predicted to shade

Dipsastraea speciosa and *Montipora aequituberculata* from future thermal stress on both coasts of the Mozambique Channel, shade *Acropora hyacinthus* in the southern Red Sea, and shade *Dipsastraea speciosa, Montipora aequituberculata, Stylophora pistillata* in the northern Red Sea (Table 3.3). The Gulf of Oman and Persian Gulf are predicted to shade *Dipsastraea speciosa, Montipora aequituberculata,* and *Stylophora pistillata* from ocean warming, and turbid locations in the Arafura Sea were predicted to protect most of the coral species in this study from future thermal stress (see online supplementary document) (Table 3.3).

The results of the generalized linear mixed model showed that the range in tidal amplitude had a significant positive effect on turbidity ($p<0.001$). There was also a strong positive relationship between chlorophyll *a* concentrations and turbidity throughout the oceans ($r_s=0.97$), however the extent of coupling varied geographically (Figure 3.2). Tidal amplitude and chlorophyll *a* coupled across most of the eastern Pacific and Indian Oceans (longitudes 50 to 180 East), except between the equator and 20^{o}N (Figure 3.2a). By contrast, the area known for upwelling, from the 180th meridian and the Pacific coast of the Americas, showed that tidal amplitude and chlorophyll *a* were decoupled south of the equator (Figure 3.2b), consistent with ephemeral upwelling along coastal Peru. In combination, the results show strong coupling between turbidity and tidal amplitudes between 20–30^{o} N and 15–25^{o}S,

which suggests a stable turbidity regime where reef-coral turbidity refuges were purported to be located.

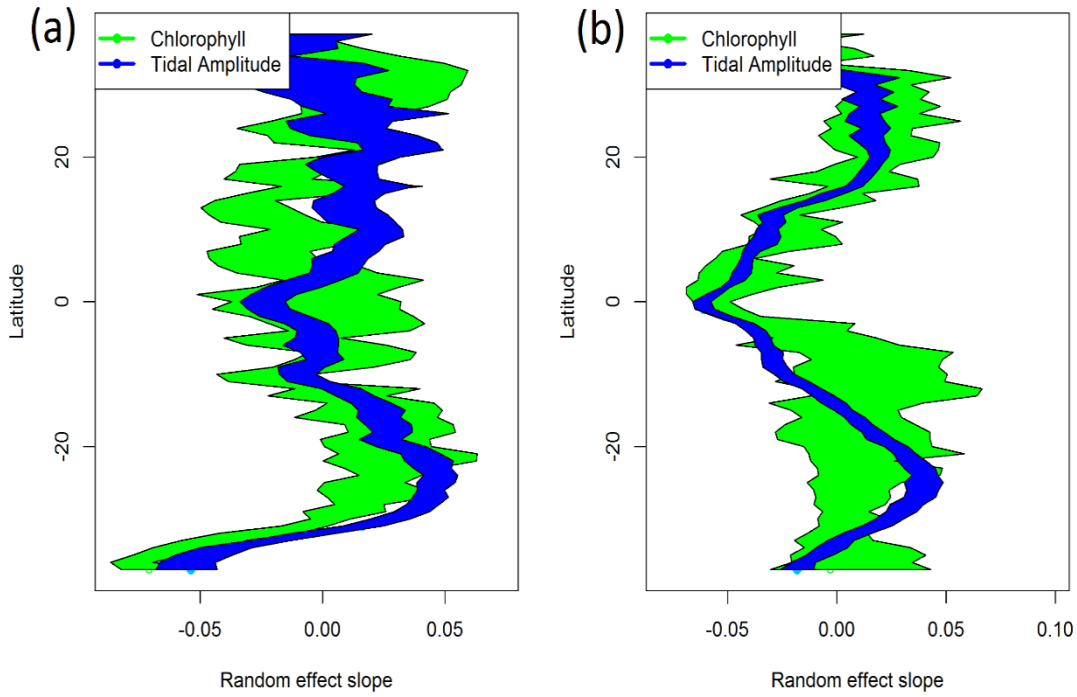

Figure 3.2 Coupling between chlorophyll *a* concentrations and tidal amplitudes on the effects of turbidity (**a**) between 37° N and S, from 50° E to the 180th meridian, and (**b**) between 37° N and S, from the 180th meridian to the Pacific coast of the Americas.

Table 3.3. The geographic location of the turbid-nearshore refuges (≤ 30 m) for reef-corals presented by geographic location, and the most prominent coral species that will likely be affected in the Pacific and Indian Oceans by 2100 under Representative Concentration Pathway 8.5 (W m^{-2}).

Latitude	**Longitude**	**Location**	**Coral species**
Northern hemisphere			
13ºN	109 ºE	eastern Vietnam	*Acropora digitifera, Acropora hyacinthus, Cyphastrea chalcidicum, Dipsastraea speciosa, Coelastrea aspera, Montipora aequituberculata,* and *Stylophora pistillata*
13 ºN	121 ºE	Philippines	*Acropora digitifera, A. hyacinthus, Cyphastrea chalcidicum, Dipsastraea speciosa, Coelastrea aspera, Leptastrea pruinosa, Montipora aequituberculata,* and *Stylophora pistillata*
23 ºN	124 ºE	Ryukyu Islands	*Dipsastraea speciosa*
25 ºN	34 ºE	Northern Red Sea	*Dipsastraea speciosa, Montipora aequituberculata, Stylophora pistillata*
14 ºN	42 ºE	Southern Red Sea	*Acropora hyacinthus*
25 ºN	54 ºE	Gulf of Oman and Persian Gulf	*Dipsastraea speciosa, Montipora aequituberculata,* and *Stylophora pistillata*
Equatorial			
1 ºS	99 ºE	western Sumatra	*Porites lobata*
Southern hemisphere			
24 ºS	113 ºE	Eastern Australia	*Acropora digitifera, A. hyacinthus, Cyphastrea chalcidicum, Dipsastraea speciosa, Coelastrea aspera, Montipora aequituberculata,* and *Stylophora pistillata*
23 ºS	157 ºE	New Caledonia and Western Australia	*Acropora digitifera, A. hyacinthus, Cyphastrea chalcidicum, Dipsastraea speciosa, Coelastrea aspera, Montipora aequituberculata,* and *Stylophora pistillata*
26 ºS	47 ºE	Southern and eastern Madagascar	*Acropora digitifera, A. hyacinthus, Cyphastrea chalcidicum, Dipsastraea speciosa, Favites halicora, Coelastrea aspera, Montipora aequituberculata,* and *Stylophora pistillata*
20 ºS	39 ºE	Mozambique Channel	*Dipsastraea speciosa* and *Montipora aequituberculata*
14 ºS	138 ºE	Arafara sea	*Acropora digitifera, A. hyacinthus, Cyphastrea chalcidicum, Dipsastraea speciosa, Coelastrea aspera, Montipora aequituberculata,* and *Stylophora pistillata*

DISCUSSION

The present study identified several turbid-nearshore locations in the Pacific and Indian Oceans that were predicted to shade corals from climate-change induced thermal stress. Specifically, the most prominent turbidity refuges were evident along the eastern and western coasts of Australia, New Caledonia, central Indonesia, eastern Vietnam, the northern Philippines, the Ryukyu Islands (Japan), on both coasts of the Mozambique Channel, the southern Red Sea, and the Persian Gulf. In general, the turbid-nearshore climate-change refuges were located at latitudes 20–30°N, and 15–25°S (Figure 3.3). Some of these locations, particularly the Persian Gulf, already support thermally tolerant corals (Coles and Riegl 2013), and resistant combinations of thermally tolerant *Symbiodinium* species (Mostafavi et al. 2007; Hume et al. 2013).

At a coral species-specific level, the present study predicts that turbidity will shade some coral species more than other coral species from climate-change thermal stress. Corals species that presently occupy the most extensive reef areas, such as *Porites lobata* (Figure 3.1d), were predicted to benefit less from turbidity in a warm ocean than the less ubiquitous species in the family Merulinidae. Indeed, with ocean warming, *Porites lobata* is predicted to increase its range by 3% because of shading by turbidity. Such a slight increase in range is most likely a consequence of an already ubiquitous distribution, and indeed there are few locations where *Porites lobata* does not already occupy. By contrast, with ocean warming, *Dipsastraea*

speciosa (Figure 3.1e) was predicted to increase its range by 31% because of shading by turbidity. It was encouraging that the models predicted that the tabulate *Acropora hyacinthus* (Figure 3.1a), a major reef-building coral, would be protected from thermal stress by turbidity in the future. The foliose coral species *Montipora aequituberculata* was also predicted to be protected from thermal stress by turbidity in the near future. These results are not surprising since *Montipora* species are most commonly found on highly turbid reefs in the Pacific Ocean (van Woesik and Done 1997; DeVantier *et al.,* 1998). Coral species that were very sensitive to thermal stress, such as *Porites horizontalata,* were unlikely to be protected from thermal stress by turbidity in a warmer ocean. The lack of a beneficial effect is likely a consequence of: 1) a narrow, contemporary distribution, limiting the area where turbidity can act upon the species, and 2) idiosyncrasies of the model, such as dispersal limitations, that exclude species from habitats where they are not found on modern reefs, even though they may be tolerant to environmental conditions found outside of their contemporary distribution. In combination, *Porites*, merulinids, and *Montipora* coral assemblages are most likely to dominate turbidity refuges.

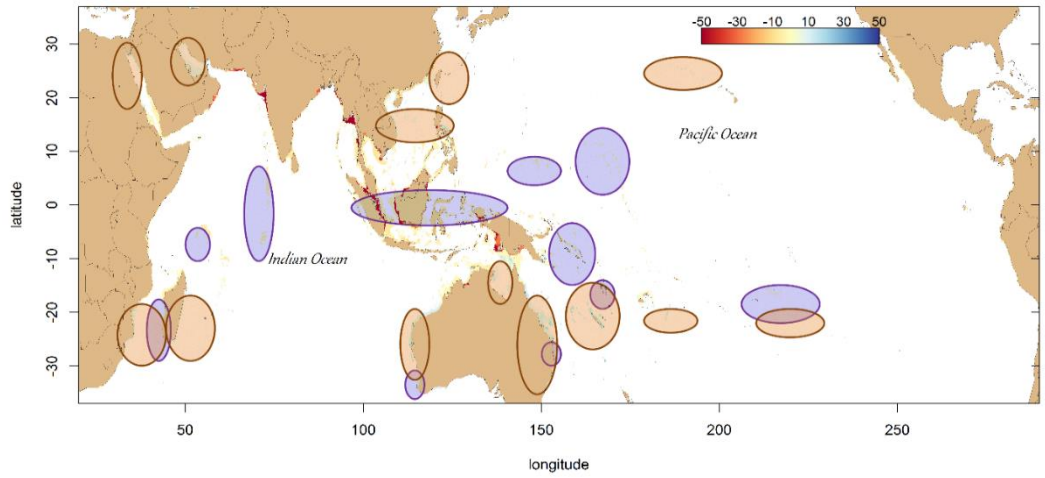

Figure 3.3 Localities of previously defined clear-water climate-change refuges in purple (from Cacciapaglia and van Woesik 2015) by 2100 under Representative Concentration Pathway (RCP) 8.5 (W m^{-2}), and the turbidity refuges defined in the present study in brown, predicted for 2100 for the Pacific and Indian Oceans.

Our model predicts that globally, turbidity will impede 16% of coral habitat under expected ocean warming. High and persistent turbidity reduces light and constricts photic zones (Tomascik et al 1991; Kleypas 1996), reduces rates of coral calcification (Anthony and Fabricius 2000), reduces coral colony survival (Tomascik 1993; Yentsch *et al.,* 2002), and can suppresses reef formation over geological time scales (Darwin 1842; Kleypas 1996). The major localities where turbidity impeded corals included the area between eastern Sumatra (Indonesia) and southern Malaysia, the southwestern coast of Kalimantan (Indonesia), the Gulf of Martaban (Myanmar), the southern coast of China, western India, and southern Papua New Guinea. These areas, with < 250 µmol m^{-2} at 3 m, were predicted to exclude all 12 of the coral

species into the near future under climate change, by continuing to restrict irradiance and compress the photic zone.

Although moderate turbidity can reduce thermal stress and bleaching, poor-water quality, with high levels of pollutants and nutrients, increases the likelihood of coral stress and mortality during anomalous-temperature events (Wooldridge 2009; Wooldridge and Done 2009; Wagner et al., 2010). For example, Wagner et al., (2010) showed that reefs in the Florida Keys that consistently experienced high dissolved inorganic nitrogen loads, with poor water quality, were more susceptible to coral bleaching under regional temperature stress. Similarly, on the Great Barrier Reef during thermal anomalies, localities with high-nutrient concentrations suffered greater bleaching and coral mortality than localities with low-nutrient concentrations (Wooldridge and Done 2009). Consistently high-nutrient concentrations are likely to increase the pigment and symbiont concentrations within corals, damaging the photosynthetic reaction centers in the coral symbionts during calm, clear-water conditions that occur during thermal-stress events (Falkowski et al. 1993; Cunning and Baker 2013).

High-nutrient concentrations also lead to high-ocean productivity, which is reflected as high chlorophyll *a* concentrations in satellite images. Although turbidity, tidal range, and chlorophyll *a* are all closely inter-related, highly productive, yet ephemeral, plankton blooms are unlikely to shade corals persistently. By contrast, consistent turbidity caused by tidal fluctuations are more likely to be permanent

fixtures of the seascape, and will most likely act as persistent shade for corals in a warming ocean. The results of the present study showed a strong coupling between turbidity and tidal fluctuations between latitudes 20–30°N and 15–25°S, where the purported reef-coral refuges were located. These results suggest that the turbidity refuges reported here are most likely stable refuges, caused by astronomical tidal fluctuations, rather than by ephemeral refuges caused by pulses of phytoplankton blooms.

Previously, Cacciapaglia and van Woesik (2015) predicted the location of 12 clear-water climate-change reef-coral refuges in the Pacific and Indian Oceans. There was considerable overlap between the previously defined clear-water refuges in the southern hemisphere (Cacciapaglia and van Woesik, 2015), and turbidity refuges defined in the present study (Figure 3.3). However, none of the clear-water refuges in the northern hemisphere, previously defined by Cacciapaglia and van Woesik (2015), overlapped with the presently defined turbidity refuges. Therefore, there are several opportunities and incentives to highlight the presently identified turbid, nearshore areas as coral refuges. Localities that deserve particular attention are the turbid-nearshore habitats of Hawaii, the reefs in the northern Philippines, in the southern Japanese islands, and in the northern gulfs of the Indian Ocean. These turbid-nearshore locations, identified in the present study, are less aesthetically appealing than the charismatic, clear-water locations. However, based on decades of physiological studies on the response of corals to irradiance (Iglesias-Prieto et al.

1992; Iglesias-Prieto and Trench 1994; Warner et al. 1999; Anthony et al. 2004; Anthony and Connolly 2004; Takahashi et al. 2004), these turbid locations could play crucial roles in preserving reef-corals by acting as key refuges in a rapidly warming ocean. Conserving these turbid locations, alongside the previously identified climate-change locations, will broaden the geographic scope and strengthen the network of locations that may act as critical reef-coral refuges. In conclusion, ocean sea-surface temperatures are predicted to increase over the next century, causing further harm to reef-corals. Reduction of irradiance through natural, yet moderate turbidity can shade corals and facilitate coral survival in warming oceans.

CHAPTER 4. MARINE SPECIES DISTRIBUTION MODELING AND THE EFFECTS OF GENETIC ISOLATION UNDER CLIMATE CHANGE

ABSTRACT

Coral reefs are experiencing both an increasing frequency and intensity of anomalously warm ocean temperatures because of climate change. Studies show that the majority of coral populations will likely decline as temperatures continue to increase, although some previous species-distribution models predict that ubiquitous species, such as the primary reef-building coral species *Porites lobata,* will increase their distribution under projected climate change. These predictive models, however, assume that all individuals are able to tolerate the entire range of environmental conditions within the species' geographic range. The effects of genetic isolation and local adaptation are not considered in species-distribution models that assume genetically contiguous populations. We aim to determine the effects of genetic isolation and local adaptation in species-distribution modeling of the ubiquitous species *P. lobata* under three climate change scenarios by comparing contiguous and isolated subpopulations.

We ran a novel species-distribution model for *P. lobata,* segregated as five geographically isolated regions across the Indian and Pacific Oceans, and examined the species response to three climate-change scenarios (i.e., Representative Concentration Pathways 8.5, 6.0, and 4.5 Wm^{-2}) by the year 2100. By contrast with previous homogeneous species-distribution models that predict a global expansion

of *P. lobata,* (~ 8 ± 1%), we predict major losses of suitable habitat for *P. lobata* in four of the five regions examined, particularly in the smallest region of the eastern Pacific Ocean (>99% ± < 0.1% in all climate scenarios). Indeed, when geographic and genetic isolation were considered, our predictions suggested that *P. lobata* would lose between 64–68 ± 7% of its habitat, depending on the climate-change scenario, mainly in the Pacific Ocean. In conclusion, genetic isolation will likely play a major role in the persistence of coral species under climate change, and small isolated populations may be more vulnerable to climate change than populations in large, highly connected regions.

INTRODUCTION

Since the early evolution of scleractinian corals, in the Triassic, corals have built reefs (Stanley, 2006). Although the climate has fluctuated considerably over that 250 million year period, the contemporary rate of change in ocean temperature is historically unprecedented (Zeebe and Zachos, 2013). Ocean temperatures are expected to increase even further in the near future, and are highly dependent on the rates of emissions of CO_2 and other greenhouse gases (IPCC, 2013). The future spatial distributions of coral species are being predicted by a range of effective tools based on: (i) the contemporary distribution of species, (ii) the environmental conditions in which species are found, and (iii) the forecasted environmental conditions from climate models (Elith and Leathwick, 2009; Cacciapaglia and van Woesik, 2015).

With the current rate of climate change, corals are being repeatedly subjected to thermal stress events. These thermal-stress events lead to bleaching, mortality, and changes in reef composition (Glynn 1993; Loya et al., 2001; van Woesik et al., 2011). Some models predict that few reef corals will survive the temperature rise that is predicted for the tropical oceans within the next hundred years (Frieler et al., 2012), yet other models predict high spatial heterogeneity in temperature changes (IPCC, 2013), with correspondingly high geographic heterogeneity in the extent of temperature stress (Thompson and van Woesik, 2009; van Hooidonk et al., 2013).

Therefore, there is an urgent need to identify regions where corals might survive into the future.

A common tool that defines local and global climate-change refugia is species-distribution models (Elith and Leathwick, 2009). One assumption of species-distribution models is that all individuals of a population can tolerate the entire range of environmental conditions within the geographic range of the species (Elith and Leathwick, 2009), even if the species is widely distributed. Yet, local adaptation is apparent in some widely dispersed, eurytopic species (Jain and Bradshaw, 1966; Sork et al., 1993; Polato et al., 2010; Kenkel et al., 2013), and only locally-adapted individuals can tolerate extreme conditions at the margins of a given geographic range (Bush, 1975). Therefore, neglecting local adaptation, at the edge of a distribution range, may unrealistically project the entire population into future habitats, which may be geographically unattainable given realistic dispersal kernels. For example, subpopulations that are locally adapted to an extreme temperature range are likely to survive ocean warming. Yet if combined with a ubiquitous subpopulation, which is not locally adapted to such temperature extremes, the species-distribution model would predict widespread survival to ocean warming, throughout, and potentially beyond, its contemporary geographic range. For instance, using a species-distribution model, the ubiquitous species *Porites lobata,* a dominant reef-building coral in the Pacific and Indian Oceans, was predicted to increase its

distribution by ~8% under projected climate change scenarios (Cacciapaglia & van Woesik, 2015).

Although coral-larval dispersal models are becoming predictive (Kleypas et al., 2016; Wood et al., 2016), species-distribution models seldom account for genetic connectivity, because genetic data are sparse for corals, especially across large ocean basins. A rare exception is a recent gene-flow study by Baums et al. (2012), of the ubiquitous coral *P. lobata* in the Indo-Pacific region. Baums et al. (2012) showed that *P. lobata* was composed of at least four isolated geographic subpopulations across the Indo-Pacific region, with the exception of Clipperton Atoll, in the eastern Pacific Ocean, which grouped genetically with the population in the central Pacific. We hypothesize that the geographical isolation of *P. lobata* may have major implications for modeling the distribution of the species into the future, and isolation may potentially reduce its range under climate change. Here we re-examine the assumption of treating populations as homogenous throughout their geographic range, and consider the response of *P. lobata* to climate change by taking a novel approach by incorporating geographic barriers into species-distribution models. We have restricted our analysis to *P. lobata*, again because of a lack of genetic data on other coral species. The primary objective of the present study is to identify to what extent the lack of gene flow affects the predicted distribution of *P. lobata* into the future under three climate change scenarios, Representative Concentration Pathways (RCPs) 8.5, 6.0, and 4.5 Wm^{-2} (IPCC, 2013).

MATERIALS AND METHODS

The distribution of *P. lobata* was conservatively subdivided into five large geographic regions. Four regions were based on the genetic results from Baums et al., (2012): (1) the eastern Pacific Ocean; (2) the Hawaiian Islands and Johnston atoll, (3) central Pacific Ocean, and (4) the western Pacific Ocean. The fifth region partitioned the well-known divide between the Indian and the Pacific Ocean regions (Hobbs et al., 2009) (Figure 4.1a). There may be additional subpopulations discovered for *P. lobata* (for example Boulay *et al.*, 2014), and the specifics of the model outputs will differ with those discoveries, however the concept tested by the present study will not differ, which was to examine the differences in species persistence when species-distribution models are considered as contiguous or as geographically isolated subpopulations. The future distributions of *P. lobata* were predicted using a model adapted from Cacciapaglia and van Woesik (2015), running the model independently for each genetically isolated region for model calibration, validation, and projection. We then compared the outputs of the contiguous and geographically isolated models.

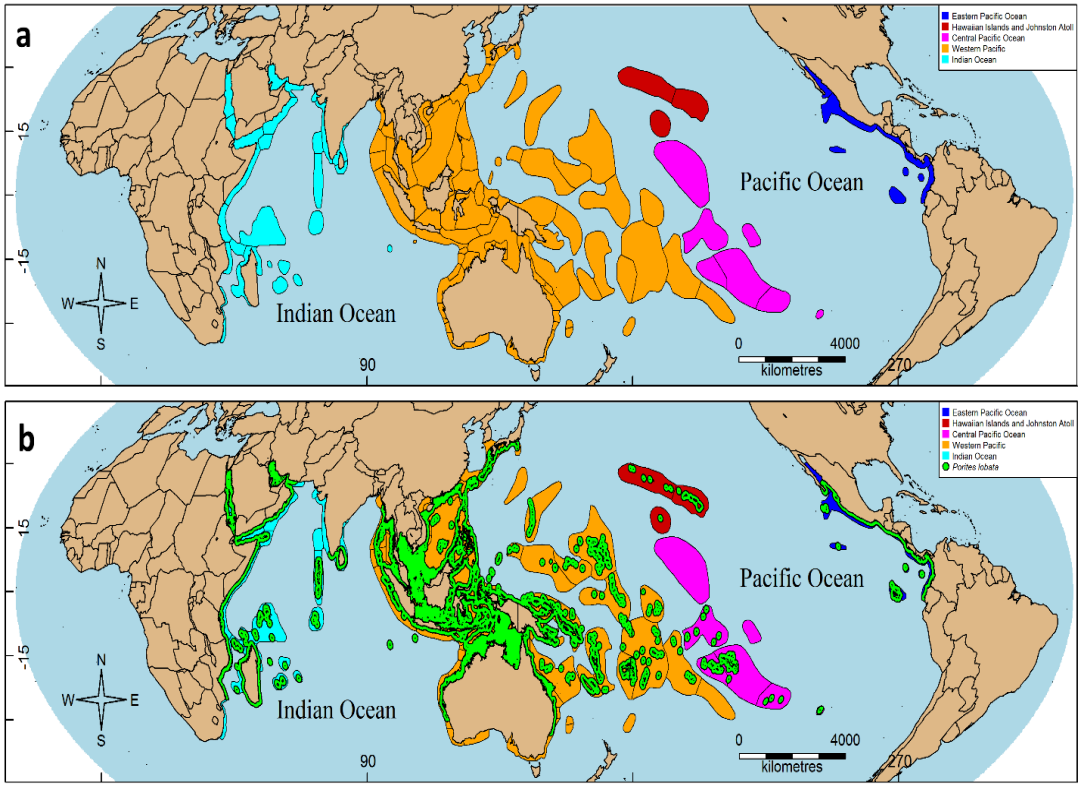

Figure 4.1 **a)** Subdivision of *P. lobata* into five geographically isolated regions in the Indian and Pacific Oceans, based on genetic data from Baums *et al.* (2012) and Hobbs *et al.* (2009) used in the present study's species-distribution model. **b)** Distribution of *Porites lobata* (green) within the five geographically isolated regions depicted in 1a, from which presence points were drawn. The distribution is based on data from the International Union for the Conservation of Nature (IUCN, 2014; IUCN Red List Data) and validated using Veron (2000), and then used in the present study's predictive model.

Both modeling approaches used two variables, irradiance and temperature, along with the contemporary distribution of *P. lobata* to project the distribution of the species under climate change scenarios RCPs 8.5, 6.0, and 4.5 Wm^{-2} by the year 2100. Specifically, the range in Sea Surface Temperature (SST) and the range of photosynthetically active radiation (PAR) were chosen as the environmental proxies

for temperature and irradiance. We chose range for both variables because the scope of aerobic performance, or physiological response, is based on the range of the environmental variables (Portner and Farrell, 2008). In addition, "range limits are commonly niche limits", as suggested by Lee-Yaw et al. (2016). Temperature and PAR were chosen because thermal stress occurs only when water temperature is outside of the normal range for an extended period, but only when solar irradiance (or PAR) is high. Thermal stress and coral bleaching is based on the response of coral to both irradiance and temperature; reduce irradiance under high temperature, and the likelihood of coral bleaching is substantially reduced (Takahashi et al., 2004). Therefore, both temperature and irradiance influence photosynthesizing organisms such as corals. Other temperature indices were excluded from this analysis to (i) avoid collinearity between variables, (ii) because averages do not capture niche space, and (iii) because the range of SST includes both the minimum and maximum temperatures, thereby increasing model parsimony.

CLIMATIC PARAMETERS

Sea-surface temperature (SST) data were downloaded from Bio-ORACLE (Ocean Rasters for Analysis of Climate and Environment) (http://www.oracle.ugent.be/) (Tyberghein *et al.*, 2012) at 5 arcmin, (*c*. 9.2 km cell size). Contemporary SST data were gathered from Aqua-MODIS (Moderate Resolution Imaging Spectroradiometer) satellite measurements. The contemporary range of SST, using

monthly intervals, was calculated for the years 2002 to 2009. Projected SST data were gathered from World Climate Research Programme Coupled Model Inter-comparison Project (WCRP CMIP3) for scenario A2 (business as usual; >800 ppm CO_2 by 2100), A1B (stabilizing CO_2 emissions by 2100; 700 ppm CO_2 by 2100), and B1 (stabilizing CO_2 emissions by 2050, then reduced emissions; 500–600 ppm CO_2 by 2100). These data were derived from the HADCM3 SRA2 model runs, and represent similar pathways to Representative Concentration Pathways (RCPs) 8.5, 6.0, and 4.5 Wm^{-2}, respectively (IPCC 2013). To align with contemporary terminology (IPCC 2013), the CMIP3 pathways (A2, A1B, and B1) are referred to as RCP 8.5, 6.0 and 4.5. The predicted increase in mean global temperature, under these three scenarios, is +3.4ºC for RCP 8.5, + 2.8ºC for RCP 6.0, and +1.8ºC for RCP 4.5. The projected range of SST was calculated using projections for the years 2087–2096. We used data from Bio-ORACLE (Tyberghein et al., 2012) that were downscaled using in-situ data to refine Global Climate Models (GCMs), assuming that the future climate will respond similarly. Bias was minimized in the present study since the in-situ data matches the modeled forecast data, under the highest resolution. Irradiance data were derived from the satellite Sea-Viewing Wide Field-of-View Sensor (SeaWiFS) (http://gdata1.sci.gsfc.nasa.gov/daac-bin/G3/gui.cgi?instance_id=ocean_month) as Photosynthetically Available Radiation (PAR, E m^{-2} d^{-1}) at the same resolution as that of the SST data (5 arcmin,

or grid size of 9.2 km). The extent of these data was cropped at 37°N and 37°S, and the models were run between these latitudes.

SPECIES DISTRIBUTIONS

The distribution of *P. lobata* was derived from International Union for Conservation of Nature (IUCN) distribution data (IUCN Red List Data) and validated using Veron (2000). One hundred and forty one sub-regions, from Veron et al. (2009) (called ecoregions by Veron), were then populated with either presence or absence data by overlaying the IUCN distribution with the sub-regions (Fig. 1b). These sub-regions were then amalgamated as five genetically isolated regions. Within each of the five regions, sub-regions that overlapped with the (IUCN) species distribution were considered to support *P. lobata*. The species was considered to be absent from a sub-region if: (1) the sub-region was outside the region of interest; or (2) if the sub-region was inside the region, but did not overlap the IUCN distribution, and if there was >95% confidence that the species was not in that sub-region, following a probability of detection algorithm found in Cacciapaglia and van Woesik (2015). We then sampled 3000 presence and absence coordinates, taken proportionally, representing the number of present versus absent sub-regions, where the total number of samples summed to 3000. The sample size was chosen to cover the geographic extent of this study. The presence and absence coordinates were taken from reef locations defined in ReefBase (www.reefbase.org).

The contemporary environmental data were extracted at the same coordinates as the 3000 presence and absence points, and a logistic regression was trained and tested using a generalized linear model (GLM) in R (R Core Team, 2015). A GLM was chosen over a variety of other model types after an initial assessment of model strengths and weaknesses. The GLM was chosen over a generalized additive model because of the consistently higher area under receiver operating characteristic curve (AUC) scores. We chose not to use the black-box methodology of neural networks, and avoided the problems of pseudo-absences associated with maximum entropy (Maxent) models. The random forest models yielded higher AUC scores than the GLM, but the model output showed very pixelated, discontinuous results, unlike natural biological systems with interconnected habitats. Therefore, we determined that a GLM, using a binomial distribution and a logit-link function, was the best model for our system of interest. We used k-fold sampling (k-fold from R package 'dismo', Hijmans et al., 2014), using 80% of the data for training, and 20% of the data for testing. This k-fold algorithm was repeated 100 times and the model with the highest AUC was used to predict the distribution under climate scenarios RCPs 8.5, 6.0, 4.5 Wm^{-2}. This process was repeated 25 times to gain confidence in the model, and an ensemble was created using the 25 highest scoring models, of the 2500 model runs. A threshold for presence and absence of each of the 25 model runs was determined as the point where the sum of the sensitivity and specificity was the highest. Confidence in the model predictions was evaluated using the 25 model runs.

Z-scores were used to determine whether predicted cells were significantly different ($p<0.05$) than the contemporary state of those cells. Masks were applied to the geographic distribution of the species, to reduce false positives without decreasing model credibility.

The following masks were considered for all models. First, a realistic dispersal kernel was used to restrict dispersal to no greater than 10 km a year, beyond the contemporary range of each species. This kernel was based on reproduction studies (Miller and Munday, 2003; Shanks et al., 2003; van Woesik, 2010), genetic studies (Ayre and Hughes, 2000), and recent modeling studies that show a reduction in dispersal with ocean warming (O'Connor et al., 2007; Figueiredo *et al.,* 2014). Second, only reef habitats in the euphotic zone < 30 m depth were considered. Bathymetric data were gathered from NOAA using the getNOAA.bathy function from the 'marmap' package (Pante and Simon-Bouhet, 2013). Third, because of freshwater mortality effects, reefs were excluded that were adjacent to the outflow of the largest rivers in the Indian and Pacific Oceans. This mask was applied as a function of distance from each rivermouth in accordance with the size of each drainage basin. Fourth, habitats < 18^{o}C at any time of the year were masked because corals are intolerant to temperatures below 18^{o}C for extended periods (Veron, 1995), and because reef accretion is unlikely below 18^{o}C (Kleypas, 1999). Fifth, appropriate continental barriers that prohibited unrealistic genetic connectivity were imposed. All five masks followed the procedures in Cacciapaglia and van Woesik (2015). All

code was written in R (R Core Team, 2015) and is available in the online supplementary document.

Table 4.1. Change in habitat through time (until 2100) for climate scenario Representative Concentration Pathway (RCP) **8.5 Wm^{-2}**, where AUC is the area under the receiver operating characteristic curve.

Geographic Region	*Current habitat km^2*	*Lost habitat km^2*	*Future habitat km^2*	*New habitat km^2*	*% habitat change*	*AUC*
Contiguous	4466534±59157	6144±2660	4838145±37051	397462±41261	8.4 ± 1	0.963±0.006
Eastern Pacific	97271±904	45734±3524	54312±4373	2775±499	-44.3 ± 4.3	0.824±0.007
Hawaii	19834±229	18278±587	1556±572	0±0	-92.2 ± 2.9	0.879±0.006
Central Pacific	40885±456	40780±447	105±17	0±0	-99.7 ± 0	0.96±0.002
Western Pacific	2188125±78476	1535289±19721	751878±87746	102499±2247	-66.3± 2.9	0.911±0.003
Indian Ocean	52034±7484	37511±4186	60705±5562	46183±2436	22.3±7.3	0.851±0.004
Regions combined	2398149±87549	1677592±28465	868556±98270	151457±5182	-63.8 ± 5.4	N/A

RESULTS

When *P. lobata* was previously modeled as a homogenous population, without geographic isolation (Cacciapaglia and van Woesik, 2015), the species was predicted to increase overall habitat occupation by 8% $\pm$ 1%, ~380,000 km^2, irrespective of climate change scenario (Tables 4.1–4.3). By contrast, the present study showed that when the five genetically isolated regions of *P. lobata* were modeled as segregated regions, the species was predicted to lose suitable habitat. *P. lobata* is predicted to lose 64% ± 5% of its suitable habitat by 2100 under climate scenario RCP 8.5 Wm^{-2} (Table 4.1; Figure 4.1), lose 68% ± 4% of its suitable habitat by 2100 under climate scenario RCP 6.0 Wm^{-2} (Table 4.2; Figure 4.2), and lose ~67% ± 7% of its suitable habitat by 2100 under climate scenario RCP 4.5 Wm^{-2} (Table 4.3; Figure 4.3). The difference between the genetically connected and disconnected models represents over a 70% swing in predicted habitat occupancy caused by regional isolation.

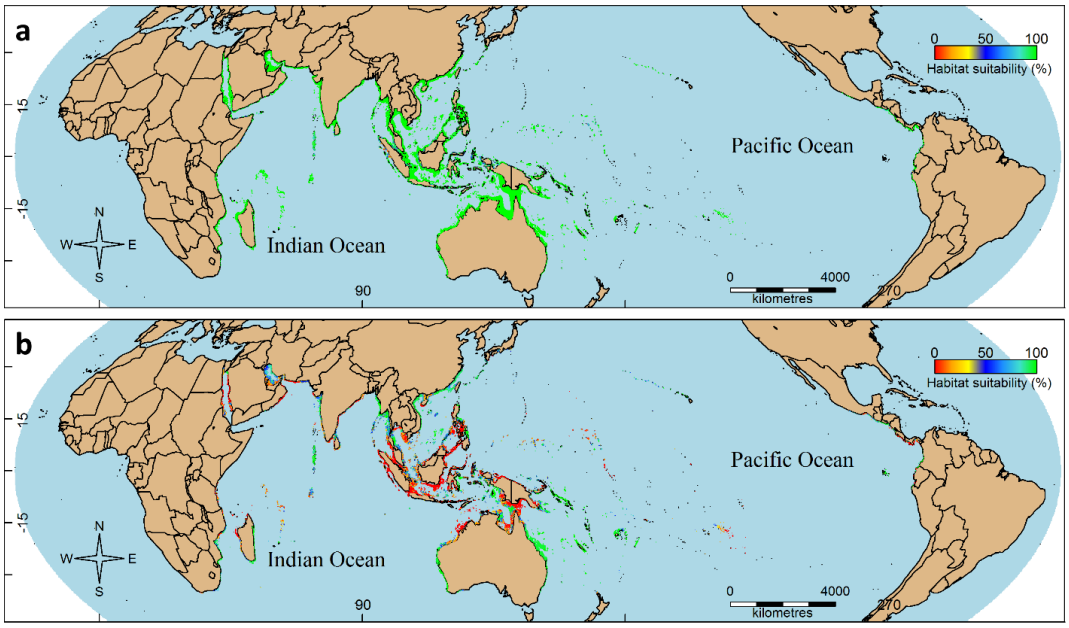

Figure 4.2 Predicted distribution of *Porites lobata* modeled as: **a)** a geographically homogenous population, and **b)** five geographically isolated subpopulations. Both models were run for the Indian and Pacific Oceans under climate scenario Representative Concentration Pathway (RCP) **8.5** Wm^{-2}. Green indicates where the suitable habitat for *P. lobata* is predicted to be maintained by 2100, red indicates were suitable habitat for *P. lobata* is predicted to be lost by 2100.

The percentage loss of *P. lobata* habitat was highest in the smallest geographic regions. For example, in the central Pacific Ocean, under each climate scenario, *P. lobata* is expected to lose 99.7% ± <0.1%, ~40,000 km^2, of the suitable habitat by 2100, because of the high temperatures that are predicted in that region (Tables 4.1–4.3). Similarly, the Hawaiian archipelago is predicted to lose between 60–92%, ~12,000–18,000 km^2, of the suitable habitat for *P. lobata* by 2100, depending on the climate scenario (Tables 4.1–4.3). The largest region, the western Pacific Ocean, is predicted to lose between 66% ± 3%, 72% ± 2%, and 68% ± 3%, of habitat suitable for *P. lobata* under respective climate scenarios RCPs 8.5, 6.0,

and 4.5 Wm^{-2}. This loss accounts for the largest absolute habitat change (~ 1,500,000 km^2), for any given region, by the year 2100 (Tables 4.1–4.3). The Indian Ocean, by contrast, is predicted to gain between 22–39%, ~9,000–18,000 km^2, of the habitat suitable for *P. lobata* by the year 2100.

Table 4.2. Change in habitat for *Porites lobata* through time (until 2100) for climate scenario Representative Concentration Pathway (RCP) **6.0 Wm^{-2}**, where AUC is the Area Under the receiver operating characteristic Curve.

Geographic Region	*Current habitat km²*	*Lost habitat km²*	*Future habitat km²*	*New habitat km²*	*% habitat change*	*AUC*
Contiguous	4415411±56215	4666±1297	4771203±25220	379440±44705	8 ± 1	0.97±0.01
Eastern Pacific	89515±2761	17569±1508	87424±1616	15478±2576	-2 ± 4	0.84+0.01
Hawaii	19956±246	10996±619	8035±756	0	-60 ± 3	0.87±0.01
Central Pacific	41019±486	40667±442	359±90	7±9	-99 ± 0	0.96±0
Western Pacific	2179827±74891	1660011±19888	612448±63530	96948±3427	-72.0 ± 2	0.91±0
Indian Ocean	46249±4699	35610±2690	63446±5171	52807±3126	39.2 ± 5	0.845±0.01
Regions combined	2376566±83083	1764853±25147	771712±71163	165240±9138	-67.5 ± 4.2	N/A

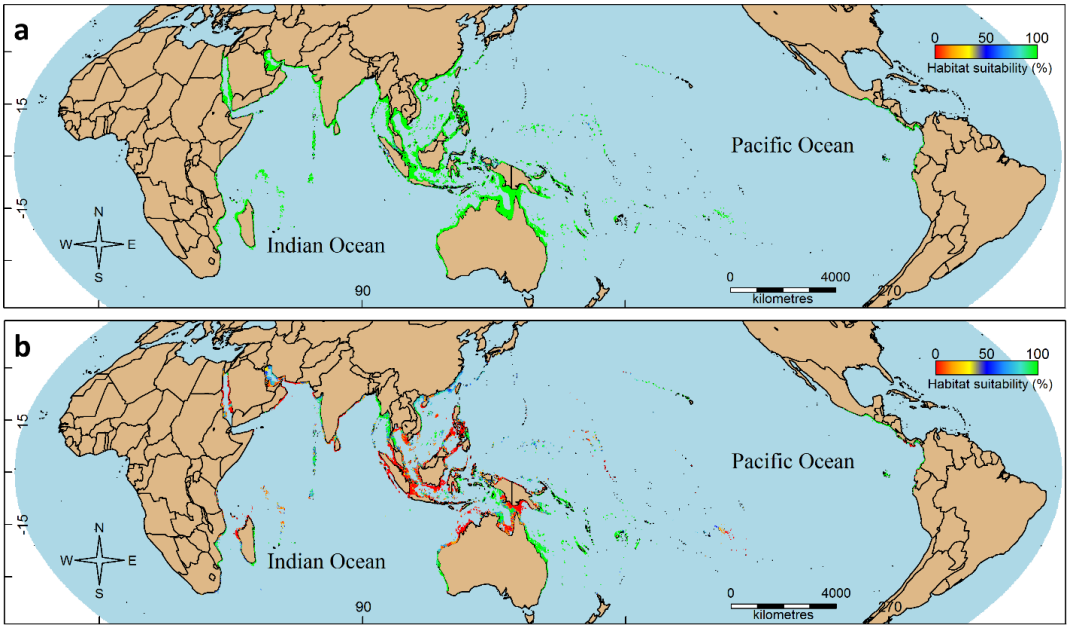

Figure 4.3 Predicted distribution of *Porites lobata* modeled as: **a)** a geographically homogenous population, and **b)** five geographically isolated subpopulations. Both models were run for the Indian and Pacific Oceans under climate scenario Representative Concentration Pathway (RCP) **6.0** Wm^{-2}. Green indicates where the suitable habitat for *P. lobata* is predicted to be maintained by 2100, red indicates were suitable habitat for *P. lobata* is predicted to be lost by 2100.

Table 4.3. Change in habitat of *Porites lobata* through time (until 2100) for climate scenario Representative Concentration Pathway (RCP) **4.5 Wm^{-2}**. The differences in suitable habitat (km^2) for the five independently run subpopulations and the genetically homogeneous (no genetic isolation) models are shown below. AUC is the Area Under the receiver operating characteristic Curve.

Geographic Region	*Current habitat km²*	*Lost habitat km²*	*Future habitat km²*	*New habitat km²*	*% habitat change*	*AUC*
Contiguous	4415411±56215	4601±1382	4767132±24601	376712±45835	8.1 ± 1.2	0.968±0.005
Eastern Pacific	89515±2761	18851±1695	86112±1780	15448±2595	-3 ± 4.4	0.837±0.007
Hawaii	19956±246	14109±542	4123±640	0	-79.5 ± 3	0.87±0.006
Central Pacific	41019±486	40951±476	67±17	0	-99.8 ± 0	0.958±0.003
Western Pacific	2179827±74891	1580245±18777	722178±83184	127012±3057	-67.5 ± 2.8	0.907±0.003
Indian Ocean	46249±4699	35076±2500	63917±6756	52744±4466	+38.6 ± 5.1	0.845±0.005
Regions combined	2376566±83083	1689232±23990	876397±92377	195204±10118	-66.9 ± 7.0	N/A

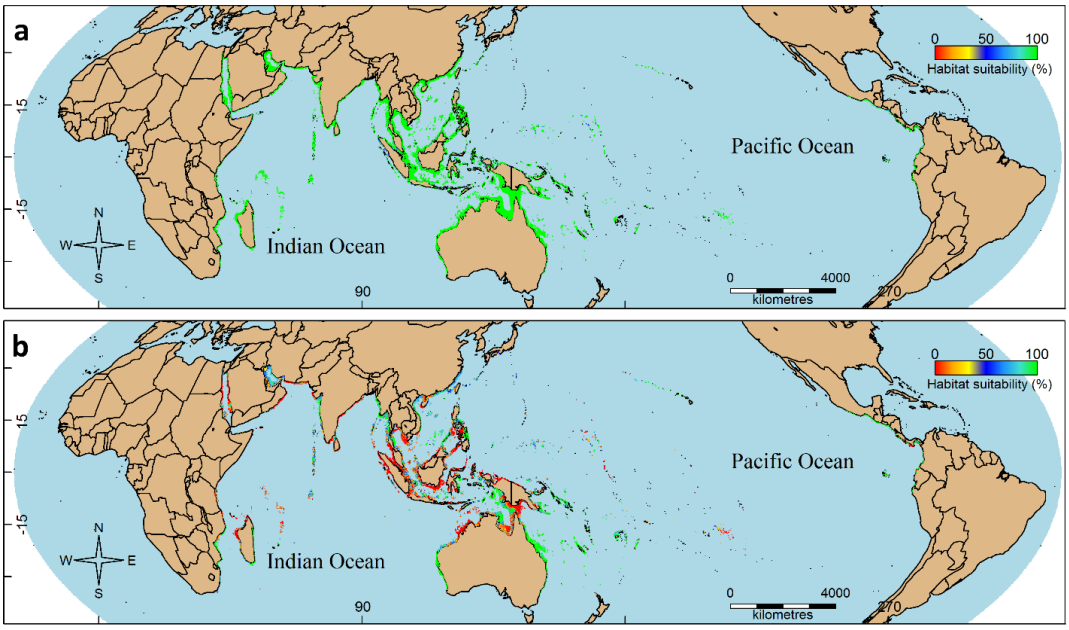

Figure 4.4 Predicted distribution of *Porites lobata* modeled as: **a)** a geographically homogenous population, and **b)** five geographically isolated subpopulations. Both models were run for the Indian and Pacific Oceans under climate scenario Representative Concentration Pathway (RCP) **4.5** Wm^{-2}. Green indicates where the suitable habitat for *P. lobata* is predicted to be maintained by 2100, red indicates were suitable habitat for *P. lobata* is predicted to be lost by 2100.

The differing climate scenarios did not greatly change the overall habitat loss of *P. lobata* when modeled as separate regions (Tables 4.1–4.3), except in the eastern Pacific, and in the Hawaiian archipelago, regions. By the year 2100, under RCP 8.5 Wm^{-2}, the west coast of Central America and equatorial South America is predicted to experience a significant loss of suitable habitat for *P. lobata* (44 %± 4.3%) (Table 4.1). Whereas under RCPs 4.5 and 6.0 Wm^{-2}, the eastern Pacific region is not predicted to lose a significant amount of habitat (2% ± 4%, and 3 ± 4% respectively;

Tables 4.2 and 4.3). Similarly, the loss of *P. lobata* habitat in the Hawaiian archipelago region was also variable, and dependent upon the climate-change scenario. The Hawaiian archipelago is predicted to lose 92% ± 3% under climate scenario RCP 8.5 Wm^{-2}, 60% ± 3% under climate scenario RCP 6.0 Wm^{-2}, and 80% ± 3% under climate scenario RCP 4.5 Wm^{-2} by the year 2100 (Tables 4.1–4.3). In the Indian Ocean, *P. lobata* is expected to gain 22% ± 7% suitable habitat for climate scenario RCP 8.5, and between 38–39% ± 5% suitable habitat for climate scenarios RCP 4.5 and 6.0.

DISCUSSION

The results of the present study show that genetic isolation may play a major role in the persistence of coral species under climate change. When the species-distribution model was run as a single homogeneous population, *P. lobata* is expected to increase its geographic range by approximately 8% by the year 2100. However, when the present model was run as five genetically isolated subpopulations, *P. lobata* is expected to decrease in geographic range by approximately 66%. The reason that the models differed so vastly was, in part, a consequence of the inherent assumptions of species-distribution models.

The homogenous species-distribution model assumes that individuals of widely distributed coral species are able to tolerate the entire range of environmental conditions in which the species is found. For example, *P. lobata* is found in tropical environments, where temperatures only range from 27–31^{o}C (Veron, 2000; Lough and Barnes, 2000; van Woesik et al., 2012), and in subtropical environments, where temperatures range from 18–28^{o}C (Veron, 2000; Fallon et al., 1999). Therefore, the tolerance range of all individuals of the species is assumed to extend from 18–31^{o}C, whereas in reality only a subset of the population can tolerate 31^{o}C, and likewise only a subset of the population can tolerate 18^{o}C for any length of time. Therefore, even under an RCP 8.5 climate scenario, the geographic expansion of the homogenous population is function of latitudinal range expansion. Yet, years of local adaptation have allowed some individuals of the species to adjust to marginal,

extreme environments, allowing those species to become widely distributed. Neglecting these local adaptations in marginal environments may inflate future distribution ranges when using species-distribution models as predictive tools.

Previous work on other systems, have considered the need to incorporate the effects of the environment on the development of phenotypes when modeling populations through climate change (Chevin et al. 2010; Atkins and Travis 2010; Valladares et al., 2014). Indeed, selection for phenotypic plasticity may have important consequences on a population's fitness (Chevin et al. 2010). Research in temperate forests has also predicted future species distributions by including the effects of isolation on phenotypic plasticity. For example, Valladares et al. (2014) showed that when subpopulations, which differ in thermal niches across a species' range, were forecasted under a warming climate, the projected outcomes were considerably less desirable than when modeling homogenous populations across the same geographic range. The fate of the populations varied, however, depending on whether phenotypic responses to environmental variables were more plastic near the margins or near the center of the species' range. Subtleties in phenotypic plasticity across a species' geographic range may have also played a critical role in determining which subpopulations survived within microrefugia through glacial cycles (Mosblech et al., 2011), and will also play a role in determining which subpopulations will survive contemporary extinction.

While selection for phenotypic plasticity may have important consequences on fitness and population persistence, the present species-distribution models do not include the inherent capacity of populations to live in environments outside the immediate range of their contemporary distribution. Clearly, some populations may have an inherent capacity to respond to climate change through phenotypic plasticity (Chevin et al., 2010), or through transgenerational adaptation (Dixon et al., 2015). Determining how much adaptation will realistically occur by the year 2100 is difficult, especially when attempting to disentangle the effects of phenotypic plasticity from adaptation. Besides, phenotypic plasticity may be an adaptive trait upon which natural selection can act (Via, 1993; Scheiner, 1993; Nussey et al., 2005). Still, why would a tropical species, which lives in water temperatures that only vary by 3^{o}C every year, have inherent properties that allows persistence outside that narrow temperature range? It may be just as reasonable to ask: Why would tropical populations purge any thermally tolerant pre-adapted genotypes, when there is relatively low selective pressure in benign tropical environments? As Fisher (1930, p. 37) stated: “The rate of increase in fitness of any organism at any time is equal to its genetic variance in fitness at that time”. Populations with high genotypic variance also may have latent genotypes that would allow some individuals to tolerate non-analogue future environments (Polato et al., 2013). It is however challenging, without experimental evidence, to model latent responses of tropical organisms to

conditions outside their immediate habitats, especially considering the unknown interactions that may also affect their future distribution and dispersal.

When the predictive model was run as one continuous population, *P. lobata* gained habitat, particularly in the Indian Ocean. Similarly, when *P. lobata* was modeled as five distinct populations, including a separate subpopulation for the central and western Indian Ocean (Fig. 1), *P. lobata* gained habitat in the Indian Ocean. There was a 22% increase predicted for climate scenario RCP 8.5, and nearly a 40% increase in habitat in the Indian Ocean for climate scenario RCP 4.5 and RCP 6.0. This habitat expansion was predicted within the southern Red Sea, and along Somalia (Figures 4.2–4.4), although habitat expansion along the coast of Somalia may be substrate limiting. Most habitat loss was predicted in the Gulf of Oman.

There was a close geographic alignment of climate-change refuges in the present study and those defined previously by Cacciapaglia and van Woesik (2015) (Figure 4.2). There were however several exceptions, including the Chagos Archipelago, Seychelles, northern Indonesia, the northern Marshall Islands, and French Polynesia (Figure 4.2). These localities were predicted to be safe-haven refuges under ocean warming when *P. lobata* was modeled as a homogenous population (Cacciapaglia and van Woesik, 2015). However, the present study identified these same areas as potentially vulnerable to climate change when *P. lobata* was modeled as geographically isolated. In conclusion, genetic connectivity will likely play a major role in the ability of corals to persist under climate change.

Indeed, modeling the ubiquitous species *P. lobata* as five genetically isolated subpopulations decreased the predicted habitat occupancy by more than 60%, when compared with model predictions of a single genetically homogenous population.

CHAPTER 5. REEF ACCRETION THROUGH SEA-LEVEL RISE

ABSTRACT

Coral reefs are one of the world's most diverse and valuable marine ecosystems. Since the mid-Holocene, some 5000 years ago, sea-level rise has been stable in the Pacific and Indian Oceans and reef accretion has occurred primarily along the reef edges. Contemporary climate change is however causing rapid sea-level rise, and is generating vertical accommodation space on coral reefs worldwide. Yet, we know little about whether modern coral reefs can keep pace with projected sea-level rise as the oceans continue to warm. Here we examine the response of four primary reef accreting species, selected as a proxy for reef-building assemblages throughout the Pacific and Indian Oceans. We use a species-distribution model with a 9 km resolution to identify locations within the Indo-Pacific where these corals can persist into the future. We use the species-distribution model alongside a reef-accretion model, which incorporates the best available information on calcification, sedimentation, and erosion rates, to identify where these coral assemblages can potentially accrete reefs fast enough to keep up with projected increases in sea level by the year 2100. Reefs are projected to keep up with sea-level rise in the Maldives, the Chagos Archipelago, northern Indonesia, Micronesia, the Marshall Islands, the Solomon Islands, Vanuatu, and Fiji. In contrast, reefs are likely to drown in locations

predicted to have increasing thermal stress, and at high latitudes where reduced light and temperature are not conducive for rapid accretion.

INTRODUCTION

Millions of people rely on coral reefs to protect them from storm surges, and to provide fisheries. Nations such as the Maldive, who inhabit coral atolls, are entirely dependent on the maintenance of healthy reef systems for their survival. Coral reefs are also diverse ecosystems that provides a physical wave barrier and resources for millions of coastal residents worldwide. Over the last three decades, however, coral assemblages have been repeatedly subjected to anomalously high thermal-stress events, which have resulted in coral bleaching, subsequent coral mortality, and changes in reef composition (Hoegh-Guldberg 1999; Loya et al. 2001; Hughes et al. 2003; Hoegh-Guldberg et al. 2007; Pandolfi et al. 2011; van Woesik et al. 2011). A change in reef composition and the loss of major reef-building corals would reduce the potential rates of reef accretion, and impair the capacity of reefs to keep up with projected sea-level rise. On average, sea level is rising by 2 mm per year, although those rates are expected to increase to 9 mm per year over the next several decades (Vermeer and Rahmstorf 2009; IPCC 2013; Jevrejeva et al. 2013). Consequently, coral reefs are experiencing an increase in vertical accommodation space on reef flats (van Woesik et al. 2015). Yet it is largely unknown where coral reefs are expected to accumulate carbonate fast enough to keep up with projected increases in sea-level rise while the oceans continue to warm.

A rapid rise in sea level followed the last ice age, around 18,000 years ago (Lambeck and Chappell 2001), when sea level was approximately 130 m lower than today. On a global scale, sea-level rise was not homogenous but was dependent on local and regional isostatic rebound effects from continental ice masses, and regional tectonics (Lambeck and Chappell 2001). Depending on their locality and reef-building capacity, coral reefs eitherkept up with sea-level rise, eventually caught up with sea level, when sea level stabilized in the mid-Holocene, some 5000 years ago (Chappell and Shackelton 1986), or (iii) did not keep up with sea-level rise through the glacial transgression period and 'drowned' (Neumann and Macintyre 1985). In the Indian and Pacific Oceans, since the mid-Holocene, reef flats have been constrained by aerial exposure at low-water-spring tides, at modern sea level, and reef flats have existed largely in a dormant state (Woodroffe et al. 2012; Roff et al. 2015). The expansion of coral reefs in these oceans has occurred primarily along the reef edges, often referred to as lateral progradation (Roff et al. 2015).

Historically, the maximum rates of reef accretion in the Indo-Pacifichas been estimated at 12 kg $CaCO_3$ m^{-2} y^{-1} (Edinger et al. 2000), which is equivalent to approximately 7–10 mm of reef growth per year (Smith and Kinsey 1976). A 'healthy' coral reef was thought to accumulate, on average, ~4 kg $CaCO_3$ m^{-2} y^{-1}, which translates to 3–5 mm per year of vertical growth, and a reef with low coral cover was thought to accumulate less than 1 kg $CaCO_3$ m^{-2} y^{-1} (~ 1 mm per year of growth) (Smith and Kinsey 1976; Buddemeier and Hopley 1988). Past estimates of rates of

reef accretion were calculated using either geological cores (Hubbard 2008), or *in situ* measurements of change in total alkalinity (Smith and Kinsey 1976). Most recently, however, rates of reef accretion have been estimated using both high-precision U-series ages of coral cores (Roff et al. 2015) and *in situ* measurements of reef composition to model estimates of net accretion (Perry 2008; Perry et al. 2015). For example, Roff et al. (2015) estimated that over the last 1000 years, reef slopes along the inner Great Barrier Reef have laterally prograded on average 11.5 ± 1.1 mm per year. Similarly, Perry et al. (2015) estimated that, recently, the majority of Caribbean reefs have been undergoing net erosion, because the estimates of local rates of erosion exceeded local rates of accretion.

Through geological time, reef growth has only occurred at locations where the local production of calcium carbonate has exceeded the local destruction (Darwin 1842; Neumann and MacIntyre 1985; Buddemeier and Hopley 1988; Glynn 1997; van Woesik and Done 1997; Perry et al. 2013; Pandolfi 2015). Local production occurs by the incremental buildup of calcifying organisms, particularly corals and coralline algae, and through the accumulation of calcareous sediment (Adey 1978; Davies 1983; Edinger et al. 2000; Perry et al. 2008; Perry et al. 2012; van Woesik 2013). Local destruction occurs by the removal of calcium carbonate, which can take three forms: (i) physical erosion,; (ii) chemical erosion; and (iii) biological erosion.

Physical erosion occurs primarily during large storms, including cyclones (Gouezo et al 2015). Reefs near the equator are locally unadapted to cyclones, and when they do occur, the storm-associated waves can be highly destructive (Roff et al. 2015). By contrast, reefs are highly cemented where cyclones are common, and reef corals are morphologically tolerant of the intense and frequent wave impact (Chappell 1980; Madin and Connolly 2006). For example in Guam and Okinawa, which experience multiple cyclones every year, reefs barely show signs of damage following the passage of the cyclone (van Woesik, pers. obs.).

Reef erosion can be also chemical. The recent literature suggests that chemical erosion may be playing a larger role on modern and future reefs than it did historically, primarily because of recent increases in ocean acidification (Hoegh-Guldberg et al. 2007; Doney et al. 2009; Veron et al. 2009). Ocean acidification can increase the rate of dissolution of bare calcium carbonate (Ries 2010), whereas live corals may buffer themselves from ocean acidification by modifying their internal chemistry (McCulloch et al. 2012). A multitude of living reef organisms can erode calcium carbonate, including sponges and worms (Glynn 1997), sea urchins (Bak 1993; Silva and McClanahan 2001), and herbivorous fishes. Biological erosion is inherently heterogeneous in its effects as it is influenced by biotic, e.g., fish denisities, and abiotic factors, e.g., ocean chemistry (Pandolfi et al. 2011). Further complexity is added by human-induced alteration of local ecosystems through adjacent landuse, pollution, and fishing (Connell 1997; De'ath and Fabricious 2010).

For example, localities with high fishing pressure can release sea-urchin populations from predation pressure, which can be detrimental to reefs when these sea-urchin densities are high (McClanahan 1990; McClanahan 1994). Additionally, high nutrient loads can increase populations of boring sponges, polychaetes, and sipunculids (Glynn 1997; Edinger et al. 2000; Grand and Fabricius 2011) that can cause high internal bioerosion. Most coastal reefs, with high human densities, have both high fishing pressure and high nutrient loads (Vitousek et al. 1997). In combination, these stressors lead to high erosion rates of nearshore reefs (Perry et al. 2015). An extreme example is evident in the polluted Jakarta Bay, along The Thousand Islands (Kepulauan Seribu), Indonesia, where Tomascik et al. (1993) reported erosion of entire reef flats, which had previously supported diverse coral assemblages some decades earlier (Umbgrove 1929).

As in the past, rates of reef accretion in the future will depend on the persistence of framework-building coral species, and on their capacity to calcify and accumulate faster than the erosional processes. Over the next century, the ocean temperatures are expected to rise between 1.0 – and 3.7°C. These conditions will consequently increase the risk of coral bleaching, cause a decline in coral growth, and induce widespread coral mortality. Thermal stress events in the oceans, however, vary spatially and temporally (Burrows et al. 2011), and the same locations that have experienced high thermal stress in the past century have recently experienced the most severe thermal stress impacts (Thompson and van Woesik 2009). If these

patterns persist into the near future, as most global-climate models suggest (IPCC 2013), then some localities will receive both more intensive and more frequent thermal stress than other localities. By contrast, some locations may act as climate-change refuges (Cacciapaglia and van Woesik, 2015), where sea-surface temperature are not predicted to increase rapidly. These locations may provide thermal safe havens where coral reefs are able to keep up with sea-level rise. Identifying coral refuges is an important research priority. This study is a first-order approximation of rates of reef accretion in the face of ocean warming across the Pacific and Indian Oceans. Reef accretion estimates allowed us to identify where reefs will most likely accrete carbonate at rates sufficient to maintain vertical growth and keep up with predicted rates sea-level rise by the year 2100.

METHODS

SPECIES DISTRIBUTION MODEL

Species-distribution models were used to identify habitats that were potentially suitable for coral species under climate-change scenarios. These models fit the geographic distribution of a species to the environment in which it is currently living. Geographical projections of the same environmental parameters from climate models were then used to predict where the species is likely to persist into the future. The species-distribution models considered: (i) the contemporary distribution of species, (ii) the environmental conditions in which the species is found, and (iii) the forecasted environmental conditions from climate models. This study focused on four reef-building coral species, *Acropora digitifera, Acropora hyacinthus, Porites lobata,* and *Porites rus*, chosen to represent the general response of reef-building corals to sea-level rise and thermal stress in the Indian and Pacific Oceans. The four species were also chosen for their capacity to contribute to reef growth, and for their variation in susceptibility to thermal stress. *Porites lobata* and *P. rus* are generally more tolerant to thermal stress than *Acropora* species (Loya et al. 2001).

The geographic localities of the four coral species were recorded as either present or absent, for which we were 95% certain that the coral species of interest were indeed absent using a probability-of-detection algorithm (see Cacciapaglia and van Woesik 2015). The geographical distribution of the coral species were

determined using Veron (2000), IUCN's Red List http://www.iucnredlist.org/technical-documents/spatial-data, and Wallace (1999). Environmental conditions at grid cells of 9.2 km (outlined below) were extracted at 3000 points where the species was present and absent, enough points to cover the geographic extent of the study,. We used a hierarchical Bayesian-generalized-linear mixed model, with a flat prior following a gamma distribution. The environmental covariates were: (i) range in sea surface temperature, (ii) range in irradiance, and (iii) turbidity. Turbidity was expressed as a random effect, binned to remove no-analog scenarios. The bin size for turbidity was optimized to reduce the model's Akaike's Information Criterion (AIC) score. An ensemble of twenty-five SDM runs, each using the model with the highest area under the receiving operating curve (AUC) value from 100 random iterations, were run to predict contemporary and future distributions for each of the four species following Cacciapaglia and van Woesik (2016).

Mechanistic constraints were applied to the SDM output to realistically constrain model estimates without increasing model complexity. These mechanistic constraints were based on the study by Cacciapaglia and van Woesik (2016), and were implemented as follows. First, a dispersal restriction was implemented to limit the distance of annual range expansion to 10 km per year based on reproductive studies (Miller and Munday, 2003; Shanks et al., 2003; van Woesik, 2010), dispersal

models incorporating warming oceans (O'Connor et al., 2007; Figueiredo et al., 2014), and genetic studies (Ayre and Hughes, 2000). Second, the outflow areas of large rivers, where freshwater effects jeopardize coral survival, were masked out as viable habitats based on drainage size. Third, a cold-water mask was implemented, excluding all reef habitats that experience <18ºC at any time of the year (Kleypas 1997; Kleypas et al. 1999). Fourth, a mask was applied outside of the contiguous oceanic region, where species experience geographic vicariance. Fifth, any site that experienced <250 μmol m^{-2} s^{-1} irradiance at 3 meters depth was masked out as the water was considered too turbid for substantial photosynthesis and reef growth (Kleypas et al. 1999). The difference between modern-day species distributions and future species distributions was interpolated linearly through time, which allowed us to estimate intermediate probabilities of species presence, at each time step of the model, based on modern-day and future distributions (all the R code for the model is available in the supplementary document).

REEF-ACCRETION MODEL

In its simplest form, reef accretion (kg $CaCO_3$ m^{-2}) was modeled at a given locality *i*, (with a spatial resolution of 5 arc min, or 9.2 km cell size) at a given time, *t*, as:

$$Reef\,accretion_{i,t} = Cal_{i,t} + \mathrm{sgn}(x)\,Sed_{i,t} - Eros_{i,t} \quad (1),$$

where *Cal* is the rate of calcification by reef-building corals, sgn is positive when local sedimentation (*Sed*) is low, and negative when local sedimentation is high, and *Eros* is the rate of erosion (after van Woesik 2013). Calcification was assumed to follow optimal performance curves, or niche space, taking the form of Gaussian distributions, dependent on water temperature and irradiance (supplementary document). The temperature component of the model varied through time, assessed at 5-year intervals based on Representative Concentration Pathway (RCP) 8.5 Wm^{-2} model scenarios from the Coupled Model Intercomparison Project Phase 5 (CMIP5) (Cacciapaglia and van Woesik, 2016). Optimal values for temperature and irradiance were derived from the respective median and mean values of current environmental data extracted at the presence points where the species were located.

Maximum calcium carbonate deposition under modern-day climate is approximately 12 kg $CaCO_3$ m^{-2} (Edinger et al. 2000). In a natural leeward setting, *Porites lobata* may be the sole contributor to rapid reef-accretion rates, and likewise on windward reefs *Acropora* may be the primary contributor to rapid reef accretion (Blanchon et al. 2014). For the purpose of this model, however, given the spatial resolution of 9.2 km, we assumed that reef accretion was most optimal, in a given locality, *i,* in the presence of all four species. We therefore allocated a maximum reef-building capacity of 3 kg $CaCO_3$ m^{-2} per year for each species. The rationale was to examine where, geographically, all four species might maintain their reef-building

capacity, and contribute to reef accretion as a general response of reef-building corals to sea-level rise and thermal stress. To account for the allometric reduction in reef height as calcium carbonate increases, mass accretion (kg $CaCO_3$ m^{-2} y^{-1}) was translated to vertical reef accretion (mm y^{-1}) using:

$$Vertical\ reef\ accretion = kg - 0.01 * kg^{((kg+1)/kg*1.45)} \quad (2),$$

where *kg* is the amount of 2-dimensional accretion of calcium carbonate per year (kg $CaCO_3$ m^{-2}).

SEDIMENTATION

Sedimentation (mg cm^{-2} d^{-1}) was estimated using the log inverse of average water-flow rate. Flow-rate data (ms^{-1}) were collected from the Integrated Climate Data Center (ICDC; http://icdc.zmaw.de/). The zonal and meridional velocities of water flow, at 5 m depth, were averaged from 2006 to 2010, and their product was taken to find directionless flowrate per locality (at a spatial resolution of 9.2 km). This flow-rate proxy for sedimentation was previously validated with *in-situ* data collected by sedimentation traps from studies by Rogers (1990) and by Szmytkiewicz and Zalewska (2013). For the purposes of the model, flow rate was assumed to remain constant through time. If the rate of sedimentation was between 0–5 mg cm^{-2} d^{-1} then the sign of sedimentation, in equation 1, was positive, if sedimentation was greater than 5 mg cm^{-2} d^{-1} then the sign was negative (van Woesik, 2013). The maximum reduction of calcification rates caused by sedimentation was adjusted to

match the total growth of the reef in each 9.2 km cell, so that the effect of sedimentation, in this model, could inhibit reef growth, but would not cause erosion. We also assumed that about two thirds of the sediments were exported from the reef (Hubbard 1986).

EROSION

Reef erosion was broken down into three major components, defined as:

$$Eros_{i,t} = phy.erosion_{i,t} + chem.erosion_{i,t} + bio.erosion_{i,t} \quad (3),$$

where *phy.erosion* is the physical erosion caused by cyclones, *chm.erosion* is the chemical dissolution of reef caused by ocean acidification, and *bio.erosion* is the biological erosion caused by marine organisms. To determine physical erosion, cyclone data were collected from International Best Track Archive for Climate Stewardship (IBTrACS; http://www.ncdc.noaa.gov/ibtracs/index.php?name=ibtracs-data) as spatial points and imported into R (R Core Team 2016, version 3.22). These data were subset into storm categories based on wind speed, according to the Saffir-Simpson scale. A raster file for the spatial frequency of cyclones was made in Quantum Geographical Information Systems (QGIS) using the 'heatmap' function, with a radius matching the radius of damaging winds (>26 ms^{-1}; Moyer et al. 2007) for each cyclone category (supplementary information). These radii followed an analysis by Moyer et al. (2007), and considered 50 years of consistent sampling effort, between 1964 and

2014. Individual yearly raster files were summed, and then divided by 50 years, to determine the average number of cyclones per cell (9.2 km), per year. A raster for the magnitude of the cyclones was created by interpolating wind speeds across all storm tracks using the inverse distance weighted interpolation in QGIS. For the model, the maximum amount of $CaCO_3$ that any given cyclone could remove was set to 1350 kg $CaCO_3$ m^{-2}, which was applied to localities that reported infrequent, yet large magnitude storms. This matches 1 meter of vertical reef accretion over the entire reef, which has been observed after large cyclones pass over reefs that infrequently experience cyclones (van Woesik et al. 1991). Storm frequency was represented as a binomial distribution following the equation:

$$Storm\ frequency = \binom{T * 365}{k} \left(\frac{p}{365}\right)^{k} \left(1 - \frac{p}{365}\right)^{T*365-k} \quad (4),$$

where k is the estimated number of cyclones over time T (years), and p is the average number of storms observed per year, per raster cell. The estimated number of cyclones over the projected time was then multiplied by the potential storm damage in each raster cell, i.

Chemical erosion was incorporated into the model by using pH as a proxy for ocean acidification. The CMIP5 projected pH data, for the global climate model of RCP 8.5 Wm^{-2}, were collected as global raster images for the years 2006–2100 from ftp://data1.gfdl.noaa.gov/11/CMIP5/output1/NOAA-GFDL/GFDL-ESM2M/rcp85/mon/ocnBgchem/Omon/r1i1p1/v20110601/ph/ as a 1x1 degree

raster. These raster data were collected at 5-year-averaged intervals, and transformed to match the environmental parameters used in the SDM. A linear model, using data from van Woesik et al. (2013), was run to determine how much $CaCO_3$ is potentially lost, based on pH. This relationship follows the following equation:

$$Chm.erosion = (6.65 - 0.81\ x)^{1.667} \quad (5),$$

where $chm.erosion$ is the kg CaCO3 m^{-2} yr^{-1} reduction in $CaCO_3$. The level of chemical erosion was predicted in each cell of the raster, based on the projected pH at each 5-year time interval. The sum of predicted erosion, for all time slices between 2006 and 2100, was calculated in each raster cell and summed to determine the overall potential loss of $CaCO_3$. Chemical erosion was modeled as an effect of calcium carbonate dissolution, and not as an effect of reef-growth inhibition because of the ability of corals to internally regulate pH (McCulloch et al. 2012).

Biological erosion was broken down into two primary components: (i) bioerosion from sea urchins, and (ii) bioerosion from infaunal organisms, such as boring sponges, polychaetes, and siphuculids. The rate of bioerosion by urchins on reefs is directly related to the density of sea urchins (Silva and McClanahan 2001). Sea urchin densities were assumed to be minimal at localities where secondary trophic-level fishes (i.e., invertivores) were high and vice versa (McClanahan and Shafir 1990). Maximum bioerosion (22.3 kg m^{-2} yr^{-1}) was estimated in locations where the biomass of invertivore fishes was minimal (Williams et al. 2011). Williams

et al. (2011) showed that fishing pressure and the density of invertivore fishes, was a function of human population density, following the function:

$$Biomass = -2.73 * log10(population + 1) + 17.23 \quad (6),$$

where *biomass* is the biomass of secondary-trophic level fishes, and *population* is the human population summed within a 30 km radius of each grid cell. Geotagged data from Williams et al. (2011) were compared with the current human population raster (2015), from the Center for International Earth Science Information Network (CIESIN). These data were aggregated to match the 9.2 km resolution of the environmental variables. Varying buffer sizes were tested to estimate the distance at which the coastal population matched the populations in Williams et al. (2011). The best match occurred when all cells in the raster, within a 30 km radius, were summed. Human population was projected into the year 2100 using birth and death rates for each country (collected from the World Bank as the adjusted UN census for 2015), and the difference between birth and death represented growth rate. A carrying capacity of 11.2 billion was used, matching estimates from the United Nations. Population growth rates were attached to shapefiles, and converted to raster data. A moving-window analysis, using the 'focal' function from the package raster (Hijmans, 2015), was applied to each predicted population raster to match the 30 km aggregation of population, in each cell at every time step. This aggregated-population

raster was then used in equation 6 to predict invertivore biomass and sea-urchin densities. Coastal populations were reassessed at 5-year intervals, and erosion was summed throughout the model run (supplementary document).

Eutrophic areas often have high bioerosion (Hallock and Schlager 1986; Edinger and Risk 1994). In this model, locations that had high and persistent concentrations of chlorophyll *a*, were considered eutrophic. We used time-averaged chlorophyll *a* as a proxy for infaunal bioerosion. Chlorophyll *a* data were collected from SeaWIFS satellite observations, and time averaged from 1998–2007. These data were cropped between the latitudes 45ºS and 45ºN, and used as a proxy for internal bioerosion of micro- and macro-boring organisms. The maximum rate of internal erosion, 2.4 kg m^{-2} yr^{-1}, from Pari et al. (1998), was used to scale the chlorophyll raster into a proxy for internal erosion. In this model, internal bioerosion is assumed to remain constant into the future.

SEA-LEVEL RISE

Sea-level rise data were extracted from the Integrated Climate Data Center (ICDC) as the RCP 8.5 Wm^{-2} ensemble mean. These data were extracted at yearly intervals so that the model could be run for each year leading up to 2100. The rate of

sea-level rise was compared with rates of vertical reef accretion (equation 1) at a spatial resolution of 9.2 x 9.2 km^2 through to the year 2100.

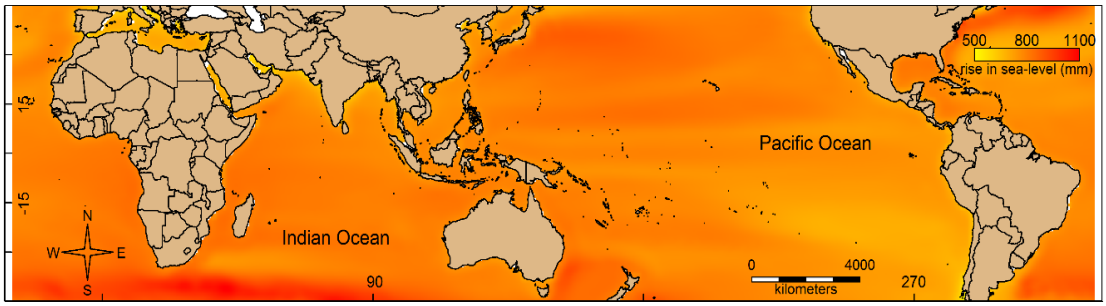

Figure 5.1 Projected rise in sea-level by 2100 under climate scenario Representative Concentration Pathways (RCP) 8.5.

RESULTS

REEF ACCRETION

Overall, localities optimal for reef growth are predicted to decline into the year 2100. The maximum allocated reef-building capacity of each species in the model was set at 3 kg $CaCO_3$ m^{-2} per year, or approximately 3 mm yr^{-1} (equation 2). The coral species varied considerably in their extent of contribution to vertical-reef growth. *Acropora digitifera* had a modern-day contribution to vertical-reef growth of approximately 1.90 mm yr^{-1}, and by the year 2100, *A. digitifera* is expected to contribute 1.26 mm yr^{-1} (Table 1). *Acropora hyacinthus* had similar contribution rates as *A. digitifera*, accreting at 1.90 mm yr^{-1} on modern reefs, and 1.31 mm yr^{-1} by the year 2100. *Porites lobata,* and *Porites rus* had similar modern-day contribution rates (2.33 and 2.17 mm yr^{-1} respectively), but differed in projected contributions for the year 2100 (2.25 and 1.70 mm yr^{-1} respectively). The two *Porites* species were projected to contribute more to vertical-reef growth into the year 2100 than the two *Acropora* species (Table 1). The species projected to contribute the highest gross carbonate to reefs in the Indo-Pacific was *Porites lobata*. Net accretion closely followed calcification rates for each species, however, accretion rates were often higher than calcification rates, because of the incorporation of low-level calcareous sediment (<5 mg cm^{-2} d^{-1}) into the reef (Table 1).

SEDIMENTATION

Overall, sedimentation reduced vertical accretion, rather than contributing to net accretion across the Indo-Pacific. The largest increase in reef-accretion rates from calcareous sedimentation was predicted in the Seychelles, Chagos Archipelago, the

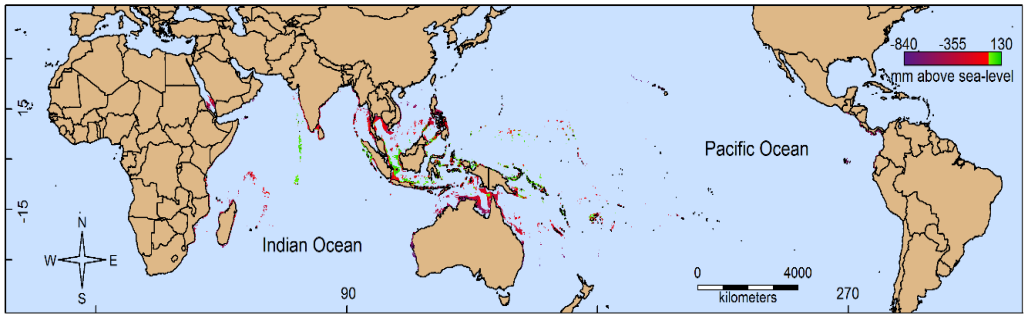

Figure 5.2 Projected reef height relative to sea-level rise in the year 2100 by accretion of four primary reef building species under climate scenario Representative Concentration Pathways (RCP) 8.5. Red to purple scale indicates 'sinking' reefs, light green to dark green scale indicates reefs that are able to keep up with sea-level rise.

Maldives, the Marshall Islands, the Galapagos Islands, and the Solomon Islands. The largest reduction in vertical accretion was predicted along the northern coast of Australia, Malaysia and the Gulf of Thailand, eastern Madagascar, Borneo and the Sulu Sea, the Red Sea, the Persian Gulf, and the Philippines.

Table 5.1. Predicted contribution of calcification, erosion, and net accretion in the **year 2100** averaged over the spatial distribution for each species.

Species	Contribution of calcification ($mm.yr^{-1}$)	Contribution of erosion ($mm.yr^{-1}$)	Net accretion ($mm.yr^{-1}$)
Acropora digitifera	1.2577	0.3485	1.6945
Acropora hyacinthus	1.3097	0.3587	1.6636
Porites lobata	2.2502	0.3583	2.3768
Porites rus	1.7026	0.3597	1.9440
Combined	6.5203	1.4252	7.6789

EROSION

Erosion rates were very similar on reefs occupied by each species in the model, averaging a 0.06 mm yr^{-1} reduction in vertical accretion on contemporary reefs, and a 0.36 mm yr^{-1} reduction in vertical accretion by the year 2100. Cyclones were responsible for a maximum reduction of approximately 13.5 mm of vertical

Table 5.2. Estimates of **modern** contributions of calcification and erosion, and estimates of net accretion averaged over the spatial distribution of each species.

Species	Contribution of calcification ($mm.yr^{-1}$)	Contribution of erosion ($mm.yr^{-1}$)	Net accretion ($mm.yr^{-1}$)
Acropora digitifera	1.8939	0.0710	1.9434
Acropora hyacinthus	1.8954	0.0465	1.9252
Porites lobata	2.3284	0.0439	2.3302
Porites rus	2.1706	0.0720	2.1577
Combined	8.2884	0.2335	8.3565

accretion loss per year. However, when reef degradation by cyclones was averaged over all areas that experience such storms, loss of accretion was only ~0.3 mm yr^{-1}. The zones of highest physical erosion were predicted to be located just above and below the doldrums (between 10 degrees N and S of the equator), particularly in the northern hemisphere, and near the outskirts of where storms frequently occur. Chemical erosion by ocean acidification was predicted to be minimal throughout the study region, with an average global loss of 11.5 mm over the projected 94 years. Most areas of high chemical erosion were identified in upwelling areas, primarily in the southern hemisphere, as well as in northern Malaysia, and western Japan. Biological erosion was the largest component of total erosion. Maximum reef erosion from organisms reached ~16.5 mm y^{-1} over the 94 year time frame. The highest rates of erosion were located in close proximity to dense coastal populations such as in India, China, sub-Saharan Africa, Madagascar, Central America, and much of Indonesia. Most bioerosion was predicted to occur by echinoid biomass. Boring infauna and eutrophied habitat accounted for less than 10% of the total biological erosion, and was locally restricted to locations where chlorophyll *a* was persistent throughout the year.

SEA-LEVEL RISE VS ACCRETION

Over 690,000 km^2 of reef was projected to keep up with sea-level into the year 2100 (Figure 5.2). Most of these reefs were near equatorial latitudes, rather than

at higher latitudes. The rate of vertical reef accretion was projected to keep pace with sea-level rise in (i) the Maldives, (ii) the Chagos Archipelago, (iii) northern Indonesia, (iv) Micronesia, (v) the Marshall Islands, (vi) the Solomon Islands, (vii) Vanuatu, and (viii) Fiji (Figure 5.2). An estimated 2,100,000 km^2 of reef habitat was projected to be unable to deposit enough $CaCO_3$ to keep up with rising sea-levels.

DISCUSSION

The combined contribution of the four coral species to reef accretion was projected to outpace sea-level rise where environmental conditions, particularly temperature, remained conducive to support the species, and where rates of biological erosion were minimal. The model predicted that many low-latitude reefs will keep up with the rate of sea-level rise, at least until the year 2100. These reefs almost exclusively lie within previously identified refugia (Cacciapaglia and van Woesik, 2015; Cacciapaglia and van Woesik, 2016). In fact, seven of the eight locations identified in this study were aligned with previously identified climate-change refugia. These locations are (i) the Maldives, (ii) the Chagos Archipelago, (iii) northern Indonesia, (iv) Micronesia, (v) the Marshall Islands, (vi) the Solomon Islands, and (vii) Vanuatu. The one location not tagged as a climate-change refuge but capable of keeping up with sea-level rise was Fiji, where the habitat is predicted to become too warm for many species in the future. The disparity between the outcomes of the studies may be a consequence of the ubiquitous distributions of the four coral species modeled in the present study compared with the more variable suite of distributions, and hence more variable environmental tolerances, of the twelve coral species modeled in Cacciapaglia and van Woesik (2015). The present study suggests, therefore, that some localities may lose diversity but might still have the capacity to keep up with sea-level rise if they continue to support the major reef

builders. High reef accretion in low diversity systems has been observed in the eastern Pacific by Toth *et al*. (2012) supporting this concept.

Sea-level rise was also predicted to outpace reef accretion in some of the localities that were previously identified as climate-change refugia. In particular, reefs along both the western and eastern coasts of Australia, along the coasts of Madagascar, the Seychelles, and French Polynesia were previously identified as climate-change refuges, where corals will likely be tolerant to future thermal stress. Yet, many of these reefs, including the Seychelles, French Polynesia, and eastern Australia, had projected vertical accretion rates that were only slightly slower than the rate of sea-level rise. Indeed, if the maximum accretion rate of the model was increased from 12 to 14 kg $CaCO_3$ m^{-2}, these reefs would be able to keep up with the rate of sea-level rise. Such high rates of reef accretion are reasonable. For example, using high-precision U-series ages, Roff et al. (2015) estimated that over the last 1000 years reef slopes along the inner Great Barrier Reef have grown rapidly, up to 35 mm per year, with an average rate of 11.5 ± 1.1 mm per year. Yet averaging over geological time may conceal the capacity of modern reefs to keep up with modern sea-level rise (Kiessling and Eichenseer, 2014). Although reef growth has long been considered to be a geological process (Darwin 1842; Hubbard 1997), and the product of the gradual accumulation of skeletons of diverse coral species over time (Hopley 1982; Blanchon et al. 2014), time averaging may conceal the maximum rates at which reefs are capable of responding to sea-level rise. Given the contemporary

accommodation space, massive and branching *Porites*, in particular, are capable of rapid response, particularly on reef flats (van Woesik et al. 2015). More troubling however is the potential decline in the growth rates of reef-building corals as the oceans continue to warm.

Warmer oceans will reduce the rates at which reefs will be able to vertically accrete and keep up with sea-level rise. Although *Porites* are generally considered resilient to acute thermal-stress events, and have not undergone extensive mortality in past bleaching events (van Woesik et al. 2012), long-term increases in temperature have resulted in declines in calcification and growth rates (Tanzil et al. 2009, De'ath et al. 2009). Recently van Woesik et al. (2015) examined the response of massive *Porites* growth rates under a range of average temperatures, from 60 sites. The results showed a unimodal function (i.e., a dome-shaped reaction norm to temperature), with extension rates increasing with increasing temperatures, peaking at 28.9ºC, beyond which the extension rates declined. For every degree Celsius increase in temperature beyond ~29ºC, extension rates declined by approximately 4.48 +1.71 mm yr^{-1}. The unimodal response and decline in growth at higher temperatures are similar to those previously reported for *Porites* calcification rates (Lough & Cantin 2014). These rates are also similar to that of Tanzil et al. (2009), whom estimated that for every 1°C increase in temperature, rates of extension would reduce growth by 41–56%. These rates of decline in potential coral growth rates will also depend on the Representative Concentration Pathways (RCPs) (IPCC 2013). A reduction in the

rapid increase in greenhouse gas emissions, corresponding to the difference between RCP 8.5 and 6.0 pathways, may make the difference between some reefs keeping up with sea-level rise, or ultimately drowning under rising seas.

The present study assumed a strong link between rates of bioerosion and populations of humans along the coasts. Consequently, protecting reefs from overfishing will positively influence the rates of reef accretion. Yet we assumed a constant radius of influence from coastal populations of 30 km, which will likely increase in the future, and cause further erosional problems as radius expands. Although local erosion can take three forms, physical, chemical, and biological, most erosive problems were identified as biological. Still, the current model did not consider the increase in the intensification of future cyclones, which have been widely reported, and future projections indicate that ocean warming will increase the overall global intensity of tropical cyclones by 2-11% by the year 2100 (Knutson et al. 2100). Although our study uses the best estimates of model parameters, and better information in the near future will improve estimates of rates of reef accretion, the regional trends will likely remain the same. The high latitude reefs are more likely to drown than reefs near the equator, because of limiting irradiance at high latitudes (Muir et al. 2015). The reefs that did show promise at low latitudes (Figure 5.2), and are likely to keep up with sea-level rise and continue to provide a protective barrier from storms, should be assigned the highest possible conservation status.

CHAPTER 6. SYNTHESIS AND CONCLUSIONS

One of the most important contemporary issues for coral reefs is to understand the vulnerability of reef corals to climate change, and to identify climate-change refugia. This study identified 19 refugia with global species distribution models using two primary predictive variables, the range in both photosynthetically available radiation and sea-surface temperature. These two environmental variables were used as our main predictors because corals extract most of their metabolic resources from their endosymbionts that photosynthesize, and because symbiotic dysfunction, observed as coral bleaching and subsequent coral mortality, occurs through the interaction between high light (photoinhibition) and anomalously high temperature. Using these predictive variables we identified 12 climate refugia with our first model.The identified climate refugia are: (i) south western Madagascar, (ii) the Maldives, (iii) the Chagos Archipelago, (iv) Western Australia, (v) the Seychelles, (vi) northern Indonesia, (vii) Micronesia, (viii) the northern Marshall Islands, (ix) the southern Great Barrier Reef, (x) the Solomon Islands, (xi) Vanuatu, and (xii) French Polynesia.

A comment on our first model by Keppel and Kavousi (2015) suggested that we examined only "one global stressor (ocean warming)" when in fact we examined two stressors – temperature and irradiance – and the interaction between these variables. They also suggested that we ignored ocean acidification, which we did purposely in that model. We also ignored many other secondary factors in the first

two models, including flow rates and the concentration of nutrients, although we did examine chlorophyll a concentrations in the second, turbidity model. We did attempt to model the above mentioned predictors, including ocean acidification, storm frequency, flow rates, and nutrient concentrations in the reef accretion (fourth) model, because of their local influence in reef accretion and dissolution or erosion. Yet, recent incubation experiments show little sensitivity of corals to reduced pH (Ohki et al. 2013; Comeau et al. 2013), and field measurements in Palau showed high diversity and high coral cover in nearshore systems that experience on average a pH of 7.85 (Shamberger et al. 2014). Moreover, corals can upregulate their internal pH through hydrogen pumping (McCulloch et al. 2012), and therefore have the potential to tolerate decreased ocean pH. Together these contemporary results show that the effect of ocean acidification on live reef corals, through to 2100, may be more subtle than previously suspected (Mumby and van Woesik, 2014), although the problems involved in carbonate framework dissolution under ocean acidification will remain (van Woesik et al. 2013), and are accounted for in modeling reef accretion in our fourth model.

By contrast, the primary predictors used in this study to model species survival, temperature stress and its interaction with irradiance, are anything but subtle (Hoegh-Guldberg et al 2007; Baker et al. 2008). It is difficult for corals to adjust to high temperature and irradiance stressors. Because of this adjustment problem, thermal anomalies that elevate sea-surface temperature 2–3^{o}C have caused

severe coral mortality in many localities around the globe, sometimes changing the composition of corals on reefs (Loya et al. 2001; van Woesik et al. 2011). Even in some of the world's warmest waters, for example in the northern Persian Gulf, coral bleaching occurs when the water temperature is above 33.5^{o}C (Kavousi et al. 2014). The temperatures of the oceans will continue to rise rapidly (IPCC 2013), potentially increasing by an average of 3^{o}C by the year 2100, and therefore dealing with increasing temperatures is *the* most immediate and critical stressor that marine organisms must face.

The second model identified nine turbid water refugia. These turbidity-driven refugia are a product of turbid waters mitigating the harmful interaction of high thermal stress and intense irradiance. Turbidity-driven refugia were identified in (i) the northwestern Hawaiian Islands, (ii) the northern Philippines, (iii) the Ryukyu Islands (Japan), (iv) eastern Vietnam, (vi) eastern Australia, (vi) Western Australia, (vii) New Caledonia, (viii) the northern Red Sea, and (ix) the Arabian Gulf.

The third model found that genetic connectivity is a critical component of reef persistence through climate change into the future. This model highlights, in particular, the importance of maintaining genetic connectivity for ubiquitous species. It is unlikely that future subpopulations of a species will be completely isolated across their entire geographic range. However, some reduction in genetic connectivity between subpopulations, similar to the pattern exhibited by *P. lobata,* is likely to occur in widely distributed species, and modeling such broadly distributed

species under the assumption that the entire population is genetically homogenous is likely to drastically overestimate projected species survival into the future.

The fourth model identified locations in the Indo-Pacific where reefs will likely keep up with sea-level rise into the future. These identified reef locations are (i) the Maldives, (ii) the Chagos Archipelago, (iii) northern Indonesia, (iv) Micronesia, (v) the Marshall Islands, (vi) the Solomon Islands, (vii) Vanuatu, and (viii) Fiji (Figure 5.2). All of these locations with the exception of Fiji, are within previously identified refugia from the climate refugia model. The reefs at higher latitudes, on the edge of species distributions had problems keeping up with sea-level rise. Sea-level rise was also predicted to outpace reef accretion in some of the localities that were previously identified as climate-change refugia, including reefs along both the western and eastern coasts of Australia, along the coasts of Madagascar, the Seychelles, and French Polynesia. However, projected vertical accretion rates were only slightly slower than the rate of sea-level rise at these localities.

Even though our global species distribution models show significant loss of corals as the oceans warm, they also highlight regions where corals might persist and even thrive, at least until 2100. These refugia deserve increased conservation effort. Our study moves away from local marine protected areas as the only management option for coral reefs, and leads the way toward the use of global sanctuaries as a more comprehensive management strategy. Our study identifies locations where we

should invest conservation effort, while we simultaneously work toward reducing green-house gas emissions.

LITERATURE CITED

Adey W (1978) Coral reef morphogenesis: a multidimensional model. *Science* **202***,* 831–837.

Al-Horani FA, Al-Moghrabi SM, de Beer D (2003) The mechanism of calcification and its relation to photosynthesis and respiration in the scleractinian coral *Galaxea fascicularis*, *Marine Biology* 142: 419-426

Allemand D, Ferrier-Pagès C, Furla P, Houlbrèque F, Puverel S, Reynaud S, Tambutté E, Tambutté S, Zoccola D (2004) Biomineralisation in reef-building corals: from molecular mechanisms to environmental control, *Comptes Rendus Palevol* 3: 453–467

Anthony KRN and Connolly SR (2004) Environmental limits to growth: physiological niche boundaries of corals along turbidity-light gradients. Oecologia **141**: 373-384

Anthony KRN, Fabricius KE (2000) Shifting roles of heterotrophy and autotrophy in coral energetics under varying turbidity. *J. Exp. Mar. Biol. Ecol.* **252**, 221–253. (doi:10.1016/S0022-0981(00)00237-9)

Anthony KRN, Ridd PV, Orpin AR, Larcombe P, Lough JM (2004) Temporal variation in light availability in coastal benthic habitats: effects of clouds, turbidity and tides. Limnol Oceanogr **49**(6): 2201-2211

Arai K, Sarusawa Y (2013) Spatial-temporal variations of turbidity and ocean current velocity of the Ariake Sea area, Kyushu, Japan through regression analysis with remote sensing satellite data. *International Journal of Advanced Computer Science and Applications*, **4 (**3), 20-25.

Araujo MB, Pearson RG, Thuiller W (2005) Validation of species-climate impact models under climate change. *Global Change Biology,* **11,** 1504-1513.

Ashcroft MB (2010) Identifying refugia from climate change. *Journal of Biogeography* **37,** 1407–1413.

Ashcroft MB, Chisholm LA, French KO (2009) Climate change at the landscape scale: predicting fine-grained spatial heterogeneity in warming and potential refugia for vegetation. *Global Change Biology,* **15,** 656–667.

Ateweberhan M, McClanahan TR (2010) Relationship between historical sea-surface temperature variability and climate change-induced coral mortality in the western Indian Ocean. *Marine Pollution Bulletin,* **60,** 964–970.

Ateweberhan M, McClanahan TR, Graham NAJ, Sheppard CRC (2011) Episodic heterogeneous decline and recovery of coral cover in the Indian Ocean. *Coral Reefs,* **30,** 739–752.

Atkins, K.E. & Travis, J.M.J. (2010) Local adaptation and the evolution of species' ranges under climate change. *Journal of Theoretical Biology*, **266**, 449–457.

Atkinson MJ, Bilger RW (1992) Effects of water velocity on phosphate uptake in coral reef-flat communities. *Limnol Oceanogr* 37: 273–279

Avise JC (2000) *Phylogeography: The History and Formation of Species*. Harvard University Press, pp 447.

Ayre, D.J. & Hughes, T.P. (2000) Genotypic Diversity and Gene Flow in Brooding and Spawning Corals Along the Great Barrier Reef, Australia. *Evolution*, **54**, 1590–1605.

Baird AH, Bhagooli R, Ralph PJ, Takahashi S (2009) Coral bleaching: the role of the host. *Trends in Ecol. Evol.* **24**, 16–20.

Baird AH, Sommer B, Madin JS (2012) Pole-ward range expansion of *Acropora* spp. along the east coast of Australia. Coral Reef, **31**(4), 1063.

BakerAC, PW Glynn, B Riegl (2008) Climate change and coral reef bleaching: An ecological assessment of long-term impacts, recovery trends and future outlook. *Estuarine, Coastal and Shelf Science* 80: 435–471

Barkley H.C, Anne L. Cohen, Yimnang Golbuu, Victoria R. Starczak, Thomas M. DeCarlo, Kathryn E. F. Shamberger (2015) Changes in coral reef communities across a natural gradient in seawater pH. *Science Advances*: e1500328

Barnes DJ & Lough JM (1989) The nature of skeletal density banding in scleractinian corals: fine banding and seasonal patterns. *J Exp Mar Bio Eco* 126: 119-134

Baums, I.B., Boulay, J.N., Polato, N.R. & Hellberg, M.E. (2012) No gene flow across the Eastern Pacific Barrier in the reef-building coral Porites lobata. *Molecular Ecology*, **21**, 5418–5433.

Birkeland C, Miller MW, Piniak GA, Eakin CE, Weijerman M, McElhany P, Dunlap M, Brainard RE (2013) Safety in numbers? Abundance may not safeguard corals from increasing Carbon Dioxide. *BioScience,* **63,** 967-974.

Bivand R, Keitt T, Rowlingson B (2014) rgdal: Bindings for the Geospatial Data Abstraction Library. R package version. http://CRAN.R-project.org/package=rgdal

Bivand R, Pebesma E, Gomez-Rubio V (2013) Applied spatial data analysis with R. Springer, pp 405

Blanchon P., Granados-Corea M, Abbey M, Braga JC, Braithwaite C, Kennedy DM, Spencer T, Webster JM, Woodroffe CD (2014) Postglacial fringing-reef to barrier-reef conversion on Tahiti links Darwin's reef types. *Scientific Reports*: 4, 4997; doi:10.1038/srep04997

Blangiardo M and Cameletti M (2015) Spatial and Spatio-temporal Bayesian Models with R – INLA, John Wiley and Sons Ltd., London.

Boulay, J.N., Hellberg, M.E., Cortés, J. & Baums, I.B. (2013) Unrecognized coral species diversity masks differences in functional ecology. Proc Royal Soc B, **281**, 20131580. DOI: 10.1098/rspb.2013.1580

Brown BE, Suharsono (1990) Damage and recovery of coral reefs affected by El Niño related seawater warming in the Thousand Islands, Indonesia. *Coral Reefs,* **8,** 163–170.

Brown BE. (1997) Coral bleaching: causes and consequences. *Coral Reefs* **16**, S129–S138. (doi:10.1007/s003380050249)

Budd AF, Klaus JS, Johnson KG (2011) Cenozoic diversification and extinction patterns in Caribbean reef corals: A review. *Paleontol Soc Papers,* **17,**: 79-94.

Buddemeier R W and Hopley D (1988) Turn-ons and turn-offs: Causes and mechanisms of the initiation and termination or coral reef growth. *Proc 6th Int Coral Reef Sym* Vol 1: 253-261

Burrows M, schoeman DS, Buckley LB, Moore P, et al. (2011) The pace of shifting climate in marine and terrestrial ecosystems. *Science* 334: 652-655

Bush, G.L. (1975) Modes of animal speciation. *Annual Review of Ecology and Systematics*, 339–364.

Cacciapaglia C and van Woesik R. (2015) Reef-coral refugia in a rapidly changing ocean. *Global Change Biology* 21, 2272-2282

Cacciapaglia C and van Woesik R. (2016) Climate-change refugia: shading reef corals by turbidity. *Global change biology*, **22**, 1145–1154.

Cesar H, Burke L, Pet-Soede L (2003) The economics of worldwide coral reef degradation. *Cesar Environmental Economics Consulting,* 6828GH Arnhem, The Netherlands, 23 pp.

Chappell J, Shackleton NJ. (1986) Oxygen isotopes and sea-level. *Nature* 324, 137-140

Chevin, L.-M., Lande, R. & Mace, G.M. (2010) Adaptation, Plasticity, and Extinction in a Changing Environment: Towards a Predictive Theory. *PLoS Biology*, **8**.

Coates AG, Jackson JBC (1985) Morphological themes in the evolution of clonal and aclonal marine invertebrates. In: Jackson JBC, Buss LW, Cook RE (eds) Population biology and evolution of clonal organisms. Yale University Press, New Haven, CT, pp 67-106.

Coles SL, Riegl BM (2013) Thermal tolerances of reef corals in the Gulf: A review of the potential for increasing coral survival and adaptation to climate change through assisted translocation. *Marine Pollution Bulletin* **72**: 323-332.

Colinvaux PA, Bush MB, Steinitz-Kannan M, Miller MC (1997) Glacial and Postglacial Pollen Records from the Ecuadorian Andes and Amazon. *Quaternary Research,* **48,** 69–78.

Comeau S, Carpenter RC, Nojiri Y, Putnam HM, Sakai K, Edmunds PJ (2014) Pacific-wide contrast highlights resistance of reef calcifiers to ocean acidification. Proc. R. Soc. B 281: 20141339. http://dx.doi.org/10.1098/rspb.2014.1339

Connell, J.H. (1997) Disturbance and recovery of coral assemblages. *Coral reefs*, **16**, S101–S113.

Costanza R, d'Arge R, de Groot R, Farber S, Grasso M, Hannon B, Limburg K, Naeem S, O'Neill RV, Paruelo J, Raskin RG, Sutton P, van den Belt M (1998) The value of the world's ecosystem services and natural capital. Ecological Economics , **25**(1), 67-72.

Costanza R, de Groot R, Sutton P, van der Ploeg S, Anderson SJ, Kubiszewki I, Farber S, Turner K (2014) Changes in the global value of ecosystem services. *Global Environmental Change,* **26,** 152–158.

Cryonak et al. 2013 Cyronak T, Santos IR, Eyre BD. (2013). Permeable coral reef sediment dissolution driven by elevated *p*CO2 and pore water advection. *Geophysical Research Letters* 40:1–6

Cunning R, Baker AC (2013) Excess algal symbionts increase the susceptibility of reef corals to bleaching. Nature Climate Change 3: 259-262.

Darwin CR (1842) The structure and distribution of coral reefs. London: Smith Elder and Co., pp. 230;237.

Davies PJ (1983) Reef growth. In: Perspectives on coral reefs (Editor DJ Barnes), publisher, Australian Institute of Marine Sciences, pp 69-106

De'ath G, Lough JM, Fabricius KE. (2009) Declining coral calcification on the Great Barrier Reef, *Science* 323, 116-119

De'ath, G. & Fabricius, K. (2010) Water quality as a regional driver of coral biodiversity and macroalgae on the Great Barrier Reef. *Ecological Applications*, **20**, 840–850.

Dennison and Barnes (1988) Effect of water motion on coral photosynthesis and calcification. *J Exp Mar Biol and Ecol* 115, 67-77

DeVantier LM, De'Ath G, Done TJ, Turak E (1998) Ecological assessment of a complex natural system: a case study from the Great Barrier Reef. *Ecol. Appl.* **8**, 480–496.

Dixon, G.B., Davies, S.W., Aglyamova, G.V., Meyer, E., Bay, L.K. & Matz, M.V. (2015) Genomic determinants of coral heat tolerance across latitudes. *Science*, **348**, 1460–1462.

Dobrowski SZ (2011) A climatic basis for microrefugia: the influence of terrain on climate. *Global Change Biology,* **17,** 1022–1035.

Donner SD, Skirving WJ, Little CM, Oppenheimer M, Hoegh-Guldberg O (2005) Global assessment of coral bleaching and required rates of adaptation under climate change. *Global Change Biology,* **11,** 2251-2265.

Dorie V (2014) blme: Bayesian Linear Mixed-Effects Models. R package version 1.0-2. http://CRAN.R-project.org/package=blme

Dullo WC (2005) Coral growth and reef growth: a brief review. *Facies* 51:33–48

Easton WH, Ku TL. (1980) Holocene sea-level changes in Palau, West Caroline-Islands. *Quaternary Research* 14, 199-209

Edinger EN, Limmon GV, Jompa J, Widjatmoko W, Heikoop JM, Risk MJ. (2000) Normal coral growth rates on dying reefs: are coral growth rates good indicators of reef health? *Marine Pollution Bulletin* 40, 404-425

Edinger EN, Risk MJ (1994) Oligocene-Miocene extinction and geographic restriction of Caribbean corals: roles of turbidity, temperature, and nutrients. *Palaios,* **9,** 576-598.

Edmunds PJ, Carpenter RC, Comeau S (2013) Understanding the treats of ocean acidification to coral reefs. *Oceanography* 26: 149-152

Ekebom J, Laihonen P, Suominen T (2003) A GIS-based step-wise procedure for assessing physical exposure in fragmented archipelagos. *Estuarine and Coastal Shelf Science* 57: 887-898

Elith, J. & Leathwick, J.R. (2009) Species distribution models: ecological explanation and prediction across space and time. *Annual Review of Ecology, Evolution, and Systematics*, **40**, 677.

England MH, McGregor S, Spence P, Meehl GA, Timmermann A, Cai W, Gupta AS, McPhaden MJ, Purich A, Santoso A (2014) Recent intensification of wind-driven circulation in the Pacific and the ongoing warming hiatus. *Nature Climate Change,* **4,** 222–227.

Eyre BD, Andersson AJ, Cyronak T (2014) Benthic coral reef calcium carbonate dissolution in an acidifying ocean. *Nature Climate Change* 4: 969-976

Falkowski PG, Dubinsky Z, Muscatine L, McCloskey L (1993) Population control in symbiotic corals. Bioscience 43: 606–611.

Fallon, S.J., McCulloch, M.T., van Woesik, R. & Sinclair, D.J. (1999) Corals at their latitudinal limits: laser ablation trace element systematics in Porites from Shirigai Bay, Japan. *Earth and Planetary Science Letters*, **172**, 221–238.

Figueiredo J, Baird AH, Harii S, Connolly SR (2014) Increased local retention of reef coral larvae as a result of ocean warming. *Nature Climate Change,* 4, 498-502.

Fisher, R.A. (1930) *The genetical theory of natural selection*, Dover Publications Inc., New York.

Frieler K, Meinshausen M, Golly A, Mengel M, Lebek K, Donner SD, Hoegh-Guldberg O (2013) Limiting global warming to 2 °C is unlikely to save most coral reefs. *Nature Climate Change,* **3,** 165–170.

Fuentes M, Henry J, Reich B (2013) Nonparametric spatial models for extremes: application to extreme temperature data. *Extremes* 16:75–101, doi:10.1007/s10687-012-0154-1

Futuyma DJ (2009) *Evolution.* 2nd ed. Sinauer Associates, Sunderland, Massachusetts, pp. 545.

Gallegos CL, Moore KA (2000) Factors contributing to water-column light attenuation. pp. 16-27. In Batiuk, R. A. et al. [eds.], *Chesapeake Bay submerged aquatic vegetation water quality and habitat-based requirements and restoration targets: A second technical synthesis.* US EPA, Chesapeake Bay Program, Annapolis, MD. USA, pp 106.

Glynn PW (1993) Coral reef bleaching: ecological perspectives. *Coral Reefs* **12**:1-17

Glynn PW (1997) Bioerosion and coral-reef growth: A dynamic balance. In: Birkeland C (eds.) Life and Death of Coral Reefs. Chapman & Hall. Chapter 4: 68-95

Golbuu Y, Wolanski E, Idechong JW, Victor S, Isechal AL, Oldiais NW, Idip D, Richmond R, van Woesik R (2012) High reef density increases coral recruitment in Palau. *PLoS One* 7(11): e50998

Grinsted A, Moore JC, Jevrejeva S (2004) Application of the cross wavelet transform and wavelet coherence to geophysical time series *Nonlinear Processes in Geophysics*, European Geosciences Union (EGU), 11 (5/6), pp.561-566

Grinsted A, Moore JC, Jevrejeva S (2012) Projected Atlantic hurricane surge threat from rising temperatures. *PNAS* 110: 5369–5373

Guest JR, Baird AH, Maynard JA, Muttaqin E, Edwards AJ (2012) Contrasting Patterns of Coral Bleaching Susceptibility in 2010 Suggest an Adaptive Response to Thermal Stress. PLoS ONE, 7(3), e33353.

Hijmans R, van Etten J (2014) "raster: Geographic data analysis and modeling. 2–2.1. http://CRAN.R-project.org/package=raster

Hijmans, R., Phillips, J., Leathwick, J. & Elith, J. (2014) dismo: Species distribution modeling. R package version 0.9-3.

Hobbs, J.-P.A., Frisch, A.J., Allen, G.R. & Van Herwerden, L. (2009) Marine hybrid hotspot at Indo-Pacific biogeographic border. *Biol. Lett*, **5**, 258–261.

Hoegh-Guldberg O (1999) Climate change, coral bleaching and the future of the world's coral reefs. *Mar. Freshwater Res.* **50**, 839–866.

Hoegh-Guldberg O, Mumby PJ, Hooten AJ, Steneck RS, Greenfield P, Gomez E, Harvell CD, Sale PF, Edwards AJ, Caldeira K, Knowlton N, Eakin CM, Iglesias-Prieto R, Muthiga N, Bradbury RH, Dubi A, Hatziolos ME (2007) Coral reefs under rapid climate change and ocean acidification. *Science,* **318,** 1737–1742.

Hoegh-Guldberg, O (1999) Climate change, coral bleaching and the future of the world's coral reefs. *Mar Fresh Res* 50, 839–866

Hopley, D. (1982) *The geomorphology of the Great Barrier Reef: Quaternary development of coral reefs*, John Wiley & Sons.

Hopley D, Smithers S, Parnell KE. (2007) *The Geomorphology of the Great Barrier Reef. Development, Diversity and Change* (Cambridge University Press), pp. 546.

Hubbard DK (1997) Reefs as dynamic systems. In: Birkeland C (eds.) Life and Death of Coral reefs. Chapman & Hall. Chapter 2: 43-67

Hubbard JAEB & Pocock YP (1972) Sediment rejection by recent scleractinian corals: a key to paleoenvironmnetal reconstruction. Geological Rundsch 61: 598-626

Hughes TP, Baird AH, Bellwood DR, Card M, Connolly SR, Folke C, Grosberg R, Hoegh-Guldberg O, Jackson JBC, Kleypas J, Lough JM, Marshall P, Nystrom M, Palumbi SR, Pandolfi JM, Rosen B, Roughgarden J (2003) Climate change, human impacts, and the resilience of coral reefs. *Science,* **301,** 929–933.

Hume B, D'Angelo C, Burt J, Baker AC, Wiedenmann J (2013) Corals from the Persian/Arabian Gulf as models for thermotolerant reef-builders: Prevalence of clade C3 *Symbiodinium*, host fluorescence and *ex situ* temperature tolerance. *Marine Pollution Bulletin* **72**: 313-322.

Iglesias-Prieto R, Matta JL, Robins WA, Trench RK (1992) Photosynthetic response to elevated temperature in the symbiotic dinoflagellate *Symbiodinium microadriaticum* in culture. *PNAS* **89**, 10302-10305.

Iglesias-Prieto R, Trench RK (1994) Acclimation and adaptation to irradiance in symbiotic dinoflagellates. I. Responses of the photosynthetic unit to changes in photon flux density. *Mar. Ecol. Prog. Ser.* **113**, 163–175.

IPCC (2013) Climate Change 2013: The Physical Science Basis. Contribution of Working Group I to the Fifth Assessment Report of the Intergovernmental Panel on Climate Change [Stocker T.F., D. Qin, G.-K. Plattner, M. Tignor, S.K. Allen, J. Boschung, A. Nauels, Y. Xia, V. Bex and P.M. Midgley (eds.)]. Cambridge University Press, Cambridge, United Kingdom and New York, NY, USA, 1535 pp, doi:10.1017/CBO9781107415324.

Jain, S.K. & Bradshaw, A.D. (1966) Evolutionary divergence among adjacent plant populations. I. The evidence and its theoretical analysis. *Heredity*, **21**, 407–441.

Jevrejeva S, Moore JC, Grinsted A, Matthews AP, Spada G. (2013) Trends and acceleration in global and regional sea levels since 1807. *Global and Planetary Change* 113, 11-22

Karnauskas KB, Cohen AL (2012) Equatorial refuge amid tropical warming. *Nature Climate Change,* **2,** 530–534.

Kayanne H, Yamano H, Randall RH. (2002) Holocene sea-level changes and barrier reef formation on an oceanic island, Palau Islands, western Pacific. *Sedimentary Geology* 150, 47-60

Kearney M, Porter W (2009) Mechanistic niche modelling: combining physiological and spatial data to predict species' ranges. *Ecol. Lett.***12**, 334–350. (doi:10.1111/j.1461-0248.2008.01277.x)

Kenkel, C.D., Meyer, E. & Matz, M.V. (2013) Gene expression under chronic heat stress in populations of the mustard hill coral (*Porites astreoides*) from different thermal environments. *Molecular Ecology*, **22**, 4322–4334.

Keppel G, Van Niel KP, Wardell-Johnson GW, Yates CJ, Byrne M, Mucina L, Schut AGT, Hopper SD, Franklin SE (2012) Refugia: identifying and understanding safe havens for biodiversity under climate change. *Global Ecology and Biogeography,* **21,** 393–404.

Kiessling W and Eichenseer K (2014) The scaling law of climate change and its relevance to assessing (palaeo)biological responses. Geophysical Research Abstracts, EGU General Assembly, Vol 14. EGU2014-15790

Klaus JS, Budd AF (2003) Comparison of Caribbean coral reef communities before and after Plio-Pleistocene faunal turnover: Analyses of two Dominican Republic reef sequences. *Palaios,* **18**(1), 3-21.

Kleypas JA (1996) Coral reef development under naturally turbid conditions: fringing reefs near Broad Sound, Australia. *Coral Reefs* **15**, 153–167.

Kleypas JA (1997) Modeled estimates of global reef habitat and carbonate production since the last glacial maximum. *Paleoceanography* **12**, 533–545.

Kleypas JA, Mcmanus JW, Meñez LaB (1999) Environmental Limits to Coral Reef Development: Where Do We Draw the Line? *Amer. Zool.* **39**, 146–159. (doi:10.1093/icb/39.1.146)

Kleypas, J.A., Thompson, D.M., Castruccio, F.S., Curchitser, E.N., Pinsky, M. & Watson, J.R. (2016) Larval connectivity across temperature gradients and its potential effect on heat tolerance in coral populations. *Global change biology*.

Lambeck K, Chappell J. (2001) Sea level change through the last glacial cycle. *Science* 292, 679-686

Larcombe P, Woolfe KJ (1999) Increased sediment supply to the Great Barrier Reef will not increase sediment accumulation at most. *Coral Reefs* **18**, 163–169. (doi:10.1007/s003380050174)

Lau K-M, Wu H-T (2007) Detecting trends in tropical rainfall characteristics, 1979–2003. *Int. J. Climatol,* **27,** 979–988.

Lee-Yaw, J.A., Kharouba, H.M., Bontrager, M., Mahony, C., Cserg\Ho, A.M., Noreen, A.M., Li, Q., Schuster, R. & Angert, A.L. (2016) A synthesis of transplant experiments and ecological niche models suggests that range limits are often niche limits. *Ecology letters*, **19**, 710–722.

Loh WKW (2007) Predominance of clade D *Symbiodinium* in shallow-water reef-building corals off Kish and Larak Islands (Persian Gulf, Iran). *Marine Biology* **153**: 25-34.

Lough JM, Barnes DJ. (2000) Environmental controls on growth of the massive coral *Porites*. *J. Exp. Mar. Biol. Ecol.* **245**, 225-243

Lough JM, Cantin NE. 2014 Perspectives on massive coral growth rates in a changing ocean. *Biological Bulletin* 226, 187-202

Loya, Y, Sakai K, Yamazato K, Nakano Y, Sambali, H, van Woesik R (2001) Coral bleaching: the winners and the losers. *Ecol. Lett.* **4**, 122–131. (doi:10.1046/j.1461-0248.2001.00203.x)

Lunn D, Jackson C, Best N, Thomas A, Spiegelhalter (2013) The Bugs Book: A practical introduction to Bayesian analysis. CRC Press, pp 381

Maina J, Venus V, McClanahan TR, Ateweberhan M (2008) Modelling susceptibility of coral reefs to environmental stress using remote sensing data and GIS models. *Ecological Modelling,* **212,** 180–199.

Marshall PA, Baird AH (2000) Bleaching of corals on the Great Barrier Reef: differential susceptibilities among taxa. *Coral Reefs,* **19,** 155–163.

Maxwell WGH (1968) Atlas of the Great Barrier Reef. Elsevier, New York, 260 pp.

McClanahan TR, Ateweberhan M, Muhando CA, Maina J, Mohammed MS (2007) Effects of climate and seawater temperature variation on coral bleaching and mortality. *Ecological Monographs,* **77,** 503–525.

McClanahan TR, Baird AH, Marshall PA, Toscano MA (2004) Comparing bleaching and mortality responses of hard corals between southern Kenya and the Great Barrier Reef, Australia. *Marine Pollution Bulletin,* **48,** 327–335.

McClanahan TR, Maina J (2003) Response of coral assemblages to the interaction between natural temperature variation and rare warm-water events. *Ecosystems,* **6,** 551–563.

McClanahan TR, Maina JM, Muthiga NA (2011) Associations between climate stress and coral reef diversity in the western Indian Ocean. *Global Change Biology,* **17,** 2023–2032.

McCulloch M, Falter J, Trotter J,Montagna P. (2012) Coral resilience to ocean acidification and global warming through pH up-regulation. *Nature Climate Change* 2:623–627

Miller, K. & Mundy, C. (2003) Rapid settlement in broadcast spawning corals: implications for larval dispersal. *Coral Reefs*, **22**, 99–106.

Moberg F, Folke C (1999) Ecological goods and services of coral reef ecosystems. *Ecol. Econ.* **29**, 215–233.

Morgan and Kench (2012) Skeletal extension and calcification of reef-building corals in the central Indian Ocean. *Marine Environmental Research* 81: 78-82

Moritz C, Agudo R (2013) The future of species under climate change: resilience or decline? *Science,* **341,** 504–508.

Mosblech NAS, Bush MB, van Woesik R. (2011) On metapopulations and microrefugia: palaeoecological insights. *Journal of Biogeography,* **38,** 419–429.

Mostafavi PG, Fatemi SMR, Mohammad Hassan Shahhosseiny MH, Hoegh-Guldberg O,

Muir, P.R., Wallace, C.C., Done, T. & Aguirre, J.D. (2015) Limited scope for latitudinal extension of reef corals. *Science*, **348**, 1135–1138.

Muller EM, and van Woesik R, (2014).Genetic susceptibility, colony size, and water temperature drive white-pox disease on the coral *Acropora palmata. PLoS One* 9(11): e110759.

Mumby P, Chisholm J, Edwards A, Andrefouet S, Jaubert J (2001) Cloudy weather may have saved Society Island reef corals during the 1998 ENSO event. *Marine Ecology Progress Series,* **222**, 209–216.

Mumby PJ, van Woesik R (2014) Consequences of ecological, evolutionary and biogeochemical uncertainty for coral reef responses to climatic stress. *Current Biology,* **24,** R413–R423.

Nakamura T and van Woesik R (2001) Differential survival of corals during the 1998-bleaching event is partially explained by water-flow rates and passive diffusion. *Marine Ecology Progress Series* 212; 301-304

Nakamura T, Yamasaki H, van Woesik R. (2003) Water-flow treatment facilitates recovery from bleaching in the coral *Stylophora pistillata*. *Marine Ecology Progress Series* 256: 287-291

Neumann AC, Macintyre I. (1985) Reef response of sea level rise: keep-up, catch-up or give-up. In *Proceedings of the Fifth International Coral Reef Congress,* Eds: Gabrie C, Toffart JL, Salvat B (Tahiti) Volume 3, 105-110

Nussey, D.H., Postma, E., Gienapp, P. & Visser, M.E. (2005) Selection on heritable phenotypic plasticity in a wild bird population. *Science*, **310**, 304–306.

O'Connor, M.I., Bruno, J.F., Gaines, S.D., Halpern, B.S., Lester, S.E., Kinlan, B.P. & Weiss, J.M. (2007) Temperature control of larval dispersal and the implications for marine ecology, evolution, and conservation. *PNAS*, **104**.

Ohki S, T. Irie, M. Inoue, K. Shinmen, H. Kawahata, T. Nakamura, A. Kato, Y.Nojiri, A.Iguchi, A. Suzuki, K. Sakai, R van Woesik (2013) Symbiosis increases coral tolerance to ocean acidification. *Biogeosciences Discussion*, 10, 7013–7030

Pandolfi JM (2015) Incorporating uncertainty in predicting the future response of coral reefs to climate change. *Ann Rev Ecol Evol Syst* 46: 281-303

Pandolfi JM, Connolly SR, Marshall DJ, Cohen AL (2011) Projecting Coral Reef Futures Under Global Warming and Ocean Acidification. *Science* **333**, 418–422. (doi:10.1126/science.1204794)

Pante E, Simon-Bouhet B (2013) Marmap: a package for importing, plotting and analyzing bathymetric and topographic data in R. *PLoS One* **8**, e73051.

Pastroyok RA and Bilyard GR (1985) Effects of sewage pollution on coral reef communities. *Marine Ecology Progress Series* 21: 175-189

Patterson MR (1992) A mass-transfer explanation of metabolic scaling relations in some aquatic invertebrates and algae. *Science* 255:1421–1423

Patterson MR, Sebens KP (1989) Forced convection modulates gas exchange in cnidarians. *Proc Natl Acad Sci* USA 86: 8833–8836

Patterson MR, Sebens KP, Olson RP (1991) In situ measurements of flow effects on primary production and dark respiration in reef corals. *Limnol Oceanogr* 36:936–948

Perry CT, Edinger EN, Kench PS, Murphy GN, Smithers SG, Steneck RS, Mumby PJ (2012) Estimating rates of biologically driven coral reef framework production and erosion: a new census-based carbonate budget methodology and applications to the reefs of Bonaire. *Coral Reefs* 31: 853-868

Perry CT, Murphy GN, Kench PS, Smithers SG, Edinger EN, Steneck RS, Mumby PJ. (2013) Caribbean-wide decline in carbonate production threatens coral reef growth. *Nature Communications* 4, 1402, doi: 10.1038/ncomms2409

Perry CT, Spencer T, Kench PS (2008) Carbonate budgets and reef production states: a geomorphic perspective on the ecological phase-shift concept. *Coral Reefs* 27: 853-866

Perry, C. T. *et al.* (2015) Remote coral reefs can sustain high growth potential and may match future sea-level trends. *Sci. Rep.* 5, 18289; doi: 10.1038/srep18289.

Pierson DC, Kratzer S, Strömbeck N, Hakansson B (2008) Relationship between the attenuation of downwelling irradiance at 490 nm with the attenuation of PAR (400 nm–700 nm) in the Baltic Sea. *Remote Sens. Environ.* **112**, 668–680.

Polato, N.R., C.R. Voolstra, J. Schnetzer, M.K. DeSalvo, C.J. Randall, A.M. Szmant, M. Medina, and I.B. Baums. (2010) Location-specific responses to thermal stress in larvae of the reef-building coral *Montastraea faveolata. PLoS ONE* 5:e11221.

Polato, N.R., N.S. Altman, and I.B. Baums. (2013) Variation in the transcriptional response of threatened coral larvae to elevated temperatures. *Molecular Ecology* 22:1366-1382.

Pörtner, H.O. & Farrell, A.P. (2008) Physiology and climate change. *Science*, **322**, 690–692.

Prachett MS, Anderson KD, Hoogenboom MO, Widman E, Baird AH, Pandolfi JM, Edmunds PJ, Lough JM (2015) Spatial, temporal and taxonomic variation in coral growth – implications for the structure and function of coral reef ecosystems. Oceanography and Marine Biology: An Annual Review 53: 215-295

R Core Team (2014) *R:* A language and environment for statistical computing. R Foundation for Statistical Computing, Vienna, Austria, 2012. ISBN 3-900051-07-0.

R Core Team. (2016) R: A language and environment for statistical computing. R Foundation for Statistical Computing. http://www.R-project.org/

Randall CJ and R. van Woesik (2015) Contemporary white-band disease in the Caribbean has been driven by climate change. *Nature Climate Change* 5: 375-379

Randall CJ, A. G. Jordán-Garza, E. M. Muller, R van Woesik (2016) Does dark-spot syndrome experimentally transmit among Caribbean corals? *PLoS ONE* 11(1): e0147493. doi:10.1371/journal.pone.0147493

Randall CJ, Jordan-Garza AG, R. van Woesik (2014) Ciliates associated with signs of disease on two Caribbean corals. *Coral Reefs* 34:243–247

Randall, C.J., A. Jordan-Garza, E. Muller, R. van Woesik (2014) Relationships between the history of thermal stress and the relative risk of Caribbean coral diseases. *Ecology* 95(7): 1981-1994

Riegl B, Piller WE (2003) Possible refugia for reefs in times of environmental stress. *Int J Earth Sci (Geol Rundsch),* **92,** 520–531.

Ries J (2011) Acid ocean cover up. *Nature Climate Change* 1:294–295

Rodolfo-Metalpa R, Houlbr`eque F, Tambutt´e E, Boisson F, Baggini C, Patti FP, Jeffree R, Fine M, Foggo A, Gattuso JP, Hall-Spencer JM (2011) Coral and mollusc resistance to ocean acidification adversely affected by warming. *Nature Climate Change* 1: 308–312

Roff G, Zhao J, Pandolfi JM (2015a) Rapid accretion of inshore reef slopes from the central Great Barrier Reef during the late Holocene. *Geology*, doi: 10.1130/G36478.1

Roff G, Iliana Chollett, Christopher Doropoulos, Yimnang Golbuu, Robert S. Steneck, Lukes Isechal, Robert van Woesik, Peter J. Mumby (2015b) Exposure-driven algal phase shift following a typhoon on a coral reef in Palau. *Coral Reefs* DOI 10.1007/s00338-015-1305-z

Rogers CS (1983) Sublethal and lethal effects of sediments applied to common Caribbean reef corals in the field. *Mar Poll Bull* 14: 378-382

Roth L, Koksal S, van Woesik R (2010) Effects of thermal stress on key processes driving coral population dynamics. *Marine Ecology Progress Series,* **411,** 73-87.

Rue H, Martino S, Chopin N (2009) Approximate Bayesian inference for latent Gaussian models by using integrated nested Laplace approximations. *J. R. Statist. Soc. B* 71:319–392.

Scheiner, S.M. (1993) Genetics and evolution of phenotypic plasticity. *Annual review of ecology and systematics*, 35–68.

Scoffin TP, Stoddart DR (1978) Nature and significance of micro-atolls. *Philosophical Transactions of the Royal Society of London Series B-Biological Sciences* 284, 99-122

Serrano X, Baums IB, O'Reilly K, Smith TB, Jones RJ, Shearer TL, Nunes FLD, Baker AC (2014) Geographic differences in vertical connectivity in the Caribbean coral *Montastraea cavernosa* despite high levels of horizontal connectivity at shallow depths. *Molecular Ecology,* **23**(17), 4226-4240.

Shamberger KEF, Cohen *AL*, Golbuu Y, McCorkle DC, Lentz SJ, Barkley HC (2014) Diverse coral communities in naturally acidified waters of a Western Pacific reef. *Geophysical Research Letters* 41(2), 1-6

Shanks, A.L., Grantham, B.A. & Carr, M.H. (2003) Propagule dispersal distance and the size and spacing of marine reserves. *Ecological Applications*, **13**, 159–169.

Silverman J, Lazor B, Cao L, Caldiera K, Erez J (2009) Coral reefs may start dissolving when atmospheric CO_2 doubles. *Geophysical Research Letters* 36:L05606, doi:10.1029/2008GLO36282.

Sinniger F, Morita M, Harii S (2012) Locally "extinct" coral species *Seriatopora hystrix* found at upper mesophotic depths in Okinawa. *Coral Reefs*, **32**(1), 153.

Smith L, Birkeland C (2007) Effects of intermittent flow and irradiance level on back reef Porites corals at elevated seawater temperatures. *J Exp Mar Biol Ecol* 341:282–294

Smith SV and Kinsey DW (1976) Calcium carbonate production, coral reef growth, and sea level change. *Science* 194:937-9

Sork, V.L., Stowe, K.A. & Hochwender, C. (1993) Evidence for Local Adaptation in Closely Adjacent Subpopulations of Northern Red Oak (Quercus rubra L.) Expressed as Resistance to Leaf Herbivores. *The American Naturalist*, **142**, 928–936.

Stanley Jr, G.D. (2006) Photosymbiosis and the evolution of modern coral reefs. *evolution*, **1**, 3.

Stearn CW, Scoffin TP,Martindale W (1977) Calcium carbonate budget of a fringing reef on the west coast of Barbados. *Bulletin of Marine Science* 27:479–510

Takahashi, S., Nakamura, T., Sakamizu, M., Woesik, R. van & Yamasaki, H. (2004) Repair Machinery of Symbiotic Photosynthesis as the Primary Target of Heat Stress for Reef-Building Corals. *Plant and Cell Physiology*, **45**, 251–255.

Tanzil JTI, Brown BE, Tudhope AW, Dunne RP (2009) Decline in skeletal growth of the coral *Porites lutea* from the Andaman Sea, South Thailand between 1984 and 2005. *Coral Reefs* 28, 519-528

Thompson, D.M. & Woesik, R. van (2009) Corals escape bleaching in regions that recently and historically experienced frequent thermal stress. *Proceedings of the Royal Society B: Biological Sciences*, **276**, 2893–2901.

Tomascik T (1991) Settlement patterns of Caribbean scleractinian corals on artificial substrata along a eutrophication gradient, Barbados, West Indies. *Mar. Ecol. Prog. Ser.* **77**, 261–269.

Tomascik T, Sander F (1986) Effects of eutrophication on reef-building corals. II. Structure of scleractinian coral communities on fringing reefs, Barbados, West Indies. *Marine Biology*, **94,** 53–75.

Tomascik T, Suharsono, Mah AJ (1993) Case histories: a historical perspective of the natural and anthropogenic impacts in the Indonesian Archipelago with a focus on the Kepulauan Seribu, Java Sea. p. 304-310. In: R.N. Ginsburg (editor) Proceedings of the Colloquium on Global Aspects of Coral Reefs: Health, Hazards and History (1993) University of Miami, Florida.

Toth, L.T., Aronson, R.B., Vollmer, S.V., Hobbs, J.W., Urrego, D.H., Cheng, H., Enochs, I.C., Combosch, D.J., van Woesik, R. and Macintyre, I.G. (2012) ENSO drove 2500-year collapse of eastern Pacific coral reefs. Science, 337(6090), pp.81-84.

Tyberghein, L., Verbruggen, H., Pauly, K., Troupin, C., Mineur, F. & De Clerck, O. (2012) Bio-ORACLE: a global environmental dataset for marine species distribution modelling. *Global Ecology and Biogeography*, **21**, 272–281.

Ulstrup KE, Hill R, Ralph PJ (2005) Photosynthetic impact of hypoxia on in hospite zooxanthellae in the scleractinian coral *Pocillopora damicornis*. Mar Ecol Prog Ser 286:125–132

Valladares, F., Matesanz, S., Guilhaumon, F., Araújo, M.B., Balaguer, L., Benito-Garzón, M., Cornwell, W., Gianoli, E., Kleunen, M., Naya, D.E. & others (2014) The effects of phenotypic plasticity and local adaptation on forecasts of species range shifts under climate change. *Ecology letters*, **17**, 1351–1364.

van Hooidonk, R., Maynard, J.A. & Planes, S. (2013) Temporary refugia for coral reefs in a warming world. *Nature Climate Change*, **3**, 508–511.

van Woesik R (2010) Calm before the spawn: global coral-spawning synchronization is explained by regional wind fields. *Proc Royal Society B*, **277,** 715-722.

van Woesik R (2013) Quantifying uncertainty and resilience on coral reefs using a Bayesian approach. *Environmental Research Letters* 8 (4): doi:10.1088/1748-9326/8/4/044051

van Woesik R and Done TJ (1997) Coral communities and reef growth in the southern Great Barrier Reef. *Coral Reefs* **16**: 103-115

van Woesik R, Houk P, Isechal AL, Idechong JW, Victor S, Golbuu Y (2012a) Climate-change microrefugia: nearshore reefs bleach less than outer reefs during a 2010 regional thermal stress event in Palau. *Ecology and Evolution* 2(10): 2474-2484

van Woesik R, Franklin EC, O'Leary J, McClanahan TR, Klaus J, Budd AF (2012b) Hosts of the Plio-Pleistocene past reflect modern-day coral vulnerability. *Proc Royal Society B,* **279,** 2448-2456.

van Woesik R, Irikawa A, Anzai R, Nakamura T (2012c) Effects of coral-colony morphologies on mass transfer and susceptibility to thermal stress. *Coral Reefs,* **31**, 633-639.

van Woesik R, Jordán-Garza AG (2011) Coral populations in a rapidly changing environment. *Journal of Experimental Marine Biology and Ecology,* **408,** 11–20.

van Woesik R, Sakai K, Ganase A, Loya Y (2011) Revisiting the winners and the losers a decade after coral bleaching. *Mar Ecol Prog Ser,* **434,** 67–76.

van Woesik R, Tomascik T, Blake S (1999) Coral assemblages and physico-chemical characteristics of the Whitsunday Islands: Evidence of recent community changes. *Marine and Freshwater Research* 50: 427-440.

van Woesik R, van Woesik K, van Woesik L, van Woesik S (2013) Effects of ocean acidification on the dissolution rates of reef-coral skeletons. *PeerJ* http://dx.doi.org/10.7717/peerj.208

van Woesik R, Y Golbuu, G Roff (2015) Keep up or drown: adjustment of Pacific coral reefs to contemporary sea-level rise. Royal Society Open Science 2: 150181. doi.org/10.1098/rsos.150181

van Woesik, R., Houk, P., Isechal, A.L., Idechong, J.W., Victor, S. & Golbuu, Y. (2012) Climate-change refugia in the sheltered bays of Palau: analogs of future reefs. *Ecology and Evolution*, **2**, 2474–2484.

Vermeer M and S Rahmstorf (2009) Global sea level linked to global temperature. *Proceedings of the National Academy of Science of the USA*, 106, 21527-21532

Veron JEN (1992) Environmental control of Holocene changes to the world's most northern hermatypic coral outcrop. *Pacific Science,* **46**(4), 405-425.

Veron JEN (1995) *Corals in Space and Time: The Biogeography and Evolution of the Scleractinia*. (Cornell University Press), pp. 321.

Veron JEN (2000) Corals of the World. *Australian Institute of Marine Science,* Townsville, Australia,1382 pp.

Veron JEN (2008) Mass extinctions and ocean acidification: biological constraints on geological dilemmas. *Coral Reefs,* **27,** 459–472.

Veron JEN, Devantier LM, Turak E, Green AL, Kininmonth S, Stafford-Smith M, Peterson N (2009) Delineating the Coral Triangle. *Galaxea, Journal of Coral Reef Studies* **11**, 91–100. (doi:10.3755/galaxea.11.91)

Via, S. (1993) Adaptive phenotypic plasticity: target or by-product of selection in a variable environment? *American Naturalist*, 352–365.

Wagner DE, Kramer P, van Woesik R (2010) Species composition, habitat, and water quality influence coral bleaching in southern Florida. *Marine Ecology Progress Series,* **408,** 65–78.

Wallace CC (1999) Staghorn Corals of the World: A Revision of the Coral Genus Acropora (Scleractinia; Astrocoeniina; Acroporidae) Worldwide, with Emphasis on Morphology, Phylogeny and Biogeography**.** CSIRO Publishing, Collingwood, Australia, pp 421.

Warner ME, Fitt WK, Schmidt GW (1999) Damage to photosystem II in symbiotic dinoflagellates: A determinant of coral bleaching. *Proc. Natl. Acad. Sci. USA* **96**, 8007–8012.

West K, van Woesik R (2001) Spatial and temporal variance of river discharge on Okinawa (Japan): inferring the temporal impact on adjacent coral reefs. *Marine Pollution Bulletin,* **42,** 864–872.

Wiggins, G. P. & McTighe, J. (2005) *Understanding by Design*. Association for Supervision and Curriculum Development (ASCD)

Wood R (1999) Reef Evolution. Oxford University Press, pp 414.

Wood, S., Baums, I.B., Paris, C.B., Ridgwell, A., Kessler, W.S. & Hendy, E.J. (2016) El Nino and coral larval dispersal across the eastern Pacific marine barrier. *Nature Communications*, **7**.

Woodroffe C, Mclean R (1990) Microatolls and recent sea-level change on coral atolls. *Nature* 344, 531-534

Woodroffe CD, McGregor HV, Lambeck L, Smithers SG, Fink D (2012) Mid-Pacific microatolls record sea-level stability over the past 5000 yr. *Geology* 40, 951-954

Wooldridge SA (2009) Water quality and coral bleaching thresholds: Formalising the linkage for the inshore reefs of the Great Barrier Reef, Australia. *Marine Poll. Bull.* **58**, 745–751.

Wooldridge SA, Done TJ (2009) Improved water quality can ameliorate effects of climate change on corals. *Ecol. Appl.* **19**, 1492–1499.

Yamano H, Sugihara K, Nomura K (2011) Rapid poleward range expansion of tropical reef corals in response to rising sea surface temperatures. *Geophysical Research Letters,* **38**(4), L04601.

Yentsch CS, Yentsch CM, Cullen JJ, Lapointe B, Phinney DA, Yentsch SW (2002) Sunlight and water transparency: cornerstones in coral research. *Exp. Mar. Biol. Ecol.* **268**, 171–183.

Zachos J, Pagani M, Sloan L, Thomas E, Billups K (2001) Trends, Rhythms, and Aberrations in Global Climate 65 Ma to Present. *Science,* **292,** 686–693.

Zeebe, R.E. & Zachos, J.C. (2013) Long-term legacy of massive carbon input to the Earth system: Anthropocene versus Eocene. Philosophical Transactions of the Royal Society A Mathematical Physical and Engineering Sciences, 371: 20120006.http://dx.doi.org/10.1098/rsta.2012.0006

Zvuloni A, Artzy-Randrup Y, Stone L, van Woesik R, Loya Y (2008) Ecological size-frequency distributions: how to prevent and correct biases in spatial sampling. *Limnol & Oceanog* 6: 144-153

APPENDICES

APPENDIX A: CLIMATE REFUGIA CODE

https://www.researchgate.net/profile/Robert_Van_Woesik2/publication/301201965_gcb13166-sup-0002-Rscripts/links/570c006308aea660813b1b6e?origin=publication_list

APPENDIX B: TURBIDITY MODEL CODE

https://www.researchgate.net/profile/Robert_Van_Woesik2/publication/301201965_gcb13166-sup-0002-Rscripts/links/570c006308aea660813b1b6e?origin=publication_list

APPENDIX C: GENETIC CONNECTIVITY CODE

```
#run confidence of p.lobata connectivity for different climate scenarios
#run on the supercomputer

#GAM with the ecoregions run for P.lobata where the species is present in all regions in the megaecoregions

#determine where the species is absent, may be easier to do manually for this one species, but set it up for later.

library(MASS)
library(audio)
library(sp)
library(foreign)
library(rgdal)
library(maptools)
library(rgeos)
library(doParallel)
library(rasterVis)
library(dismo)
library(plotKML)
library(SDMTools)
library(PBSmapping)
library(lme4)
library(blme)
#library(mailR)
library(raster)

load("C:/Users/Chris/Desktop/Comps/load data comps 10-1-2014.RData") #may need to add alternate
scenarios


#nutrients<-raster("C:/Users/Chris/Desktop/van Woesik/Chlorophyll
a/SWFMO_CHLO.CR.timeAverage.1998-2007.nc")


SST_min_futureB1<-raster("C:/Users/Chris/Desktop/van Woesik/ORACLE future temp
scenarios/B1/2100/sstmin.asc")
proj4string(SST_min_futureB1)<- CRS("+proj=longlat")
SST_min_future2B1<-crop(SST_min_futureB1,extent(-180,180,-37,37))

SST_min_futureA1B<-raster("C:/Users/Chris/Desktop/van Woesik/ORACLE future temp
scenarios/A1B/2100/sstmin.asc")
proj4string(SST_min_futureA1B)<- CRS("+proj=longlat")
SST_min_future2A1B<-crop(SST_min_futureA1B,extent(-180,180,-37,37))

kd<-raster("C:/Users/Chris/Desktop/van Woesik/Light Attenuation kd/mean kd 1998-2007 9km.nc ")#average
light attenuation 490 coefficiten to 1998 to 1007 mean of each layer NA values removed. resolution = .0833333
(9km)


change.kd_to_PLD<-function(x,Zmax=3){ #for rasters
  x2<-.6677*x^.6763 #kdPAR~kd490 pierson et al. 2007
  Y2<-exp((-1*x2)*Zmax) #percent light at depth zmax  - 3 meters depth
  return(Y2)
}
```

```
PLD<-change.kd_to_PLD(kd)

PAR.mean<-raster("C:/Users/Chris/Desktop/van Woesik/PAR global
data/SWFMO_PAR.CR.timeAverage1998-2007.nc")


#median.reef.PLD<-0.4570086#from light attenuation median
# tPARmeanFINAL<-crop(PAR.mean,extent(PLD))*median.reef.PLD #training raster

pPARmeanFINAL<-crop(PAR.mean,extent(PLD))*PLD #prediction raster

####################
####################
####################
####################
#################### SET Mechanistic values
########################################


minTolerance<-18.0        #degrees C of minimum tolerance
dispersalDist<-10        #how far the species can disperse each year (KM)
LongitudinalBuffer<-5     #the initial longitudinal buffer for dispersal uncertainty values(0:10) numeric, also
will do latitude
ProjTime<-86.0            #years until projection (2100)
AdaptationRange<-1        #how much range will the species be able to tolerate in 2100 (can change to time
relationship) - 1 degree gain in range tolerance
PAR.limit<-21.6 #value from Kleypas 1997, 250 microE/m^2/s = 21.6 E/m^2/day
Zmax<-3
turbidrun<-0
#increaseSD<-1



########################################
####################
####################
####################

#acropora hyacinthus = set 1 i<-58
#plobata = set<-2;i<-398

# cl <- makeCluster(5) #
# registerDoParallel(cl)
# registerDoParallel(cl)

#read IUCN
list1<-c(1,1,2,2,2,2,2,1,2,2,2,2)
list2<-c(58,30,65,129,140,180,238,233,395,398,455,470)

#for (vers in c(7:12)){
vers<-10
set<-list1[vers]
i<-list2[vers]

setwd("C:/Users/Chris/Desktop/van Woesik/IUCN shapes")
corals2<-read.dbf(paste("CORALS",set,".dbf",sep=""))
```

```
corals<-corals2[order(corals2$binomial),]
Species<-paste(corals[i,2])

#convert to CRS
setwd(paste("C:/Users/Chris/Desktop/van Woesik/IUCN shapes/Coral shapes/Corals",set,sep=""))
IUCN_dist2<-readOGR(".",paste("CORALS",set,"_binomial__",Species,sep=''))
IUCN_dist<-spTransform(IUCN_dist2,CRS(newproj))

sparea<-area(IUCN_dist)
#find ecregions the species is in
IUCNinECO3<-ecoregions[!is.na(over(ecoregions,IUCN_dist)[,1]),]
IUCNinECO<-as.numeric(IUCNinECO3$New_No)
#IUCNinECO<-replace(IUCNinECO2, IUCNinECO2==142, 141)

print(paste("IUCN data converted to ecoregions",Species))

########## probability ################################################
regions<-IUCNinECO;nregions<-regions #regions the spp is in
one2141<-c(1:141)
absent<- one2141[!one2141 %in% regions] #find the regions the species is not in


adjlist<-data.frame() #list of all adjacent regions to the species (includes regions species is in)
for (j in nregions){
  AdjRegions<-AdjacencyMat[j,1:10]
  adjlist<-rbind(adjlist,AdjRegions)}
noNAadjlist<-adjlist[!is.na(adjlist)]
No_Present_Or_NA_adjlist<-noNAadjlist[!noNAadjlist%in%(nregions)]########################
No_Present_Or_NA_adjlist is list of adjacent regions that do not have the species detected, not unique because
we sample through the number of iterations

########## give each initial absent region a probability of 30% to find species on first try.
problist<-data.frame()
for (i in 1:141){
  if (i %in% nregions){ # if it is in a region P(detect)=1
    x<-1}
  else{x<-.3} # if not in region P(detect)= .3
  problist<-rbind(problist,x)
}
#################################### initial values set


problist1<-c(do.call("cbind",problist))  ################ change .6 as decrease of adjacent regions
for (i in No_Present_Or_NA_adjlist){
  problist1[i]<-problist1[i]*.6}  ########### everytime a species is detected adjacent to a region the species is
absent from, probablility of detection is decreased by 40% because it is more likely the samplers missed it.

############### incorporate size into P

Plist<-problist1
for (i in absent){
  size<-sizes[i]
  ratioArea<-(minsize/size)^4 ##for regions the species is absent in take the log area of the region and divide
log min area by it
  Plist[i]<-Plist[i]*ratioArea}
problist<-Plist
```

```
if (any(!regions %in% c(123:137))==T){ ## they are not in atlantic
  problist[c(123:137)]<-1
  ATLvPAC<-1}#caribbean <- known absent

if (any(regions %in% c(123:137))==T){  ## they are in atlantic
  (problist[c(1:122,139:141)]<-1)
  ATLvPAC<-0} # pacific <- known absent

#ATLvPAC is 1 if it is a pacific species
probmat<-problist
#probmat


cl <- makeCluster(5) #
registerDoParallel(cl)


#determine which regions the species is likely to be absent

print("p2")
variance<-foreach (i = 1:141,.combine=rbind,.verbose=F) %dopar% {  ##########################loop it
for variance and Prob of Geometric
  p<-probmat[i]
  nfails<-SEF[i]

  maxSE<-max(SEF) #find the maximum value of sampling effort

  #geometric distribution for SE out of maxSE
  pgm<-pgeom(nfails,p)#probablility of finding this spp after x trials
  mx<-pgeom(maxSE,p)#prob of finding after max attempts
  PGM<-pgm /mx  #difference in probablility of finding after x trials - max attempts

  #determine variance
  VAR<-(1-p)/p^2  # get the variance
  EXP<-1/p    #expected value
  c(VAR,EXP,nfails,PGM) #combine variance, expected, sampling effort, probability of finding after SE trials
}
print("done var")

n<-1
se<-(sqrt(variance[,2]))/sqrt(n)
p<-probmat
#confidence of 95%
c95<-se*1.96 # determine the 95% confidence of regions
s95<-((log(1-.95)/log(1-p))-1) # determine the SE at which we are 95% sure we have found it.
plotsp<-cbind(variance,c95,s95,p)
rownames(plotsp)<-scip[,1]
colnames(plotsp)<-(c("var","exp","nfails","ProbFound","c95","s95","p"))
oplotsp<-plotsp[order(plotsp[,6]),]


low_confidence_regions<-foreach (i = 1:141,.combine=rbind)%dopar%{
  if(plotsp[i,4]<.95){i} ######################################## only take ones greater than 95% (could
include the confidence of that confidence?)
}
lowregions<-scip[low_confidence_regions,1]#if you need the region names
```

```
stopCluster(cl)


############# shapes of classified regions ############
#uncertain
n.regions<-as.numeric(low_confidence_regions[,1])
n.shpregions<-ereg[n.regions,604]
lowconf<-ecoregions[c(n.shpregions),]

#present
p_regions<-regions
shpregions<-ereg[regions,604]
this_spp<-ecoregions[c(shpregions),]
this_spp<-gBuffer(this_spp,width=0,byid=T)

#absent
pres_and_uncert<-c(n.regions,p_regions)
all<-c(1:141)
no<-setdiff(all,pres_and_uncert)
certainGone<-ereg[no,604]
none<-ecoregions[c(certainGone),]


############################################################  MEGAECOREGIONS !!!!! run one for each zone.. how to go abou this efficiently

# here we need to take the 5 major connectivity zones and isolate each one, then subtract the absent ecoregions from the megaecoregion, all others are also absent. but we do not include the carribbean in the absent regions for sampling the data.

#geographic barriers like the Caribbean are not counted as absent, but we include the rest of the pacific because dispersal is possible, but they are still genetically more isolated, this genetic isolation prohibits a positive, but is it necessarily abstent because it can't handle those conditions.

#Five megaregions


################################### ZONING


for(zonei in 1:6){

for(CONF in 1:25){


ZAmericas<-c(67,115:133) #western Americas
ZHawaii<-c(111:113) #Hawaii main,johnston atoll,Nhawaii
ZSpac<-c(105:110,114) #Line,Marquesas,Moorea
ZAfrica <-c(2:23,134:138,140,141,96) # all others,near africa -srilanka - cocos keeling
restof<-c(ZAmericas,ZHawaii,ZSpac,ZAfrica)
Zindo<-setdiff(all,restof)  # Marshalls, Phoenix,Samoa,Fiji indonesia
Indian_indo<-c(ZAfrica,Zindo)

zones<-list(ZAmericas,ZHawaii,ZSpac,Zindo,ZAfrica,Indian_indo)
zone<-zones[[zonei]]     #### set the zone
#present<-intersect(present,megazone)
```

```
### megaregion present
newP<-intersect(zone,p_regions)
shpregions<-ereg[newP,604]
this_spp<-ecoregions[c(shpregions),]
this_spp<-gBuffer(this_spp,width=0,byid=T) #

##megaregion Absent

allno<-setdiff(all,zone)  #everyhting outside the zone
not_in_zone<-setdiff(zone,newP) #everything in zone that is not present
absinzone<-union(allno,not_in_zone) #add these two
BLAH<-intersect(zone,n.regions)#remove all things in zone that are uncertain
abs2<-setdiff(absinzone,BLAH)
certainGone<-ereg[abs2,604]
none<-ecoregions[c(certainGone),]  #absent ,not in megaregion and 95% within megaregion
########################################### END ZONING


#Absent zones will only be sampled as absent if in same ocean as species, so Atlantic zones will not be counted
as present or absent because geographic barriers prevent distribution, not the environment.
#  plot(ecoregions)
#  plot(this_spp,add=T,col='green')
# plot(none,add=T,col='red')


### plotting the regions

#   plot(ecoregions)
#   plot(ecoregions[ereg[ZAmericas,604],],col='blue',add=T)
#   plot(ecoregions[ereg[ZHawaii,604],],col='red',add=T)
#   plot(ecoregions[ereg[ZSpac,604],],col='green',add=T)
#   plot(ecoregions[ereg[ZAfrica,604],],col='orange',add=T)
#   #plot(ecoregions[ereg[Zindo,604],],col='pink',add=T)
#   plot(ecoregions[ereg[Indian_indo,604],],col='pink',add=T)
#


######################################### MEGAECOREGIONS DONE


#sampling numbers
if(ATLvPAC==1){absentSampleNumber<-(length(none)-15)}
if(ATLvPAC==0){absentSampleNumber<-(length(none)-125)}
absentSampleNumber/(length(this_spp)+absentSampleNumber)->ratio
asamp<-round(3000*ratio);psamp<-round(3000-asamp)


print(paste("probability is determined", length(regions),"present",length(no),"absent,","presence
samples=",psamp,"absence samples=",asamp))


######################3 run it all

print('start points')
############################## extract points
```

```
if(ATLvPAC==1){Atldepth<-AtldepthP}
if(ATLvPAC==0){Atldepth<-AtldepthC}

cl <- makeCluster(5) #
registerDoParallel(cl)


ecoP<-this_spp
ecoP<-spTransform(ecoP,CRS(proj4string(reefs)),force_ring=TRUE)


inreefs2<-over(reefs,ecoP)
short<-reefs[!is.na(inreefs2[,1]),]

#absence points
ecoA<-none
ecoA<-spTransform(ecoA,CRS(proj4string(Atldepth)),force_ring=TRUE)
ecoA<-gBuffer(ecoA,width=0,byid=F)
Absintersection<-gIntersection(ecoA,Atldepth)

cuts<-round(asamp/100)
cutsamp<-round(seq(1,asamp,length.out=cuts))


abspts<-foreach(i=1:(cuts-1),.packages="sp",.combine=rbind) %dopar%{
  abspt<-spsample(Absintersection,cutsamp[i+1]-cutsamp[i], type='random',iter=100)
  coordinates(abspt)}

abspts<-SpatialPoints(abspts)
abspts.<-SpatialPointsDataFrame(abspts,data=data.frame(1:length(abspts)))

#presence points

 ####### REEFS INSIDE ECOREGIONS ################
inreefs<-as.numeric(rownames(inreefs2))

blure<-paste("determine presence points");print(blure)

#   stopCluster(cl)
#
#   cl <- makeCluster(5) #
#   registerDoParallel(cl)

if(zonei!=1){
cuts<-round(psamp/10)
cutsamp<-round(seq(1,psamp+200,length.out=cuts))
scuts<-round(seq(1,length(short),length.out=cuts))
inreefst1<-foreach(i=2:cuts,.packages=c("sp"),.combine=rbind) %dopar%{
  lrfs<-(short[scuts[i-1]:scuts[i]])
  rpoints<-spsample(lrfs,n=(cutsamp[i]-cutsamp[i-1]),"random",iter=100)
  coordinates(rpoints)
}
}

if(zonei==1){
rpoints<-spsample(short,n=psamp+200,"random",iter=100)
inreefst1<-coordinates(rpoints)
```

```
}

inreefst<-SpatialPoints(inreefst1)
Prespoints1<-SpatialPointsDataFrame(inreefst,data=data.frame(1:length(inreefst)))
proj4string(Prespoints1)<-proj4string(ecoP)
testpoint<-(over(Prespoints1,as(ecoP, "SpatialPolygons")))
tp2<-cbind(testpoint,1:length(testpoint))
shlst<-tp2[complete.cases(tp2),2] # take only complete cases
snum<-sample(shlst,psamp) #randomly sample the needed number of values
Prespoints<-Prespoints1[snum,]

stopCluster(cl)


print(paste("done sampling points"))

########################


################## Regression
##################  regression
##################  regression
##################  regression

proj4string(abspts.)<-newproj
tabs_pts<-abspts.
tpts<-Prespoints

pts<-spTransform(tpts,CRS=CRS(nextproj))
abs_pts<-spTransform(tabs_pts,CRS=CRS(nextproj))


############# CONNECTIVITY LAYER - mask outside 5 degrees  #############

longs<-(coordinates(pts)[,1]) #lon of pts
lats<-(coordinates(pts)[,2])
rlongs<-round(longs)
rlats<-round(lats)
urlon<-unique(rlongs)
urlat<-unique(rlats)
turlon<-180+urlon


today<-data.frame()
for (i in 1:LongitudinalBuffer) {
  today<-c(today,(unique(c(turlon,turlon+i,turlon-i))))
}

todayL<-data.frame()
for (i in 1:LongitudinalBuffer) {
  todayL<-c(todayL,(unique(c(urlat,urlat+i,urlat-i))))
}


unturlat<-as.numeric(unique(todayL))
unturlon<-as.numeric(unique(today))
```

```
xc1<-sub(361,1,unturlon);xc2<-sub(362,2,xc1);xc3<-sub(363,3,xc2);xc4<-sub(364,4,xc3);xc5<-
sub(365,5,xc4);xc6<-sub(366,6,xc5);xc7<-sub(367,7,xc6);xc8<-sub(368,8,xc7);xc9<-sub(369,9,xc8);xc10<-
sub(370,10,xc9)
xc<-sub( "^0",360,xc10)
xc12<-sub( "^-1$" ,359,xc);xc13<-sub( -2 ,358,xc12);xc14<-sub( -3 ,357,xc13);xc15<-sub( -4
,356,xc14);xc16<-sub( -5 ,355,xc15);xc17<-sub( -6 ,354,xc16);xc18<-sub( -7 ,353,xc17);xc19<-sub( -8
,352,xc18);xc20<-sub( -9 ,351,xc19);xc21<-sub( -10 ,350,xc20)

xct<-as.numeric(xc21)
uxct<-unique(xct)
#min(uxct);max(uxct)

mlat<-matrix(ncol=360,nrow=180)
mlon<-matrix(ncol=360,nrow=180)
mlon[,uxct]<-1
mlat[,]<-1
mlat[90-unturlat,]<-0
q<-raster(mlon)
q2<-raster(mlat)
extent(q)<-c(xmin=-180,xmax=180,ymin=-90,ymax=90)
q<-crop(q,extent(-180,180,-37,37))
proj4string(q)<-"xy"
proj4string(q)<-nextproj
extent(q2)<-c(xmin=-180,xmax=180,ymin=-90,ymax=90)
q2<-crop(q2,extent(-180,180,-37,37))
proj4string(q2)<-"xy"
proj4string(q2)<-nextproj


q<-mask(q,q2,maskvalue=1)
# plot(q)
# plot(q2,add=T)
# points(pts)

#combine lat and lon masks
q<-resample(q,SST_min_current)



print(paste("Connectivity layer done"))

################################################


######################### KFOLD for HIGHEST AUC ############################## here is first run
of the model

cl <- makeCluster(5) # 4 cores
registerDoParallel(cl)
registerDoParallel(cl)


perMutations<-100
pscoreholder <- foreach(i = 1:perMutations, .packages = c("dismo","raster","stats","blme")) %dopar% {
  kfold(pts, 5) ##subset into 5 groups
}
ascoreholder <- foreach(i = 1:perMutations, .packages = c("dismo","raster","stats")) %dopar% {
```

```
 kfold(abs_pts, 5) ##subset into 5 groups
}
AUC <- foreach(i = 1:perMutations, .packages = c("dismo","raster","stats","lme4"),.combine='c') %dopar% {
 ##subset into 5 groups

 pres_train <- pts[c(pscoreholder[[i]]) != 1, ]
 pres_test <- pts[c(pscoreholder[[i]]) == 1, ]

 abs_train <- abs_pts[c(ascoreholder[[i]]) != 1, ]
 abs_test <- abs_pts[c(ascoreholder[[i]]) == 1, ]

 #extract training values
 presvals <- extract(rasters2, pres_train,method="bilinear") #rasters has training data
 absvals <- extract(rasters2, abs_train,method="bilinear")  #rasters2 has predicitng contemporary data
 if(turbidrun==1){
  presvals<-round(presvals,1)
  absvals<-round(absvals,1)
 }
 ##format data
 pb <- c(rep(1, nrow(presvals)), rep(0, nrow(absvals)))
 sdmdata <- data.frame(cbind(pb, rbind(presvals, absvals)))

 ######



 #turbidity model
 if(turbidrun==1){
   try(gam1 <- bglmer(pb ~SST_range_current*PAR_range+(1|PLD_mean),data=sdmdata,cov.prior=gamma,
family = binomial(link = "logit")))
 }


 #non-turbidity model
 if(turbidrun==0){
  try(gam1 <- glm(pb ~ (SST_range_current)*(PAR_range),family = binomial(link = "logit"), data=sdmdata))
 }

 ### AUC = true positives/false positives
 ######
 #########
 ##############
 ##################
 ########################


 ## set up evaluation data
 testpres <- data.frame( extract(rasters, pres_test) )
 testpres<-testpres[complete.cases(testpres),]
 testbackg <- data.frame( extract(rasters, abs_test) )
 testbackg<-testbackg[complete.cases(testbackg),]
 ##

 ### evaluate and set a threshold

 gam1e <- evaluate(testpres, testbackg, gam1,allow.new.levels=T)
 gam1e@auc
```

```
}

maxAUC<-which.max(AUC)

pres_train <- pts[c(pscoreholder[[maxAUC]]) != 1, ]
pres_test <- pts[c(pscoreholder[[maxAUC]]) == 1, ]

abs_train <- abs_pts[c(ascoreholder[[maxAUC]]) != 1, ]
abs_test <- abs_pts[c(ascoreholder[[maxAUC]]) == 1, ]

#extract training values
presvals <- extract(rasters2, pres_train,method="bilinear")
absvals <- extract(rasters2, abs_train,method="bilinear")

##format data
pb <- c(rep(1, nrow(presvals)), rep(0, nrow(absvals)))
sdmdata <- data.frame(cbind(pb, rbind(presvals, absvals)))
sdmdata[,4]<-round((sdmdata[,4])*2,-1)/2


#
# maty<-(as.data.frame(matrix(rep(c(1,NA,12,NA),100),ncol=4,byrow=T)))
# names(maty)<-names(sdmdata)
# sdmdata<-rbind(sdmdata,maty)
#
# if (increaseSD>0){
#   dbt<-fitdistr(c(sdmdata[is.finite(sdmdata[,3]),3]),'gamma')   #fit gamma distribution
#   a<-dbt$estimate[1]  #shape
#   b<-dbt$estimate[2]   # rate
#
#   std<-sqrt(a/b^2)   #Standard deviation of gamma dist
#   m<-a/b           #Mean of Gamma
#
#   #paste(round(m,2),round(std,2))   #paste mean,sd
#   #hist(rgamma(1000,shape=a,rate=b),50)
#
#
#   VX<-((std)^2)/((std+(std*increaseSD))^2)   ##### equation to increase sd by one while keeping mean the
same
#   a<-a*VX  ## change a & b dependent on equation
#   b<-b*VX
#   std<-sqrt(a/b^2)   #Standard deviation of gamma dist  ##recalculate
#   m<-a/b           #Mean of Gamma
#   paste(round(m,2),round(std,2))   #paste new
#
#
#
# }


print(paste("Kfold finished"))


stopCluster(cl)
```

```
####################### RUN initail GAM with  highest AUC   #######
#################
############
#######
####

#turbid model
if(turbidrun==1){
  gam1 <- bglmer(pb ~SST_range_current*PAR_range+(1|PLD_mean),data=sdmdata, family = binomial(link =
"logit"),verbose=T,cov.prior=gamma)#,control=glmerControl(optCtrl=list(maxfun=100000) ))
}

if(turbidrun==0){
  #non turbid model
  gam1 <- glm(pb ~ (SST_range_current)*(PAR_range),family = binomial(link = "logit"), data=sdmdata)
}


####
#######
###########
###########
################
###################
### AUC = true positives/false positives
## set up evaluation data
testpres <- data.frame( extract(rasters, pres_test) )
testpres<-testpres[complete.cases(testpres),]
testbackg <- data.frame( extract(rasters, abs_test) )
testbackg<-testbackg[complete.cases(testbackg),]

# enutriTPRES<-data.frame( extract(nutrients, pres_test) )
# enutriTPRES<-enutriTPRES[complete.cases(testpres),]
# enutriTBACKG<-data.frame( extract(nutrients, abs_test) )
# enutriTBACKG<-enutriTBACKG[complete.cases(testpres),]
##
testinga<-rbind(testpres,testbackg)
### evaluate and set a threshold
testing1<-raster(ncol=1,nrow=sum(nrow(testpres),nrow(testbackg)));values(testing1)<-testinga[,1]
testing2<-raster(ncol=1,nrow=sum(nrow(testpres),nrow(testbackg)));values(testing2)<-testinga[,2]
testing3<-raster(ncol=1,nrow=sum(nrow(testpres),nrow(testbackg)));values(testing3)<-testinga[,3]
testing<-stack(testing1,testing2,testing3)
names(testing)<-names(testinga)

tstd.a <- predict(testing,gam1,type="response",na.action=na.omit,re.form=NULL,allow.new.levels=T)
#tstd<-tstd.a-(.0432*(enutriTPRES*(2.86297283611898e+13/sparea))* 1.73819020691208e-07)
tstd<-tstd.a
evald<-evaluate(values(tstd)[1:nrow(testpres)],values(tstd)[nrow(testpres):length(values(tstd))])


tr<-threshold(evald, 'spec_sens')

gam1e <- evaluate(testpres, testbackg, gam1,re.form=NULL,allow.new.levels=T)
gam1e@auc

print('predict')
pgam1.a <- predict(rasters2,gam1,type="response",na.action=na.omit,re.form=NULL,allow.new.levels=T)
```

```
#
#
# ################### FUTURE MODEL RUN ######################
pgam2.a <- predict(Future, gam1,type="response",na.action=na.omit,re.form=NULL,allow.new.levels=T)
pgam2B1 <- predict(FutureB1, gam1,type="response",na.action=na.omit,re.form=NULL,allow.new.levels=T)
pgam2A1B <- predict(FutureA1B,
gam1,type="response",na.action=na.omit,re.form=NULL,allow.new.levels=T)


#################### ADAPTATION MODEL RUN ###################
#FTA2<-TempRange2100x-AdaptationRange
#FTAB1<-TempRangeB1x-AdaptationRange
#FTAA1B<-TempRangeA1Bx-AdaptationRange

#adapRasA2<-stack(PAR_rangex,FTA2,pPARmeanFINAL)
#adapRasB1<-stack(PAR_rangex,FTAB1,pPARmeanFINAL)
#adapRasA1B<-stack(PAR_rangex,FTAA1B,pPARmeanFINAL)



# names(adapRasA2)<-c('PAR_range','SST_range_current','PLD_mean')
# adapRasA2<-crop(adapRasA2,extent(-180,180,-37,37))
# pgam3 <- predict(adapRasA2, gam1,type="response",na.action=na.omit,re.form=NULL,allow.new.levels=T)
#
# names(adapRasB1)<-c('PAR_range','SST_range_current','PLD_mean')
# adapRasB1<-crop(adapRasB1,extent(-180,180,-37,37))
# pgam3B1 <- predict(adapRasB1,
gam1,type="response",na.action=na.omit,re.form=NULL,allow.new.levels=T)
#
# names(adapRasA1B)<-c('PAR_range','SST_range_current','PLD_mean')
# adapRasA1B<-crop(adapRasA1B,extent(-180,180,-37,37))
# pgam3A1B <- predict(adapRasA1B,
gam1,type="response",na.action=na.omit,re.form=NULL,allow.new.levels=T)

print(paste("Contemporary, Future, and adaptation models run"))

#####################
#################### NUTRIENT EFFECT, bases on endinger Plobata study inference

#pgam1<-pgam1.a-(.0432*(nutrients*(2.86297283611898e+13/sparea))* 1.73819020691208e-07)
#pgam2<-pgam2.a-(.0432*(nutrients*(2.86297283611898e+13/sparea))* 1.73819020691208e-07)


######## Nutrients have no effect, to discard them from this analysis use

pgam1<-pgam1.a
pgam2<-pgam2.a



#####################
#################



############### First Masking ###############
```

```
## mask out reef, temp<18, and longitude

print('masking 1')
maskreef<-mask(pgam1,mask_deep_bathy,maskvalue=NA) #mask less than 20 meters
mask_temp_reef<-mask(maskreef,SST_min_current>minTolerance,maskvalue=0) #mask less than the
minimum tolerance degrees C
mask_temp_reef_lon<-mask(mask_temp_reef,q,maskvalue=NA) #mask outside distribution lon
mask_temp_reef_lon<-mask(mask_temp_reef_lon,riversBuffer,inverse=T) #mask rivers
if(turbidrun==1){
  mask_temp_reef_lon<-mask(mask_temp_reef_lon,pPARmeanFINAL<PAR.limit,maskvalue=1)#mask too
low light
}
mask_temp_reef_lon_ATL<-mask(mask_temp_reef_lon,ATL,inverse=T) #mask the Atlantic


###################### DISPERSAL BETWEEN TIME PERIODS ####################
print('start dispersal')
initdistr<-(mask_temp_reef_lon_ATL > tr)
initdistr[initdistr==0] <- NA
dispdistKM<-dispersalDist*ProjTime


lx<-5330-dispersalDist*333 ## random points to be taken from the distribution, should cover all # using this
formula, 1km samples 5000 pts, and 10 samples 2000, ranging linearly between
prand<-randomPoints(initdistr,lx)  #take random background points to cover extent #transform CRS for
projection

sprand<-SpatialPoints(prand)
proj4string(sprand) <- CRS(nextproj)
lox<-spTransform(sprand,CRS(newproj))

IDK<-gBuffer(lox,width=(dispdistKM*1000),byid=F) ## buffer by the distance of dispersal

#polygon to raster
sdxprand<-SpatialPolygonsDataFrame(IDK,data=data.frame(1),match.ID=F)
idk<-vect2rast(sdxprand,cell.size=70000)
rasBuf<-(raster(idk))
reprojRB2<-projectRaster(rasBuf,crs=CRS(nextproj))
reprojRB3<-reprojRB2>0
reprojRB4<-crop(reprojRB3,extent(pgam1))
reprojRB<-resample(reprojRB4,pgam1)

print(paste("DISPERSAL BETWEEN TIME PERIODS done"))


################## MODEL ACCURACY ####################
presconfusion<-data.frame(extract(pgam1,pts));names(presconfusion)<-'x'
absconfusion<-data.frame(extract(pgam1,abs_pts));names(absconfusion)<-"x"
conmat<-rbind(presconfusion,absconfusion)
pi.hat <- exp(conmat)/(1 + exp(conmat))
pball <- c(rep(1, nrow(pts)), rep(0, nrow(abs_pts)))
flop<-cbind(pball,pi.hat)
flopx<-flop[complete.cases(flop),]
Lost<-confusion.matrix(flopx$pball,flopx$x,threshold=.5)
ModelAccuracy<-(Lost[1,1]+Lost[2,2])/(Lost[1,1]+Lost[1,2]+Lost[2,1]+Lost[2,2])
OM<-omission(Lost)
Sens<-sensitivity(Lost)
```

```
Specifi<-specificity(Lost)
PropC<-prop.correct(Lost)
h1<-paste(ModelAccuracy,"Model Accuracy")
h2<-paste(OM,"omission")
h3<-paste(Sens,"sensitivity")
h4<-paste(Specifi,"specificity")
h5<-paste(PropC,"prop.correct")


print(paste("Model accuracy done"))


# ## mask out reef, temp<18, and longitude
# maskreef<-mask(pgam1,mask_deep_bathy,maskvalue=0) #mask less than 20 meters
# mask_temp_reef<-mask(maskreef,SST_min_current>minTolerance,maskvalue=0) #mask less than the
minimum tolerance degrees C
# mask_temp_reef_lon<-mask(mask_temp_reef,q,maskvalue=NA) #mask outside distribution
# mask_temp_reef_lon<-mask(mask_temp_reef_lon,riversBuffer,inverse=T) #mask rivers
# mask_temp_reef_lon_ATL<-mask(mask_temp_reef_lon,ATL,inverse=T) #mask the Atlantic


################## MASKING for PLOTTING2 ####################
#masking for  future scenarios and adaptation


cl <- makeCluster(3) #
registerDoParallel(cl)
namess<-c("2","2B1","2A1B")
SST_min_future2<-SST_min_future

listedras<-pgam2
for(str in 2:3){
  listedras<-stack(listedras,get(paste("pgam",namess[str],sep="")))}
names(listedras)<-namess

listedmin<-SST_min_future2
for(str in 2:3){
  listedmin<-stack(listedmin,get(paste('SST_min_future',namess[str],sep="")))}
#names(listedmin)<-namess


  rastermask<-foreach (prep=1:3,.packages=c('raster','sp')) %dopar%{
    maskreef2A1B<-mask(subset(listedras,prep),mask_deep_bathy,maskvalue=NA)

    #### mask out all future places where min is less than 18 degrees
    mask_temp_reef2A1B<-mask(maskreef2A1B,subset(listedmin,prep)>minTolerance,maskvalue=0) #mask
too low of temperatures
    mask_temp_reef_lon2A1B<-mask(mask_temp_reef2A1B,reprojRB>0,maskvalue=NA) #mask distribution
    mask_temp_reef_lon2A1B<-mask(mask_temp_reef_lon2A1B,riversBuffer,inverse=T) #mamsk rivers
    if(turbidrun==1){
        mask_temp_reef_lon2<-mask(mask_temp_reef_lon2,pPARmeanFINAL<PAR.limit,maskvalue=1)#mask
too low light #
      }
    mask(mask_temp_reef_lon2A1B,ATL,inverse=T) #mask atlantic ocean
  }
```

```
### assign the names of the masked rasters
for (fg in 1:3){
  assign(paste("mask_temp_reef_lon_ATL",namess[fg],sep=''),rastermask[[fg]])
}

  stopCluster(cl)

# maskreef2<-mask(pgam2,mask_deep_bathy,maskvalue=NA)
# #### mask out all future places where min is less than 18 degrees
# mask_temp_reef2<-mask(maskreef2,SST_min_future>minTolerance,maskvalue=0) #mask too low of
temperatures
# mask_temp_reef_lon2<-mask(mask_temp_reef2,reprojRB>0,maskvalue=NA) #mask distribution
# mask_temp_reef_lon2<-mask(mask_temp_reef_lon2,riversBuffer,inverse=T) #mamsk rivers
# if(turbidrun==1){
#   mask_temp_reef_lon2<-mask(mask_temp_reef_lon2,pPARmeanFINAL<PAR.limit,maskvalue=1)#mask
too low light #
# }
# mask_temp_reef_lon_ATL2<- mask(mask_temp_reef_lon2,ATL,inverse=T) #mask atlantic ocean

print(paste("masking 2 done"))
proj4string(pgam2)<-CRS("+proj=longlat")
proj4string(pgam2B1)<-CRS("+proj=longlat")
proj4string(pgam2A1B)<-CRS("+proj=longlat")
# proj4string(pgam3)<-CRS("+proj=longlat")
# proj4string(pgam3B1)<-CRS("+proj=longlat")
# proj4string(pgam3A1B)<-CRS("+proj=longlat")
proj4string(mask_temp_reef_lon_ATL)<-CRS("+proj=longlat")


#### RasterVis
#of all area

# mask_temp1<-mask(pgam1>tr,SST_min_future>minTolerance,maskvalue=0)
# mask_temp_lon1<-mask(mask_temp1,q,maskvalue=NA)
# mask_temp2<-mask(pgam2>tr,SST_min_future>minTolerance,maskvalue=0)
# mask_temp_lon2<-mask(mask_temp2,q,maskvalue=NA)
# dif<-mask_temp_lon1-mask_temp_lon2
# loss_of_hab<-mask(dif,dif,maskvalue=-1)
# loss_of_hab<-mask(loss_of_hab,ATL,inverse=T)
# loss_of_hab<-mask(loss_of_hab,riversBuffer,inverse=T)
# #of reefs
# lostras<-((mask_temp_reef_lon_ATL>tr)-(mask_temp_reef_lon_ATL2>tr))>0
# lostrass<-mask(lostras,lostras,maskvalue=0)
#


###################### AREA STATISTICS ######################
### find area of distribution #deepmask needs to be second

slick<-
matrix(ncol=3,nrow=5,data=NA,dimnames=list(c("current","lost",'future','new','change'),c("2","2B1","2A1B"))
)
strings<-c("2","2B1","2A1B") #2100 A2,B1,A1B,  Adaptation A2,Adap B1,Adap A1B
for (p in 1:3){
  i<-strings[p]

  a<-area(mask_temp_reef_lon_ATL)## the area of cells in meters^2? MAKE SURE MASS IS DETACHED
```

```
 #deepmask<-mask(a,mask_temp_reef_lon_ATL2)
 #assign(paste0("deepmask",i),mask(a,get(paste("mask_temp_reef_lon_ATL",i,sep=""))>tr))

 #current area
 curhab1<-mask(a,mask_temp_reef_lon_ATL>tr)
 curhab<-mask(curhab1,mask_temp_reef_lon_ATL>tr,maskvalue=0)
 curhabval<-(cellStats(curhab,sum)) #-66120
 slick[1,p]<-curhabval


 #lost
 pizza<-sum((get(paste("mask_temp_reef_lon_ATL",i,sep=""))>tr),(-
2*(mask_temp_reef_lon_ATL>tr)),na.rm=F)
 zz2<-mask(a,pizza==(-2),maskvalue=0)
 assign(paste0("losthab",i),mask(zz2,pizza==(-2),maskvalue=NA))
 assign(paste0("losthabval",i),cellStats(get(paste("losthab",i,sep="")),sum))
 slick[2,p]<-get(paste("losthabval",i,sep=""))

 #future area
 zz4<-mask(a,(get(paste("mask_temp_reef_lon_ATL",i,sep=""))>tr),maskvalue=0)
 assign(paste0("futarea",i),mask(zz4,(get(paste("mask_temp_reef_lon_ATL",i,sep=""))>tr),maskvalue=NA))
 assign(paste0("futareaval",i),cellStats(get(paste("futarea",i,sep="")),sum))
 slick[3,p]<-get(paste("futareaval",i,sep=""))


 #new habitat gained
 assign(paste0("gain",i),mask((get(paste("futarea",i,sep=""))),curhab,inverse=T))
 assign(paste0("gainval",i),cellStats(get(paste("gain",i,sep="")),sum))
 slick[4,p]<-get(paste("gainval",i,sep=""))


 #percent changed
 assign(paste0("habchange",i),-(1-(get(paste("futareaval",i,sep=""))/curhabval))) # change in habitat
 slick[5,p]<-get(paste("habchange",i,sep=""))

 print(i)
}

slick<-cbind(slick,c(gam1e@auc,rep(NA,4)));colnames(slick)[4]<-"auc"
slick<-cbind(slick,c(Species,rep(NA,4)));colnames(slick)[5]<-"species"
slick<-cbind(slick,c(paste(Sys.Date()),rep(NA,4)));colnames(slick)[6]<-"time"

#
# slick<-matrix(ncol=1,nrow=5,data=NA,dimnames=list(c("current","lost",'future','new','change'),c("A2")))
# for (i in 2){
#   p<-1
#
#   a<-area(mask_temp_reef_lon_ATL)## the area of cells in meters^2? MAKE SURE MASS IS DETACHED
#   #deepmask<-mask(a,mask_temp_reef_lon_ATL2)
#   #assign(paste0("deepmask",i),mask(a,get(paste("mask_temp_reef_lon_ATL",i,sep=""))>tr))
#
#   #current area
#   curhab1<-mask(a,mask_temp_reef_lon_ATL>tr)
#   curhab<-mask(curhab1,mask_temp_reef_lon_ATL>tr,maskvalue=0)
#   curhabval<-(cellStats(curhab,sum)) #-66120
#   slick[1,p]<-curhabval
#
```

```
#
#   #lost
#   pizza<-sum((get(paste("mask_temp_reef_lon_ATL",i,sep=""))>tr),(-
2*(mask_temp_reef_lon_ATL>tr)),na.rm=F)
#   zz2<-mask(a,pizza==(-2),maskvalue=0)
#   assign(paste0("losthab",i),mask(zz2,pizza==(-2),maskvalue=NA))
#   assign(paste0("losthabval",i),cellStats(get(paste("losthab",i,sep="")),sum))
#   slick[2,p]<-get(paste("losthabval",i,sep=""))
#
#   #future area
#   zz4<-mask(a,(get(paste("mask_temp_reef_lon_ATL",i,sep=""))>tr),maskvalue=0)
#   assign(paste0("futarea",i),mask(zz4,(get(paste("mask_temp_reef_lon_ATL",i,sep=""))>tr),maskvalue=NA))
#   assign(paste0("futareaval",i),cellStats(get(paste("futarea",i,sep="")),sum))
#   slick[3,p]<-get(paste("futareaval",i,sep=""))
#
#
#   #new habitat gained
#   assign(paste0("gain",i),mask((get(paste("futarea",i,sep=""))),curhab,inverse=T))
#   assign(paste0("gainval",i),cellStats(get(paste("gain",i,sep="")),sum))
#   slick[4,p]<-get(paste("gainval",i,sep=""))
#
#
#   #percent changed
#   assign(paste0("habchange",i),-(1-(get(paste("futareaval",i,sep=""))/curhabval))) # change in habitat
#   slick[5,p]<-get(paste("habchange",i,sep=""))
#
#   print(i)
# }
#
#
# slick<-rbind(slick,c(gam1e@auc));rownames(slick)[6]<-"auc"
# slick<-rbind(slick,c(Species));rownames(slick)[7]<-"species"
# slick<-rbind(slick,c(paste(Sys.Date())));rownames(slick)[8]<-"time"

if(turbidrun==1){
  slick<-rbind(slick,c(paste(print(VarCorr(gam1),comp=c("Variance"))))));rownames(slick)[7]<-"Variance"
  slick<-rbind(slick,c(paste(sqrt(diag(VarCorr(gam1)$PLD_mean))))));rownames(slick)[8]<-"Std.Dev."
}
print('slick')



#
#
#   valeus<-(zonal(losthab2>0, init(losthab2, v='row'), fun='sum'))
#   pagain<-gain2>0
#   gains<-(zonal(pagain,init(pagain, v='row'), fun='sum'))
#
#   lonplot<-40 #what lattitude you want the map to show
#   btwnlons<-lonplot-37
#
#   kmlost2<-valeus[,2]*9.3^2 #9.3*9.3 per raster cell
#   kmlost<-c(rep(0,12*btwnlons),kmlost2,rep(0,12*btwnlons))
#   rlos<-length(kmlost) #the length for the derivplot
#   zmean<-c(0,0,0)
#   for (i in 3:(length(kmlost)-4)){
#     p<-mean(kmlost[c(i-3,i-2,i-1,i,i+1,i+2,i+3)])
```

```
#    zmean<-c(zmean,p)
#   }
#   finmena<-c(zmean,0,0,0)
#
#
#   kmgain2<-gains[,2]*9.3^2
#   kmgain<-c(rep(0,12*btwnlons),kmgain2,rep(0,12*btwnlons))
#   zmean<-c(0,0,0)
#   for (i in 3:(length(kmlost)-4)){
#     p<-mean(kmgain[c(i-3,i-2,i-1,i,i+1,i+2,i+3)])
#     zmean<-c(zmean,p)
#   }
#   fingain<-c(zmean,0,0,0)
#
#
#   closeer3<-cbind(finmena,fingain)
#   closeer2<-cbind(closeer3,rowSums(closeer3));colnames(closeer2)[3]<-'sum'
#   closeer1<-cbind(closeer2,max(closeer2[,3])-closeer2[,2]);colnames(closeer1)[4]<-'g second'
#
#   tmask_temp_reef_lon_ATL2<-mask_temp_reef_lon_ATL2
#   tmask_temp_reef_lon_ATL<-mask_temp_reef_lon_ATL
#   tlosthab2<-losthab2
#
#   extent(tmask_temp_reef_lon_ATL2)<-c(0,360,-37,37)
#   tmask_temp_reef_lon_ATL2<-rotate(tmask_temp_reef_lon_ATL2)
#   extent(tmask_temp_reef_lon_ATL2)<-c(0,360,-37,37)
#
#   extent(tmask_temp_reef_lon_ATL)<-c(0,360,-37,37)
#   tmask_temp_reef_lon_ATL<-rotate(tmask_temp_reef_lon_ATL)
#   extent(tmask_temp_reef_lon_ATL)<-c(0,360,-37,37)
#
#   extent(tlosthab2)<-c(0,360,-37,37)
#   tlosthab2<-rotate(tlosthab2)
#   extent(tlosthab2)<-c(0,360,-37,37)
#
#

####################save load data comps as an workspace


print('saving')
#Save data
setwd("C:/Users/Chris/Desktop/van Woesik/Mega ecoregions connectivity/Confidence runs")
newdir<-getwd()
subDir<-"A1B"
dir.create(file.path(newdir, subDir), showWarnings = FALSE)
setwd(file.path(newdir, subDir))
subDir2<-zonei
nowdir<-getwd()
dir.create(file.path(nowdir, subDir2), showWarnings = FALSE)
setwd(file.path(nowdir, subDir2))
##save.image(paste(paste(getwd(),Species,sep="/"),".RData",sep=""))  #saves a workspace file for later use
#save raster
writeRaster((mask_temp_reef_lon_ATL > tr),paste(zonei,Species,CONF,"initial dist.nc"),overwrite=T)
writeRaster((mask_temp_reef_lon_ATL2A1B > tr),paste(zonei,Species
,CONF,"A1B","distribution.nc"),overwrite=T)
```

```
#save stats
#write.csv(slick,paste(Species,"model stats",'.csv'))
slshort<-t(c(slick[,3],slick[1,4]))
colnames(slshort)<-c("current","lost","future","new","change","AUC")
if(CONF==1){write.table(slshort,paste("C:/Users/Chris/Desktop/van Woesik/Mega ecoregions
connectivity/Confidence runs/A1B/",zonei,"/table.csv",sep=''),sep=",",row.names = F,col.names=T,append=F)}
if(CONF!=1){write.table(slshort,paste("C:/Users/Chris/Desktop/van Woesik/Mega ecoregions
connectivity/Confidence runs/A1B/",zonei,"/table.csv",sep=''),sep=",",row.names = F,col.names=F,append=T)}


#Save data
setwd("C:/Users/Chris/Desktop/van Woesik/Mega ecoregions connectivity/Confidence runs")
newdir<-getwd()
subDir<-"B1"
dir.create(file.path(newdir, subDir), showWarnings = FALSE)
setwd(file.path(newdir, subDir))
subDir2<-zonei
nowdir<-getwd()
dir.create(file.path(nowdir, subDir2), showWarnings = FALSE)
setwd(file.path(nowdir, subDir2))

##save.image(paste(paste(getwd(),Species,sep="/"),".RData",sep=""))  #saves a workspace file for later use
#save raster
writeRaster((mask_temp_reef_lon_ATL > tr),paste(zonei,Species,CONF,"initial dist.nc"),overwrite=T)
writeRaster((mask_temp_reef_lon_ATL2B1 > tr),paste(zonei,Species
,CONF,"B1","distribution.nc"),overwrite=T)

#save stats
#write.csv(slick,paste(Species,"model stats",'.csv'))
slshort<-t(c(slick[,2],slick[1,4]))
if(CONF==1){write.table(slshort,paste("C:/Users/Chris/Desktop/van Woesik/Mega ecoregions
connectivity/Confidence runs/B1/",zonei,"/table.csv",sep=''),sep=",",row.names = F,col.names=T,append=F)}
if(CONF!=1){write.table(slshort,paste("C:/Users/Chris/Desktop/van Woesik/Mega ecoregions
connectivity/Confidence runs/B1/",zonei,"/table.csv",sep=''),sep=",",row.names = F,col.names=F,append=T)}


#   zz <- file(paste(Species,"stats auto.txt"),"w")
#   sink(zz)
#
#   print(paste("INPUT"))
#   print(paste("#degrees C of minimum tolerance="  ,minTolerance))
#   print(paste("#how far the species can disperse each year KM =",dispersalDist))
#   print(paste("#the initial longitudinal buffer for dispersal uncertainty (degrees) =",LongitudinalBuffer) )
#   print(paste("years until projected time =",ProjTime))
#   print(paste("adaptation coef", AdaptationRange))
#   print(paste("    ADAPTATION VALUES"))
#   print(gam1e)
#   print(summary(gam1))
#   print(Lost)
#   cat(paste(h1,h2,h3,h4,h5, sep='\n')   )
#   sink();close(zz)
#

################## FIGURES

#   png(paste(Species,"synthesis plot.png"),width=1323,height=418)#1323,418
#
```

```
#
#   layout( matrix( c(1,1,1,1,2,2),ncol=3),widths=c(2,2,1) )
#   par(mar = c(5, 5, 6, 0))
#
image(land,col=c("white","burlywood"),xlab="Longitude",ylab="Latitude",cex.main=4,cex.lab=1.8,cex.axis=1
.2,ylim=c(-lonplot,lonplot),xlim=c(20,290))
#   image((tmask_temp_reef_lon_ATL2 > tr),add=T,col=c("#00000000","limegreen"),legend=F)  ### new
habitat
#   image((tmask_temp_reef_lon_ATL > tr),add=T,col=c("#00000000","blue"),legend=F)  ### currently
inhabited
#   image((tlosthab2>0),add=T,col=c("red"))
#   legend("topright",c("lost habitat","gained habitat","retained
habitat"),col=c("red","green","blue"),pch=c(16,16,16),box.col=NA,bg="#00000000",cex=1.4)
#   box('plot',lty='solid')
#   #compassRose(345,-30,cex=.5)
#   axis(4,tick=T,labels=F,tck=.02)
#
#
#   par(mar=c(5,0,6,5),font.lab=1,font.main=1)
#
#   plot(finmena,1:length(finmena),type="l",ylim=rev(range(c(1,rlos))),xlim=c(0,max(closeer1[,3])),ann =
FALSE,axes=F)
#   polygon(finmena,1:length(finmena),col=rgb(.8,.1,.1,alpha=1))
#   polygon(closeer1[,4],1:length(finmena),col=rgb(.0,.8,.2,alpha=.5))
#   lines(closeer1[,4],1:length(finmena))
#   axis(1,cex.axis=1.2,at=(round(seq(0,max(closeer1[,3]),length.out=8),-3)))
#
axis(3,cex.axis=1.2,at=(seq(0,max(closeer1[,3]),length.out=8)),labels=c(rev(paste(round(seq(0,max(closeer1[,3
]),length.out=8),-3)))))
#
axis(4,at=c(0,length(finmena)*.25,length(finmena)/2,length(finmena)*.75,length(finmena)),labels=c("40","20",
"0","-20","-40"))
#   title(xlab=expression(paste("Habitat lost (km"^"2",")")),cex.lab=1.8)
#   title(main=expression(paste(" Habitat gained (km"^"2",")")),cex.main=1.8,xpd=T)
#   legend(0,1070,"",pch=5,xpd=T,col=rgb(.8,.1,.1,alpha=.5),bg=rgb(.8,.1,.1,alpha=1),cex=.6)
#   legend(0,-140,"",pch=5,xpd=T,col=rgb(.0,.8,.2,alpha=.5),bg=rgb(.0,.8,.2,alpha=.5),cex=.6)
#   mtext("Latitude",4,cex=1.3,line=3)
#   dev.off()
#
#

###### notify me of species being completed
try(send.mail(from = "slipping24@gmail.com",to = c("slipping24@gmail.com"),subject = "finished a
spp",body = "<html> Duck - <img src=\"http://beehivehairdresser.com/wp-content/uploads/2010/03/duck-
butt.jpg\"></html>",html = TRUE, smtp = list(host.name = "smtp.gmail.com", port = 465, user.name =
"slipping24", passwd = "########", ssl = TRUE),authenticate = TRUE,send = TRUE))
play(sin(1:20000/17)*2)
}

try(send.mail(from = "slipping24@gmail.com",to = c("slipping24@gmail.com"),subject = "Zone done R
home",body = "<html> Duck - <img src=\"http://beehivehairdresser.com/wp-content/uploads/2010/03/duck-
butt.jpg\"></html>",html = TRUE, smtp = list(host.name = "smtp.gmail.com", port = 465, user.name =
"slipping24", passwd = "#######", ssl = TRUE),authenticate = TRUE,send = TRUE))
print(Sys.time())

}
```

```
emailME<-send.mail(from = "slipping24@gmail.com",to = c("slipping24@gmail.com"),subject = "Error R
home",body = "<html> Duck - <img src=\"http://beehivehairdresser.com/wp-content/uploads/2010/03/duck-
butt.jpg\"></html>",html = TRUE, smtp = list(host.name = "smtp.gmail.com", port = 465, user.name =
"slipping24", passwd = "#######", ssl = TRUE),authenticate = TRUE,send = TRUE)
print(Sys.time())


#stopCluster(cl)
```

APPENDIX D: REEF ACCRETION MODEL CODE

```
#Reef accretion script - run after SDM of accreting spp below, compile (in this script?)


for (sppnum in c(1,2,4,5)){

library(raster)
#as a function?
source("C:/Users/Chris/Desktop/van Woesik/R functions/revrotate..R")
source("C:/Users/Chris/Desktop/van Woesik/R functions/rotater.R")
#take all available species, and sum up the accretion of each
#Porites lobata, Porites cylindrica, Acropora hyacinthus, Acropora digitifera, Goniastrea aspera, Favia speciosa,
Porites rus

#RCP 8.5
#turbidity run

Biological_Erosion<-T
Chemical_Erosion<-T
Physical_Erosion<-T


Ttotal<-10 #how many years projected, max=94
# sppnum <-1
specnumT<-4 #total number of species accreting on reef to devide erosion values by
#Perry et al 2015 suggest Acropora dominated reefs up to 8.4 kg CaCO3 m2 y-1
#Edinger et al 2000 tells us that max reef growth is 11.68 kg CaCO3
#Blanchon et al 2014 says that Acropora reefs grow faster than Porites reefs

Growth_rates<-c(3,3,1,1,3,3)
#Acropora digitifera, Acropora hyacinthus, Favia speciosa, Goniastrea aspera,  Porites lobata, and Porites rus

#grSpp<-c(5,6,7,8,9,5) #species specific accretion coefficients - literature? assume all the same? ( should get in
kg CaCO3 yr-1)


#### accretion rates from ROB


setwd("C:/Users/Chris/Desktop/van Woesik/Manuscripts/Reef accretion spatial/work for RA/Confidence
runs")
Species<-list.files()[sppnum];Species


#
# ##################
# ################################################################################ For New
Species to get confidence in one raster
# t<-1
#  ######################################    0 or 1, t0 = initial, t1 = 2100 A2 scenario
# ######################################   input zone, 1:5
#
#   if(t==0){time<-"initial dist.nc"}
#   if(t==1){time<-"A2 distribution.nc"}
```

```
#   for (i in 1:25){
#     x<-raster(paste("C:/Users/Chris/Desktop/van Woesik/Manuscripts/Reef accretion spatial/work for
RA/Confidence runs/",Species,"/",Species," ",i," ",time,sep=""))
#
#     if(i==1){RF<-x}
#     if(i!=1){RF<-sum(RF,x,na.rm=T)}
#
#
#     print(i)
#   }
#
# R<-RF
# R[R>25]<-25
# R[R==0]<-NA
#
# specRas<-R#read in the combined raster of the species for accretion
#
# setwd(paste("C:/Users/Chris/Desktop/van Woesik/Manuscripts/Reef accretion spatial/work for
RA/Confidence runs/",Species,"/",sep=""))
# writeRaster(R,paste(Species,"conf_sum",time),overwrite=T)
#
# ##############################################################################
# ############################

##############################################################################################grow
th/accretion


# # A series of gaussian distributions
#


################################################## GET PRESENCE POINTS
library(rgdal)
library(foreign)
load("C:/Users/Chris/Desktop/Comps/load data comps 10-1-2014.RData")


list1<-c(1,1,2,2,2,2)
list2<-c(30,58,129,180,398,415)

#for (vers in c(7:12)){
vers<-sppnum
set<-list1[vers]
i<-list2[vers]


setwd("C:/Users/Chris/Desktop/van Woesik/IUCN shapes")
corals2<-read.dbf(paste("CORALS",set,".dbf",sep=""))
corals<-corals2[order(corals2$binomial),]
Species<-paste(corals[i,2])
print(Species)


#convert to CRS
setwd(paste("C:/Users/Chris/Desktop/van Woesik/IUCN shapes/Coral shapes/Corals",set,sep=""))
IUCN_dist2<-readOGR(".",paste("CORALS",set,"_binomial__",Species,sep=""))
```

```
IUCN_dist<-spTransform(IUCN_dist2,CRS(newproj))

sparea<-area(IUCN_dist)
#find ecregions the species is in
IUCNinECO3<-ecoregions[!is.na(over(ecoregions,IUCN_dist)[,1]),]
IUCNinECO<-as.numeric(IUCNinECO3$New_No)
#IUCNinECO<-replace(IUCNinECO2, IUCNinECO2==142, 141)

print(paste("IUCN data converted to ecoregions",Species))


########## probability ################################################
regions<-IUCNinECO;nregions<-regions #regions the spp is in
one2141<-c(1:141)
absent<- one2141[!one2141 %in% regions] #find the regions the species is not in


adjlist<-data.frame() #list of all adjacent regions to the species (includes regions species is in)
for (j in nregions){
  AdjRegions<-AdjacencyMat[j,1:10]
  adjlist<-rbind(adjlist,AdjRegions)}
noNAadjlist<-adjlist[!is.na(adjlist)]
No_Present_Or_NA_adjlist<-noNAadjlist[!noNAadjlist%in%(nregions)]#########################
No_Present_Or_NA_adjlist is list of adjacent regions that do not have the species detected, not unique because
we sample through the number of iterations

########## give each initial absent region a probability of 30% to find species on first try.
problist<-data.frame()
for (i in 1:141){
  if (i %in% nregions){ # if it is in a region P(detect)=1
    x<-1}
  else{x<-.3} # if not in region P(detect)= .3
  problist<-rbind(problist,x)
}
#################################### initial values set


problist1<-c(do.call("cbind",problist))  ################ change .6 as decrease of adjacent regions
for (i in No_Present_Or_NA_adjlist){
  problist1[i]<-problist1[i]*.6}  ########### everytime a species is detected adjacent to a region the species is
absent from, probablility of detection is decreased by 40% because it is more likely the samplers missed it.

################ incorporate size into P

Plist<-problist1
for (i in absent){
  size<-sizes[i]
  ratioArea<-(minsize/size)^4 ##for regions the species is absent in take the log area of the region and divide
log min area by it
  Plist[i]<-Plist[i]*ratioArea}
problist<-Plist

if (any(!regions %in% c(123:137))==T){ ## they are not in atlantic
  problist[c(123:137)]<-1
  ATLvPAC<-1}#caribbean <- known absent

if (any(regions %in% c(123:137))==T){  ## they are in atlantic
```

```
 (problist[c(1:122,139:141)]<-1)
 ATLvPAC<-0} # pacific <- known absent

#ATLvPAC is 1 if it is a pacific species
probmat<-problist
#probmat

library(doParallel)
cl <- makeCluster(5) #
registerDoParallel(cl)


#determine which regions the species is likely to be absent

print("p2")
variance<-foreach (i = 1:141,.combine=rbind,.verbose=F) %dopar% {  ##########################loop it
for variance and Prob of Geometric
 p<-probmat[i]
 nfails<-SEF[i]

 maxSE<-max(SEF) #find the maximum value of sampling effort

 #geometric distribution for SE out of maxSE
 pgm<-pgeom(nfails,p)#probablility of finding this spp after x trials
 mx<-pgeom(maxSE,p)#prob of finding after max attempts
 PGM<-pgm /mx  #difference in probablility of finding after x trials - max attempts

 #determine variance
 VAR<-(1-p)/p^2  # get the variance
 EXP<-1/p    #expected value
 c(VAR,EXP,nfails,PGM) #combine variance, expected, sampling effort, probability of finding after SE trials
}
print("done var")

n<-1
se<-(sqrt(variance[,2]))/sqrt(n)
p<-probmat
#confidence of 95%
c95<-se*1.96 # determine the 95% confidence of regions
s95<-((log(1-.95)/log(1-p))-1) # determine the SE at which we are 95% sure we have found it.
plotsp<-cbind(variance,c95,s95,p)
rownames(plotsp)<-scip[,1]
colnames(plotsp)<-(c("var","exp","nfails","ProbFound","c95","s95","p"))
oplotsp<-plotsp[order(plotsp[,6]),]


low_confidence_regions<-foreach (i = 1:141,.combine=rbind)%dopar%{
 if(plotsp[i,4]<.95){i} ######################################## only take ones greater than 95% (could
include the confidence of that confidence?)
}
lowregions<-scip[low_confidence_regions,1]#if you need the region names


stopCluster(cl)

library(rgeos)
############ shapes of classified regions ############
```

```
#uncertain
n.regions<-as.numeric(low_confidence_regions[,1])
n.shpregions<-ereg[n.regions,604]
lowconf<-ecoregions[c(n.shpregions),]

#present
p_regions<-regions
shpregions<-ereg[regions,604]
this_spp<-ecoregions[c(shpregions),]
this_spp<-gBuffer(this_spp,width=0,byid=T)

#absent
pres_and_uncert<-c(n.regions,p_regions)
all<-c(1:141)
no<-setdiff(all,pres_and_uncert)
certainGone<-ereg[no,604]
none<-ecoregions[c(certainGone),]


if(ATLvPAC==1){absentSampleNumber<-(length(none)-15)}
if(ATLvPAC==0){absentSampleNumber<-(length(none)-125)}
absentSampleNumber/(length(this_spp)+absentSampleNumber)->ratio
asamp<-round(3000*ratio);psamp<-round(3000-asamp)


ecoP<-this_spp
ecoP<-spTransform(ecoP,CRS(proj4string(reefs)),force_ring=TRUE)


inreefs2<-over(reefs,ecoP)
short<-reefs[!is.na(inreefs2[,1]),]


inreefs<-as.numeric(rownames(inreefs2))

blure<-paste("determine presence points");print(blure)

#   stopCluster(cl)
#
cl <- makeCluster(5) #
registerDoParallel(cl)


cuts<-round(psamp/10)
cutsamp<-round(seq(1,psamp+200,length.out=cuts))
scuts<-round(seq(1,length(short),length.out=cuts))
inreefst1<-foreach(i=2:cuts,.packages=c("sp"),.combine=rbind) %dopar%{
  lrfs<-(short[scuts[i-1]:scuts[i]])
  rpoints<-spsample(lrfs,n=(cutsamp[i]-cutsamp[i-1]),"random",iter=100)
  coordinates(rpoints)
}

inreefst<-SpatialPoints(inreefst1)
Prespoints1<-SpatialPointsDataFrame(inreefst,data=data.frame(1:length(inreefst)))
proj4string(Prespoints1)<-proj4string(ecoP)
testpoint<-(over(Prespoints1,as(ecoP, "SpatialPolygons")))
tp2<-cbind(testpoint,1:length(testpoint))
```

```
shlst<-tp2[complete.cases(tp2),2] # take only complete cases
snum<-sample(shlst,psamp) #randomly sample the needed number of values
Prespoints<-Prespoints1[snum,]
Prespoints<-spTransform(Prespoints,nextproj)
stopCluster(cl)


print(paste("done sampling points"))


################################################## GOT PRESENCE POINTS
#http://nomads.gfdl.noaa.gov:8080/DataPortal/getModelExperDataByTable.jsp?coupled_name=GFDL-
ESM2M&exper_name=rcp85&exper_id=exper_id_NzrgHxy3PV&realiz_id=realiz_id_ntKPD70REo
setwd("C:/Users/Chris/Desktop/van Woesik/SST CMIP5 8.5 timeseries (distorted)")
for (i in 1:length(list.files())){
 z<-raster(list.files()[i],varname="tos",stopIfNotEqualSpaced=FALSE)
 if(i==1){tosi<-z}
 if(i!=1){tosi<-stack(tosi,z)}
}


tosi<-rotater(tosi,180) #Rotate to the correct place
tosi<-rotate(tosi) #rotate to the correct place


for (i in 1:19){  #loop this until 2100
 tos1<-subset(tosi,i) # subset for the individual time slice
 tos1<-crop(tos1,extent(c(-180,180,-60,60)))  #crop the extent
 r.pts <- rasterToPoints(tos1, spatial=TRUE)  #convert to points to play with coords
 zpt<-as.data.frame(r.pts)  # To data frame to transform
 #zpt<-zpt[,1]
 nexzpt<-(abs(coordinates(r.pts)[,2])*(1/sin((96-abs(coordinates(r.pts)[,2]))*pi/180)))  #transformation based
on the curvature of the earth from a point source. however, there may be more to it, but this is close. Satellite
89.5N and 81S. not sun... should be 90 for straight source. but its a model run


 nexzpt[coordinates(r.pts)[,2]<0]<-nexzpt[coordinates(r.pts)[,2]<0]*-1 #replace coordinates to match corrected
 newcoord<-cbind(coordinates(r.pts)[,1],nexzpt/max(nexzpt/60)) #bind x and y

 coordinates(zpt)<-newcoord
 zpt<-zpt[,1]

 #plot(zpt,pch='.')
 #tos2 <- resample(tos2,tos1, crs=nextproj)

 new<-rasterize(zpt,tos1,field=names(zpt))
 #image(new)
 #points(Prespoints)

 tos<-new
 tos<-tos-273.15
 #e<-extent(c(-180,180,-81.5,89.5)) #-81.5 : 89.5
 #tos2<-crop(tos2,extent(c(-167,167,-60.5,69.5)))
 #extent(tos2)<-e

 #plot(tos2)
 #points(Prespoints)
```

```
ecrop<-extent(c(-180,180,-37,37))
tos<-crop(tos,ecrop)

#need to match rasters
#points need to align properly

#PAR.mean<-raster("C:/Users/Chris/Desktop/van Woesik/PAR global
data/SWFMO_PAR.CR.timeAverage1998-2007.nc")
PAR.mean<-raster("C:/Users/Chris/Desktop/van Woesik/Manuscripts/Reef accretion spatial/work for
RA/Growth accretion/PARwithTURB.nc")
IrrDens<-extract(PAR.mean,Prespoints)
TeDens<-extract(subset(tos,1),Prespoints)
#hist(IrrDens,30)
#hist(TeDens,30)
optIrQ<-quantile(IrrDens,na.rm=T,probs=c(0,.01,.5,.99,1));quantile(IrrDens,na.rm=T,probs=c(0,.01,.5,.99,1))
#find the outer 5% and remove to allow for spatial distortion of extracting values from presence points
optTQ<-quantile(TeDens,na.rm=T,probs=c(0,.01,.5,.99,1));quantile(TeDens,na.rm=T,probs=c(0,.01,.5,.99,1))


Te<-tos#time changing...
 # get Temp from raster for current time (average?)
Irrad= PAR.mean # seq(0,100,1) # irradiance should remain constant
Te<-resample(Te,Irrad)

optTemp=median(TeDens,na.rm=T)  # find average for extracted presence points of moving temp
#NoptTemp= (28.9-min(Te))/(max(Te)-min(Te)) #take 99% oulier? there is some spatial distortion so not min
NoptTemp= (optTemp-optTQ[2])/(optTQ[4]-optTQ[2]) #take 99% oulier? there is some spatial distortion so
not min
optIr=median(IrrDens,na.rm=T) # find average for extracted presence points of static irrad

Tedisplay=seq(optTemp-20,optTemp+20,length.out=100)
Irrdisplay<-seq(optIr-40,optIr+40,length.out=100)


#NoptIrrad= (50-min(Irrad))/(max(Irrad)-min(Irrad)) # 99%
NoptIrrad= (optIr-optIrQ[2])/(optIrQ[4]-optIrQ[2]) # 99%
#Tmax=35
#NTmax=20
#Irrmax=100
#NIrrmax=1
#a=0.9
#b=0.9
normTe = (Tedisplay-optTQ[2])/(optTQ[4]-optTQ[2])
normTe2 = (Te-optTQ[2])/(optTQ[4]-optTQ[2])
normIrr = (Irrdisplay-optIrQ[2])/(optIrQ[4]-optIrQ[2])
normIrr2 = (Irrad-optIrQ[2])/(optIrQ[4]-optIrQ[2])

sigma=0.3
sigma2=0.5


mu=NoptTemp
x=normTe2
mu2=NoptIrrad
x2=normIrr2
```

```
  Growth=(Growth_rates[sppnum]/(sqrt(2*pi)*sigma)*exp(-1*(x-
mu)^2/(2*sigma^2)))*(1/(sqrt(2*pi)*sigma2)*exp(-1*(x2-mu2)^2/(2*sigma2^2)))
  if(i==1){AccreteStac<-Growth}
  if(i!=1){AccreteStac<-stack(AccreteStac,Growth)}
  print(paste(round(i/19,2),"%"))
}


mu=NoptTemp
dx=normTe
mu2=NoptIrrad
dx2=normIrr
dGrowth = (Growth_rates[sppnum]/(sqrt(2*pi)*sigma)*exp(-1*(dx-
mu)^2/(2*sigma^2)))*(1/(sqrt(2*pi)*sigma2)*exp(-1*(dx2-mu2)^2/(2*sigma2^2)))

#
plot(Irrdisplay,dGrowth, ylab=c("Growth (mm/yr)"), xlab = expression(paste("Irradiance meanPAR"), cex =
1.5),type="l",lwd=3,col='blue')
plot(Tedisplay,dGrowth, ylab=c("Growth (mm/yr)"), xlab = expression(paste("Temperature ("*degree*C*")"),
cex = 1.5),type="l",lwd=3,col='red')

grow.stack<-AccreteStac #each raster is the average


#determine how many times to add closest raster to predicted year, to get predictions not divisable by 5
tstacks<-Ttotal/5 #how many raster stacks fall into the predicted time frame
dtstack<-tstacks-max(1:tstacks) #how many leftover years into next stack

total.grow1<-sum((subset(grow.stack,1:tstacks)*5),na.rm=T)# take the temp up until time determined
if(dtstack>0){last.grow.ras<-(5*dtstack)*subset(grow.stack,max(1:tstacks)+1)} #
if(dtstack==0){last.grow.ras<-0}
total.grow<-total.grow1+last.grow.ras #raster of growth in mm???

grow.stack<-crop(grow.stack,c(-180, 180, -37, 37))
total.grow  #raster of just growth increase until x years for 5 year intervals from 2006-2100


##################
for(NOWAY in c(5,10,89,94)){
Ttotal<-NOWAY #shortcut for same species but different time frame (start at 94)
###########

inSpecRas<-raster(paste("C:/Users/Chris/Desktop/van Woesik/Manuscripts/Reef accretion spatial/work for
RA/Confidence runs/",Species,"/",Species," conf_sum initial dist.nc",sep=""))

specRasF<-raster(paste("C:/Users/Chris/Desktop/van Woesik/Manuscripts/Reef accretion spatial/work for
RA/Confidence runs/",Species,"/",Species," conf_sum A2 distribution.nc",sep=""))


Differe<-inSpecRas-specRasF
specRasT<-inSpecRas-(Differe/94)*Ttotal

#Accumulation of species presence and growth through time
pb <- txtProgressBar(min = 1, max = Ttotal, style = 3)
for (tf in 1:Ttotal){   #always must start at 1, goes through time accumulating growth and changing presence to
Ttotal
specRasi<-inSpecRas-(Differe/94)*tf  #specrasi = current species distribution (dynamic)
```

```
if(tf==1){specRas<-specRasi}   #if initial run, SpecRas=initial contemporary conditions
if(tf!=1){specRas<-sum(specRas,specRasi)}  #adds through time
################ confidence for species rasters

if(tf==1){presRas<-specRasi>0}
if(tf!=1){presRas<-sum(presRas,specRasi>0)}


upperci <- function(x) { ((x/25)+1.96*sqrt(x/25*(1-x/25)/25))*25} #upper confidence interval calculations
lowerci <- function(x) { ((x/25)-1.96*sqrt(x/25*(1-x/25)/25))*25} #lower


high95specRasi<-calc(specRasi,upperci)
high95specRasi[high95specRasi>25]<-25
low95specRasi<-calc(specRasi,lowerci)
low95specRasi[low95specRasi<0]<-0

if(tf==1){low95specRas<-low95specRasi;high95specRas<-high95specRasi}
if(tf!=1){low95specRas<-sum(low95specRas,low95specRasi);high95specRas<-
sum(high95specRas,high95specRasi)}



growth.and.species.t<-(specRasi/25)*(subset(grow.stack,round((tf+2)/5),na.rm=T))  #species distribution at
time i as a probability 0-1 * the growth of species at each location during time i
if(tf==1){GANDSP<-growth.and.species.t}
if(tf!=1){GANDSP<-GANDSP+growth.and.species.t}

growth.and.species.tLOWER<-(low95specRasi/25)*(subset(grow.stack,round((tf+2)/5),na.rm=T))
if(tf==1){GANDSPLOWER<-growth.and.species.tLOWER}
if(tf!=1){GANDSPLOWER<-GANDSPLOWER+growth.and.species.tLOWER}

growth.and.species.tHIGHER<-(high95specRasi/25)*(subset(grow.stack,round((tf+2)/5),na.rm=T))
if(tf==1){GANDSPHIGHER<-growth.and.species.tHIGHER}
if(tf!=1){GANDSPHIGHER<-GANDSPHIGHER+growth.and.species.tHIGHER}
print(paste(tf,round((tf+2)/5)))
setTxtProgressBar(pb, tf)
}

distributionT<-specRas
GANDSPLOWER
GANDSPHIGHER
specRas<-GANDSP  ###### incorporates growth through time including dynamic species presence, dynamic
temperature, and static irradiance, with a gaussian growth model fitted to presence points determining optimal
temp and irrad.
#presRas
#units are in mm extension still here.... need to convert to kgCaCO3, do at beginning when inputting growth
rate, not after.


print('subgrow done')


################################### sedimentation values ######################
#sed<-.1 constant global value
```

```
########## Sed.i,t is the amount of sedimentation


#follows flow rate negative exponential u*v high energy decreases sedimentation, get flow need function relating sediment to flow,


#currently use the log(inverse of flowrate to determine sedimentation) - stokes law

#http://icdc.zmaw.de/las/getUI.do?dsid=id-5248d88811&catid=082B82FBCF995B62AB1AD430D459955F&varid=AMPL-id-5248d88811&plot=XY_zoomable_image&view=xy&auto=true              Take the zonal and meridional velocities average through time 2006-2010(including seasonal trends) - then multiply u*v to get flow rate
#ORA S4 zonal current M s**-1     #depth=5.022 meters

v<-stack("C:/Users/Chris/Desktop/van Woesik/Manuscripts/Reef accretion spatial/work for RA/surface velocity global/meridional current (m s-2) at 5m-depth 2006-2010.nc")
v<-subset(v,1:48) #Take the first 48 of the 49 layers to get jan-dec for 4 years (2006-2010)
velv<-abs(v) #absolute value - for flow rate
T_Av<-mean(velv) #mean flow rate in the N/S direction for these 4 years...


u<-stack("C:/Users/Chris/Desktop/van Woesik/Manuscripts/Reef accretion spatial/work for RA/surface velocity global/zonal current (m s-2) at 5m-depth 2006-2010.nc")
u<-subset(u,1:48) #Take the first 48 of the 49 layers to get jan-dec for 4 years (2006-2010
velu<-abs(u)
T_Au<-mean(velu)

flowrate1<-T_Au*T_Av #in m s-1


#####################################################
#SEDIMENTATION IS NOW ONLY be POSITIVE OR NEGATIVE IF CORAL IS THERE
flowrate<-resample(rotate(flowrate1),specRas)
sed<-log(1/flowrate)  #where if(sed<0){print('error, sedimentation cannot be less than 0')},
if(sed>=0&sed<5){sed.sgn<-1} #if sedimentation is between 0-5 then sign is positive, if(sed>5){sed.sgn<-(-1)}
#is sedimentation is > 5 then sign is negative


#if(sed<0){print('error, sedimentation cannot be less than 0')} #not necessary now

#if(sed>=0&sed<5){sed.sgn<-1} #if sedimentation is between 0-5 then sign is positive
sed.sgn<-sed<5
#if(sed>5){sed.sgn<-(-1)} #is sedimentation is > 5 then sign is negative
sed.sgn[sed.sgn==0]<- (-1)


sed.it<-(sed.sgn*sed*presRas)/specnumT

#divided by 6 to not count sedimentation for each species.

# 1 g.m-2.d-1 = 0.1 mg.m-2.d-1


print('sedimentation done')
```

```
################################### accretion values ############################

#pcal.it<-(1/(1-flowrate))/1.3 ######### f(water quality) +f(year) +eps(lag1)   #spatial water quality... flow rate?   #scale of 0-1
#can i get probability, with error and do Bayesian?
#thompson and van woesik rasterized !!!!!!!!!!!!!!!!


growth.it<-specRas


#######################################
#######################################
######################################## Erosion values ############################


####### BIOLOGICAL EROSION #should this be done for the reef rather than individual species? yes... should all erosion? not the reduction in rate by cyclones.

lrras<-raster("C:/Users/Chris/Desktop/van Woesik/Manuscripts/Reef accretion spatial/work for RA/Bioerosion/population data/lowres popras sum aggregated 9.2km.nc")
rp<-raster("C:/Users/Chris/Desktop/van Woesik/Manuscripts/Reef accretion spatial/work for RA/Bioerosion/population data/pop growthrates.nc")


##### works for 5:94 years
x<-1:Ttotal;int<-1;y<-(-1*x^(3)/3009362+int);#plot(x,y,type='l',main='carrying cap effect',ylab='population decay',xlab='years')

uhh<-c()
for (i in seq(1,Ttotal,5)){
 Ti<-i
 allpopfut1<-lrras+lrras*rp*Ti
 Differp<-lrras-allpopfut1
 popRasT<-lrras-(Differp/94)*Ti

 allpopfut<-popRasT*y[i] #rescale to UN pop predictions of 11.2 billion
 FutPop<-focal(allpopfut,w=matrix(1,nrow=7,ncol=7),na.rm=T,pad=T) # buffer to r=30km
 biomass=-2.725*log10(FutPop)+17.234
 biomass[biomass<=0.01]<-0.01
 biomass[biomass>30]<-30
 #scale biomass to erosion of .01 to 22.3 kgm2 (mcclanahan) #I can scale linear because of biomass-erosion linear relationship # or 22.8 with Pari 1998 (same location)
 bio_E_urchin<-(biomass*-1+30)/1.32

 #add through time
 uhh[i]<-cellStats(allpopfut,sum)
 if(i==tail(seq(1,Ttotal,5),1)){Bio_E_urchFIN<-bio_E_urchin*(Ttotal+1-tail(seq(1,Ttotal,5),1)) }
 if(i==1){Bio_E_urchFIN<-bio_E_urchin*5}
 if(i!=1&i!=tail(seq(1,Ttotal,5),1)){Bio_E_urchFIN<-Bio_E_urchFIN+bio_E_urchin*5}
 print((i/Ttotal))
}
plot(seq(1,Ttotal,5),uhh[!is.na(uhh)],xlab='time',ylab='population',type='l',lwd=2)

Bio_E_urchFIN
```

```
#### chla
chl<-raster("C:/Users/Chris/Desktop/van Woesik/Chlorophyll a/SWFMO_CHLO.CR.timeAverage.1998-2007.nc")
#internalerosionrange<-c(.002,2.4) Pari 1998
internalbioerosion<-chl/25*Ttotal

internalbioerosion<-crop(internalbioerosion,Bio_E_urchFIN)

biol_erosion.it<-sum(Bio_E_urchFIN,internalbioerosion,na.rm = T)/6

# Fabricius et al. 2009 for internal bioerosion


print('bio erosion done')



#############
#############
#############phy_erosion

prob.cyclone<-raster("C:/Users/Chris/Desktop/van Woesik/Manuscripts/Reef accretion spatial/work for RA/Cyclone data/frequencies combined FINAL.nc") #probability of cyclone per year, caclculated from hurricanes between 1964 and 2014 (50 years) split into the category by wind speed and average radius of damaging wind (Moyer et al. 2007) for that category used as the radius for a density plot. Sum of these categories of hurricanes' density  over the 50 years/50 gives # of hurricanes*yr-1 spatially
#plot(prob.cyclone,maxpixels=3836160)
prob.cycloneRAW<-raster("C:/Users/Chris/Desktop/van Woesik/Manuscripts/Reef accretion spatial/work for RA/Cyclone data/frequencies combined FINAL.nc")
prob.cycloneRAW[prob.cycloneRAW==0]<-NA
prob.cycloneRAW[prob.cycloneRAW<0.000703125]<-0.000703125 # 1% of the distribution of values in raster
#intensity of cyclone raster (spatially dependent)
magnitudes<-raster("C:/Users/Chris/Desktop/van Woesik/Manuscripts/Reef accretion spatial/work for RA/Cyclone data/magnitude interpolation2 FINAL.tif")
magnitudes<-crop(magnitudes,extent(prob.cyclone))


Damage.freqREMOVE<-1/prob.cycloneRAW
bin<-Damage.freqREMOVE
######### binomial raster
prob.cycloneRAW01<-prob.cycloneRAW/cellStats(prob.cycloneRAW,max)
binom<-rbinom(ncell(prob.cycloneRAW01),Ttotal*365,values(prob.cycloneRAW01)/365)
values(bin)<-binom

#1350 kgCaCO3 is 1 meter vertical accretion.
lossREMOVE<-Damage.freqREMOVE*magnitudes
lossF<-lossREMOVE/(max(values(lossREMOVE),na.rm=T)/1350)

phy_erosion.it<-lossF*bin/specnumT
phy_erosion.it[is.na(phy_erosion.it)]<-0



print('physical erosion done')
```

```
#########chemical erosion (ocean acidification) negligible? conc[aragonite] raster?
#########
#########

#ftp://data1.gfdl.noaa.gov/11/CMIP5/output1/NOAA-GFDL/GFDL-
ESM2M/rcp85/mon/ocnBgchem/Omon/r1i1p1/v20110601/ph/


# distorted pH...
setwd("C:/Users/Chris/Desktop/van Woesik/Manuscripts/Reef accretion spatial/work for RA/pH/nc data")
######## setup ph rasters
for (i in 1:length(list.files())){
  z<-raster(list.files()[i],varname="ph",stopIfNotEqualSpaced=FALSE)
  if(i==1){phs<-z}
  if(i!=1){phs<-stack(phs,z)}
}

####### rasters stacked

x1<-c(8.2,7.8)  #ph values for starting point
y1<-c(0.0,.153)  # .153 kg of loss at ph 7.8 and 0 at 8.2
md<-lm(y1^0.6 ~ x1)  # regression using van Woesik et al. 2013

x<-seq(7.7,8.3,length.out = 100)  #use function to predict to see curve
y<-(md[[1]][2]*x+md[[1]][1])^(1/.6)  # predict
#plot(x,y)
#points(x1,y1,col='red',pch=16)  # fit

chem.eros.stack<-((md[[1]][2]*phs+md[[1]][1])^(1/.6))  #each raster is the average

#determine how many times to add closest raster to predicted year, to get predictions not divisable by 5
tstacks<-Ttotal/5 #how many raster stacks fall into the predicted time frame
dtstack<-tstacks-max(1:tstacks) #how many leftover years into next stack

total.erosion1<-sum((subset(chem.eros.stack,1:tstacks)*5),na.rm=T)# take the ph up until time determined
if(dtstack>0){last.chem.ras<-(5*dtstack)*subset(chem.eros.stack,max(1:tstacks)+1)} #
if(dtstack==0){last.chem.ras<-0}
total.erosion<-total.erosion1+last.chem.ras #raster of Kg CaCO3 m-2 yr-1lost until x years for 5 year intervals
from 2006-2100

rero2<-rotater(total.erosion,180)
rero1<-rotate(rero2)
rero<-crop(rero1,extent(c(-180,180,-60,60)))

r.pts <- rasterToPoints(rero, spatial=TRUE)  #convert to points to play with coords
zpt<-as.data.frame(r.pts)  # To data frame to transform
#zpt<-zpt[,1]
nexzpt<-(abs(coordinates(r.pts)[,2])*(1/sin((96-abs(coordinates(r.pts)[,2]))*pi/180)))  #transformation based on
the curvature of the earth from a point source. however, there may be more to it, but this is close. Satellite
89.5N and 81S. not sun... should be 90 for straight source. but its a model run

nexzpt[coordinates(r.pts)[,2]<0]<-nexzpt[coordinates(r.pts)[,2]<0]*-1 #replace coordinates to match corrected
newcoord<-cbind(coordinates(r.pts)[,1],nexzpt/max(nexzpt/60)) #bind x and y
coordinates(zpt)<-newcoord
zpt<-zpt[,1]

new<-rasterize(zpt,tos1,field=names(zpt))
```

```
#image(new)
#points(Prespoints)

total.erosion<-new


chem_erosion.it <- resample(total.erosion, phy_erosion.it, method='ngb') #resample to match phy_erosion raster(cell size).


chem_erosion.it<-chem_erosion.it/specnumT #kg CaCO3 lost from lowering pH over the time frame of the study-Ttotal (very small amount)

print('chemical erosion done')

#
# ############################## test to interpolate lines in erosion #just resample...
# library(ipdw)
# library(fields)
# r.pts <- rasterToPoints(chem_erosion.it, spatial=TRUE)
# zpt<-as.data.frame(r.pts)
# pts<-randomPoints(chem_erosion.it,5000)
# dataf<-as.data.frame(cbind(pts,extract(chem_erosion.it,pts)))
# coordinates(dataf)<-~x+y
# variogram = autofitVariogram(V3~x+y,dataf,model='Gau')
# plot(variogram)
#
# test<-ipdw(r.pts,costras=chem_erosion.it,range=11)
#  # To data frame to run interpolation
# new<-rasterize(zpt,tos1,field=names(zpt))
#

##############################
###################### vertical accretion rate to transform Kg CCO3 ################


# define functions
Cal.it = (growth.it) #########Cali,t is the amount of calcification that occurs relative to time t at site i (usually expressed in kg CaCO3 m-2 yr-1) #fit the rasters to a value we have for calcification? Cal.it<-(B1)*flow rate*coral cover?, the probablility of calcifying is inherent in this because of thermal stressors.

Eros.it = sum(phy_erosion.it,chem_erosion.it,na.rm=T)+biol_erosion.it #########Erosi,t is the extent of reef erosion, which is a function of biological erosion (biol_erosioni,t) (by associated reef organisms including herbivores), physical erosion (phy_erosioni,t) (by by storms), and chemical erosion (chem_erosioni,t) (by ocean acidification)

sed.it1<-(sed.sgn*sed*presRas)/specnumT
sedneg<-sed.it
sedneg[sedneg>0]<-0
toolow<-(Cal.it+sedneg)<0 #alter it so no erosion occurs, just inhibiition of growth
nottoolow<-(Cal.it+sed.it)>0
sed.it<-(nottoolow*sed.it)-(toolow*Cal.it)

#coeff of sed rate compared to accretion? or does value directly add to reef accretion since it sin kg CaCO3 m-2 yr-1
Accretion = Cal.it - Eros.it  + sed.it
```

```
#Some function
#mmheight1<-Accretion/1.457143 ##(Smith and Kinsey 1976). 10/7 or 4/3==kgcaco3/mm, Shallow, seaward portions of modern coral reefs produce about 4 kilograms of calcium carbonate per square meter per year, and protected areas produce about 0.8 kilogram per square meter per year. The difference is probably largely a function of water motion. The more rapid rate, equivalent to a maximum vertical accretion of 3 to 5 millimeters per year, places an upper limit on the potential of modern coral reef communities to create a significant vertical structure on a rising sea.

dV<-seq(0,10,.1)
a<-.01
b<- 1.45
dH<-dV-(a*dV^((dV+1)/dV*b))
#plot(dV,dH)
#lines(0:10,0:10,type='l')
mmheight1<-Accretion-(a*Accretion^((Accretion+1)/Accretion*b))
mmheight<-revrotate(mask(mmheight1,specRas,maskvalue=0))


print('height determined')
print('saving rasters')
# Save accretion as raster to sum for all species


homedir<-"C:/Users/Chris/Desktop/van Woesik/Manuscripts/Reef accretion spatial/work for RA/final accretion rates for spp"
subDir<-Species
dir.create(file.path(homedir, subDir),showWarnings = FALSE)
setwd(paste(homedir,subDir,sep='/'))


#plot(mmheight)
writeRaster(mmheight,paste(Species," mm year",Ttotal,".nc",sep=''),overwrite=T) #maybe just run for all 6 species here then compile and save so its easier to modify one parameter and evaluate the differences.
writeRaster(Cal.it,paste(Species," calcification kgCaCO3 year",Ttotal,".nc",sep=''),overwrite=T) #maybe just run for all 6 species here then compile and save so its easier to modify one parameter and evaluate the differences.
writeRaster(Eros.it,paste(Species," erosion kgCaCO3 year",Ttotal,".nc",sep='')) # *6 for the whole reef...


SLRiseTS<-stack("C:/Users/Chris/Desktop/van Woesik/Manuscripts/Reef accretion spatial/work for RA/Sea level data/ICDC data!/Time series/RCP 8.5 ensemble mean est (m) t-series.nc")


fut.sealevel1<-subset(SLRiseTS,Ttotal)*1000 #mm sealevel rise
fut.sealevel<-resample(fut.sealevel1,mmheight)
#Global Mean Sea Level Data and Figure ########## predicted sea level rise for RCP 8.5 ensemble approach, 2006-2100
fut.reef.height<-(mmheight-fut.sealevel) #final plot for one species.
#plot(fut.reef.height,maxpixels=3836160,useRaster=F,axes=F)
#plot(revrotate(mmheight1)-fut.sealevel,maxpixels=3836160,useRaster=F,axes=F)
writeRaster(fut.reef.height,paste(Species," mm above sealevel year",Ttotal,".nc",sep='')) # *6 for the whole reef...
}
}

#stopCluster(cl)
```

APPENDIX E: SUPPLEMENTARY FIGURES FOR CHAPTER 5.

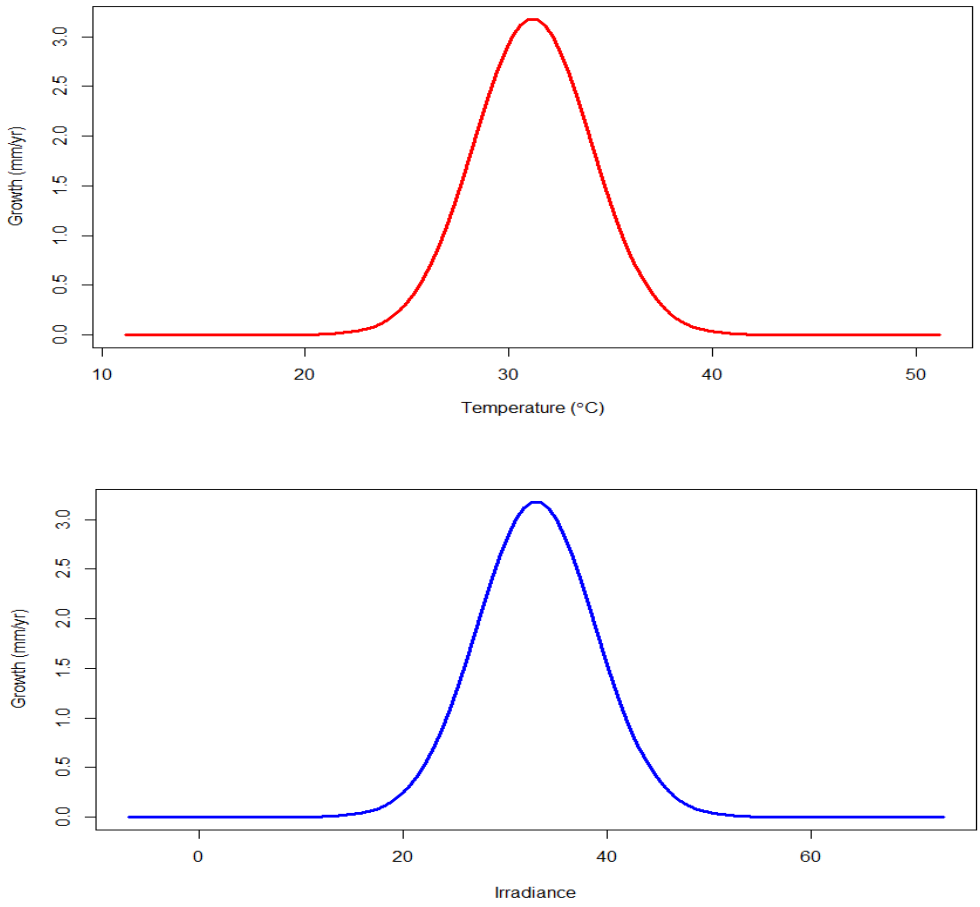

Figure S5 1. Gaussian optimal performance curves **a**) water temperature and **b**) irradiance

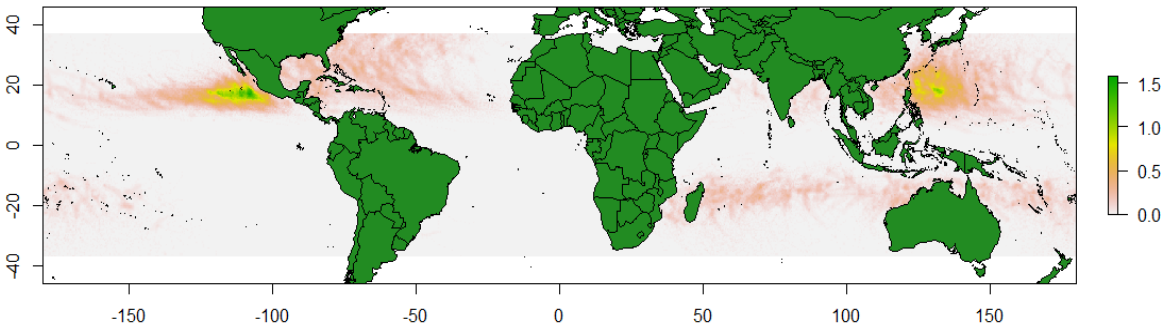

Figure S5 3. Interpolated annual cyclone frequency from the last 50 years of observations, collected from IBTrACS.

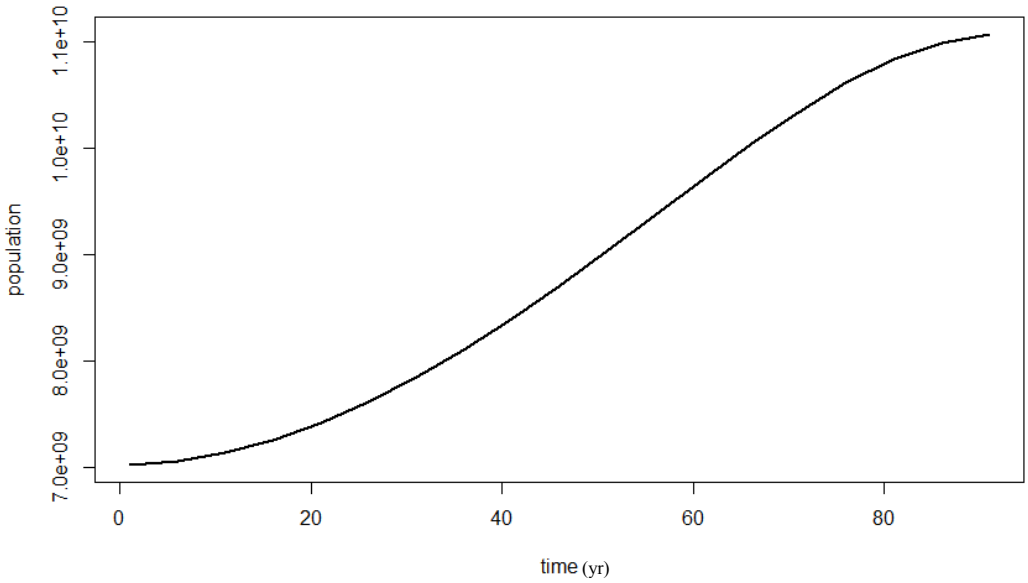

Figure S5 2. Human population model projections.